CHEMICAL REACTION IN A RADIOFREQUENCY DISCHARGE. THE OXIDATION OF HYDROGEN CHLORIDE

MASS.

by

Alexis T. Bell

S.B., Massachusetts Institute of Technology
(1964)

Submitted in Partial Fulfillment
of the Requirements for the
Degree of Doctor of Science
at the
Massachusetts Institute of Technology
August, 1967

Signature of Author .
Department of Chemical Engineering
August 21, 1967

Certified by .
Thesis Supervisor

Accepted by . . . .
Chairman, Departmental Committee
on Graduate Theses

Abstract

CHEMICAL REACTION IN A RADIOFREQUENCY DISCHARGE. THE OXIDATION OF HYDROGEN CHLORIDE

by

Alexis T. Bell

Submitted to the Department of Chemical Engineering in partial fulfillment of the requirements for the degree of Doctor of Science.

A radiofrequency electric gas discharge has been investigated for carrying out the oxidation of hydrogen chloride. Power was supplied by a Lepel Model T-2.5-1-HCl-J-B generator operating at 20 MHz. The reactor consisted of a straight quartz tube enclosed in a Lucite heat exchanger. A light petroleum oil was circulated through the heat exchanger which also acted as a calorimeter. The generator was capacitively coupled to the discharge through two sleeve electrodes placed on the outside of the quartz tube. The r.f. voltage applied across the electrodes was measured with a high voltage vacuum tube voltmeter.

Passage of a stoichiometric mixture of hydrogen chloride and oxygen through the discharge resulted in over 50% conversion of the hydrogen chloride to chlorine and water. For a fixed pressure and flow rate, the conversion for the forward reaction passes through a maximum when plotted versus power. Increasing the pressure for a constant power causes the conversion to rise to a maximum at ~ 15 Torr and to subsequently decrease. Increases in conversion can also be achieved by reducing the total molar flow rate and by increasing the ratio of oxygen to hydrogen chloride in the feed.

Studies of the reverse reaction showed that the conversion of chlorine to hydrogen chloride does not pass through a maximum as a function of power. Again, an increased conversion can be achieved by decreasing the flow rate.

When data for the forward and reverse reactions taken at constant power are plotted versus pressure, it is observed that for high pressures and low flow rates the percent of chlorine in the product mixture approaches an asymptotic value. This steady state value can be interpreted in terms of a modified theory of chemical equilibrium.

The passage of only one reactant through the discharge with subsequent addition of the second downstream showed that for the forward reaction either hydrogen chloride or oxygen could provide the necessary reactive species. A similar study on the reverse reaction showed that only the dissociation of water results in a significant conversion of chlorine.

A kinetic mechanism was proposed for the forward reaction. The primary step in this mechanism is a dissociative attachment process involving hydrogen chloride. Values for the conversion derived from the integrated rate expression for the consumption of hydrogen chloride agreed quite well with the experimental values. In addition, the proposed kinetic expression properly predicted the appearance of a maximum conversion with respect to power and the shift of this maximum to higher power for an increase in pressure.

The agreement between the calculated and the experimental values of conversion was found to be better for the assumption of well-mixed flow than for the assumption of plug flow. This observation was attributed to axial dispersion of reactants as a result of molecular diffusion.

A calculation of the degree to which the energy fed to the discharge is consumed by a particular excitation process showed that a large fraction may be used to excite hydrogen chloride to emit infrared radiation.

Thesis Supervisor: R. F. Baddour

Title: Professor of Chemical Engineering

Department of Chemical
Engineering
Massachusetts Institute
of Technology
Cambridge, Massachusetts
August 21, 1967

Professor Edward N. Hartley
Secretary of the Faculty
Massachusetts Institute of Technology
Cambridge, Massachusetts

Dear Professor Hartley:

In accordance with the regulations of the Faculty, I herewith submit a thesis entitled "Chemical Reaction in a Radiofrequency Discharge. The Oxidation of Hydrogen Chloride" in partial fulfillment of the requirements for the degree of Doctor of Science at the Massachusetts Institute of Technology.

Respectfully submitted,

Alexis T. Bell

Acknowledgements

The author wishes to express his appreciation and thanks to his advisor Professor Raymond F. Baddour for the suggestions and criticisms which he offered during the course of this work. He would also like to acknowledge the benefits of numerous discussions with Dr. Peter H. Dundas and Mr. William W. Cooper which provided new insights into theoretical aspects of the work.

Thanks are due to the National Science Foundation for its support of both the work and the author through a Graduate Traineeship.

Finally, the author would like to thank Miss Angela Carbone for typing the final draft of the thesis.

TABLE OF CONTENTS

CHAPTER		Page
I.	SUMMARY	1
	A. Introduction	1
	B. Apparatus	3
	C. Presentation and Discussion of Results	4
	D. Conclusions	14
II.	INTRODUCTION	16
	A. Background	16
	B. Previous Work	20
	C. Objective	32
III.	PHYSICAL CHEMISTRY OF AN ELECTRIC DISCHARGE	35
	A. Transfer of Energy	35
	B. Dissipation of Energy	41
IV.	APPARATUS	47
	A. General Description	47
	B. Electrical System	47
	C. Gas Handling System	48
	D. Discharge Tubes	50
	E. Heat Exchange Loop	51
	F. Water Injection System	51
V.	PROCEDURE	53
	A. Mixed Feed	53
	B. Separated Feed	55
	C. Measurement of Power Consumption	56

VI. RESULTS 57

A. Mixed Feed 57

1. Forward Reaction 57

2. Reverse Reaction 58

B. Separated Feed 60

C. Physical Observations and Visual Observations 62

VII. DISCUSSION OF RESULTS 66

A. Mixed Feed 66

1. Forward Reaction 66

a. Effect of Power on Conversion at Constant Pressure 66

b. Power Consumption 85

2. Reverse Reaction 90

a. Effect of Power on Conversion at Constant Pressure 90

B. Equilibrium 94

C. Separate Feed 101

D. Evaluation of Relative Power Losses 107

E. Estimation of Gas Temperatures 115

F. Contraction of Discharge Column 119

G. Distribution of Electric Field Strength and Emitted Light 123

H. Discussion of Errors and Reproducibility 129

1. Power Measurements 129

2. Product Composition 131

3. Reproducibility 133

VIII. CONCLUSIONS 134

IX. RECOMMENDATIONS 139

APPENDIX A. SAMPLE CALCULATIONS 141

- A. Calculation of Absorbed Power 141
- B. Calculation of Percent Conversion from the Chromatographic Data 142
- C. Calculation of the Dissociative Attachment Reaction Rate Constants 143
- D. Calculation of the Conversion for the Postulated Reaction Mechanism 145
- E. Calculation of Heat Transfer Coefficients 148
- F. Evaluation of the Effect of Axial Dispersion 152

APPENDIX B. ELECTRON DETACHMENT FROM NEGATIVE 155

APPENDIX C. REDUCTION OF REACTION KINETICS 158

APPENDIX D. DISCUSSION OF THE EXPERIMENTAL MEASUREMENT OF E/p' VERSUS T_e 165

APPENDIX E. EVALUATION OF THE ASSUMPTION OF A MAXWELLIAN DISTRIBUTION OF ELECTRON ENERGIES 169

APPENDIX F. NOMENCLATURE 171

APPENDIX G. LOCATION OF ORIGINAL DATA 175

APPENDIX H. LITERATURE REFERENCES 176

APPENDIX I. BIOGRAPHICAL NOTE 183

List of Figures

		After Page No.
Figure 1.	Percent Conversion of HCl versus Power	5
Figure 2.	The Effect of Pressure on Forward and Reverse Reactions at Constant Power	5
Figure 3.	Calculated Conversions for the Forward Reaction at 3.75 Torr	11
Figure 4.	Electron Density Distribution	39
Figure 5.	Variation of Electric Field Strength in a Hydrogen Discharge	41
Figure 6.	Electron Temperature versus E/p'	43
Figure 7.	Fractional Energy Loss per Collision versusElectron Temperature	44
Figure 8.	Distribution of Dissipated Power in Hydrogen	45
Figure 9.	Schematic of Apparatus	47
Figure 10.	Circuit Diagram of Vacuum Tube Voltmeter	48
Figure 11.	Discharge Tubes	50
Figure 12.	Apparatus for Feeding Water Vapor	51
Figure 13.	The Effect of Pressure on Conversion versus Power for $F = 7.4 \times 10^{-5}$ moles/sec	57
Figure 14.	The Effect of Pressure on Conversion versus Power for $F = 7.4 \times 10^{-5}$ moles/sec	57
Figure 15.	The Effect of Total Molar Flow Rate on Conversion versus Power for 3.75 Torr	57

Figure 16. The Effect of Total Molar Flow Rate on Conversion versus Power for 7.50 Torr 57

Figure 17. The Effect of Total Molar Flow Rate on Conversion versus Power for 11.25 Torr 57

Figure 18. The Effect of Oxygen to Hydrogen Chloride Ratio on Conversion versus Power for 3.75 Torr 58

Figure 19. Mass Spectra of Reactants and Products 58

Figure 20. The Effect of Pressure on Conversion versus Power for the Reverse Reaction 59

Figure 21. The Effect of Pressure on Forward and Reverse Reactions at Constant Power 59

Figure 22. The Effect of Discharging Hydrogen Chloride or Oxygen with the Subsequent Addition of the Second Reactant Downstream 61

Figure 23. The Effect of Adding Excess Oxygen or Chlorine to the Products of a Hydrogen Chloride Discharge 61

Figure 24. The Effect of Discharging Water Vapor with the Subsequent Addition of Chlorine Downstream 62

Figure 25. Voltage versus Current for a 20 MHz Discharge 62

Figure 26. Gas Temperature versus Power for 60 Hz Discharge 63

Figure 27. Dissociative Attachment Rate Constants for Hydrogen Chloride, Oxygen, and Water Vapor versus Electron Temperature 77

Figure 28. Dissociative Attachment Rate Constants for Hydrogen Chloride and Oxygen versus Electron Temperature 77

Figure 29. Drift Velocity versus E/p' 79

Figure 30. Calculated Conversions for the Forward Reaction at 3.75 Torr 81

Figure 31. Calculated Conversions for the Forward Reaction at 7.50 Torr 81

Figure 32. Calculated Conversions for the Forward Reaction at 11.25 Torr 81

Figure 33. Calculated Conversions for the Forward Reaction at 3.75 Torr Taking into Account Variations in O_2/HCl 84

Figure 34. Number of Hydrogen Chloride Molecules Dissociated per Unit of Energy 86

Figure 35. The Effect of Pressure on the Power Consumed per Pound of Chlorine Produced 88

Figure 36. The Effect of Flow Rate and O_2/HCl Ratio on the Power Consumed per Pound of Chlorine Produced 88

Figure 37. Calculated Conversion for the Reverse Reaction 93

Figure 38. Kinetic Curves for the Oxidation of Nitrogen 94

Figure 39. Equilibrium Conversion versus Temperature 99

Figure 40. Fractional Energy Loss by an Electron upon Collision with Carbon Monoxide and Carbon Dioxide 113

Figure 41. Infrared Spectrum of Bayol 35 119

Figure 42. Ambipolar Diffusion Coefficients as a Function of $\alpha = n_-/n_e$ 121

Figure 43. Normalized Radial Electron Distribution 122

Figure 44. Discharge Characteristics in the Presence of an Inhomogeneous Electric Field 125

Figure 45. Axial Distribution of Electron Temperature and Density near an External Electrode of a High Frequency Discharge 129

Figure A-1. Thermal Characteristics of Bayol 35 141
Figure A-2. y versus Percent Conversion 148
Figure D-1. Schematic of Drift Tube 165
Figure D-2. Average Electron Energy in Helium 168

LIST OF TABLES

TABLE		Page
1.	Characteristics of Hot and Cold Discharges	17
2.	Color of Emitted Light from Electrode and Central Discharge Volumes	64
3.	Reaction Rate Constants	71
4.	Summary of Vasil'ev's Data on Nitric Oxide Formation in an Arc	96
5.	Relative Yields of Chlorine Using a Hydrogen Chloride and an Oxygen Discharge	104
6.	Discharge Parameters	108
A-1.	Data for the Calculation of a Theoretical Conversion	148
A-2.	Calculated Values of the Natural Convection Heat Transfer Data	151

CHAPTER I

SUMMARY

A. Introduction

The prospect of a decrease in the cost of electricity has led to a re-examination of chemical processes which would depend on the direct use of electric power. The possibility of a developing chemical process using an electric gas discharge has attracted special interest because of the ability of a discharge to produce large quantities of chemically active species. These species, predominantly atoms and free radicals, could be used to promote chemical reactions which are kinetically inhibited, to form thermodynamically unstable compounds, or to induce changes in the surface characteristics of a solid material. Two forms of discharge are usually considered. The first, characterized by an arc or a plasma torch, operates under conditions in which the gas and electron temperature are equivalent and both are above several thousand degrees Kelvin. The second type of discharge, known as a glow discharge, operates with a high ratio of electron to gas temperature and a gas temperature of several hundred degrees Kelvin. Use of the second form of discharge presents several advantages over use of the former type. By maintaining a low gas temperature, a large portion of the electric energy supplied to the discharge can be diverted from heating of the gas to the performance of chemical activation. The latter effect is achieved through selective channeling of the power into the translational energy of the electrons. Materials problems in reactor construction which arise in the case of arcs and plasma jets could be eliminated because of the reduced severity of the thermal conditions. The one major disadvantage of operation with a glow discharge is the requirement that the gas pressure be maintained below $\sim$ 100 Torr. This limits the throughput of materials as well as the pressure drop available for flow. Attempts to increase the pressure would, unfortunately, cause the glow discharge to revert to the hotter form.

The objective of the present work has been to study a chemical reaction occurring in a radiofrequency discharge maintained by external electrodes. By keeping the electrodes external to the discharge volume, problems of reaction contamination are eliminated. Of specific interest has been an attempt to relate the observed chemical changes to a kinetic mechanism and rate expression which incorporate the variables which characterize the discharge. The two parameters of greatest concern are the electron temperature and density. Early work on the dissociation of hydrogen has shown that for this simple process the rate constant depends on the electron temperature, whereas the over-all rate is directly proportional to the electron density. For a complex reaction which depends on the formation of reactive intermediates via electron-molecule collisions, a similar type of relation is to be expected.

The chemical reaction chosen for this study was the oxidation of hydrogen chloride to chlorine. The reaction is one which is favored by thermodynamic equilibrium at low temperatures but which fails to proceed due to kinetic limitations. Previous work by Cooper (31) has shown that this reaction will proceed with over 50% conversion of the hydrogen chloride when carried out in a microwave discharge at pressures between 4 and 40 Torr. Unfortunately, measurements of the voltage and current through the discharge could not be made in this case. In the present study such measurements were possible (because of the lower frequency) and supplied the information necessary to determine the electron temperature and density.

B. Apparatus

Radiofrequency power for the experiments was provided by a Lepel Model T-2.5-1-MC1-J-B generator operating at 20 MHz. The generator was coupled to the discharge through a matching network and two external sleeve electrodes placed around the discharge tube. The discharge tube was enclosed in a heat exchanger which formed part of a closed heat exchange loop. The oil, circulated through the loop, served to cool the discharge tube. By measuring the temperature rise in the oil, the power supplied to the discharge could be determined. The voltage applied across the electrodes was measured with an r.f. vacuum tube voltmeter.

Reactants were fed to the discharge from a gas manifold, and the products were collected in a sample trap immersed in liquid nitrogen. Upon vaporization of the collected products, an analysis of the composition was performed via gas chromatography. The chromatographic column, which was capable of separating hydrogen chloride and chlorine, was packed with 30 - 60 mesh Haloport F (a Teflon 6 material) onto which was deposited a 10% loading of DC-11 silicone grease.

C. Presentation and Discussion of Results

The effect of the power supplied to the discharge on the conversion of hydrogen chloride to chlorine was investigated over the pressure range of 3.75 to 22.50 Torr. For a constant pressure and molar flow rate, the conversion at first increases with power but, then, attains a maximum and gradually begins to decrease. The power at which the maximum conversion occurs shifts to higher powers as the gas pressure is increased. An increase in conversion can be achieved by decreasing the total molar flow rate. The effect of diminishing the flow rate begins to decrease at lower flow rates and especially for higher pressures. Increasing the ratio of oxygen to hydrogen chloride in the feed also leads to an increase in conversion. Figure 1 illustrates these effects for the data taken at 3.75 Torr.

An evaluation of the amount of power consumed per pound of chlorine produced showed that for a fixed pressure this parameter rises with increasing power. Increasing the flow rate or increasing the ratio of oxygen to hydrogen chloride in the feed led to a decrease in the power consumption. To a limited extent a similar effect could be achieved by increasing the pressure. For the conditions covered in the present study, the lowest power consumption was 8.4 kwhr/lb of Cl_2, obtained at $P = 40$ watts, $p = 7.50$ Torr, $F = 7.40 \times 10^{-5}$ moles/sec, and $O_2/HCl = 0.25$.

A study of the reverse reaction, using a stoichiometric mixture of chlorine and water, showed that at constant pressure the conversion of chlorine does not pass through a maximum when plotted against power. As in the case of the forward reaction, a decrease in the total molar flow rate produces an increase in the conversion.

The effects of pressure and flow rate on the mole percent of chlorine in the hydrogen chloride-chlorine product mixture is shown in Figure 2 for both the forward and the reverse reactions. As the molar flow rate is

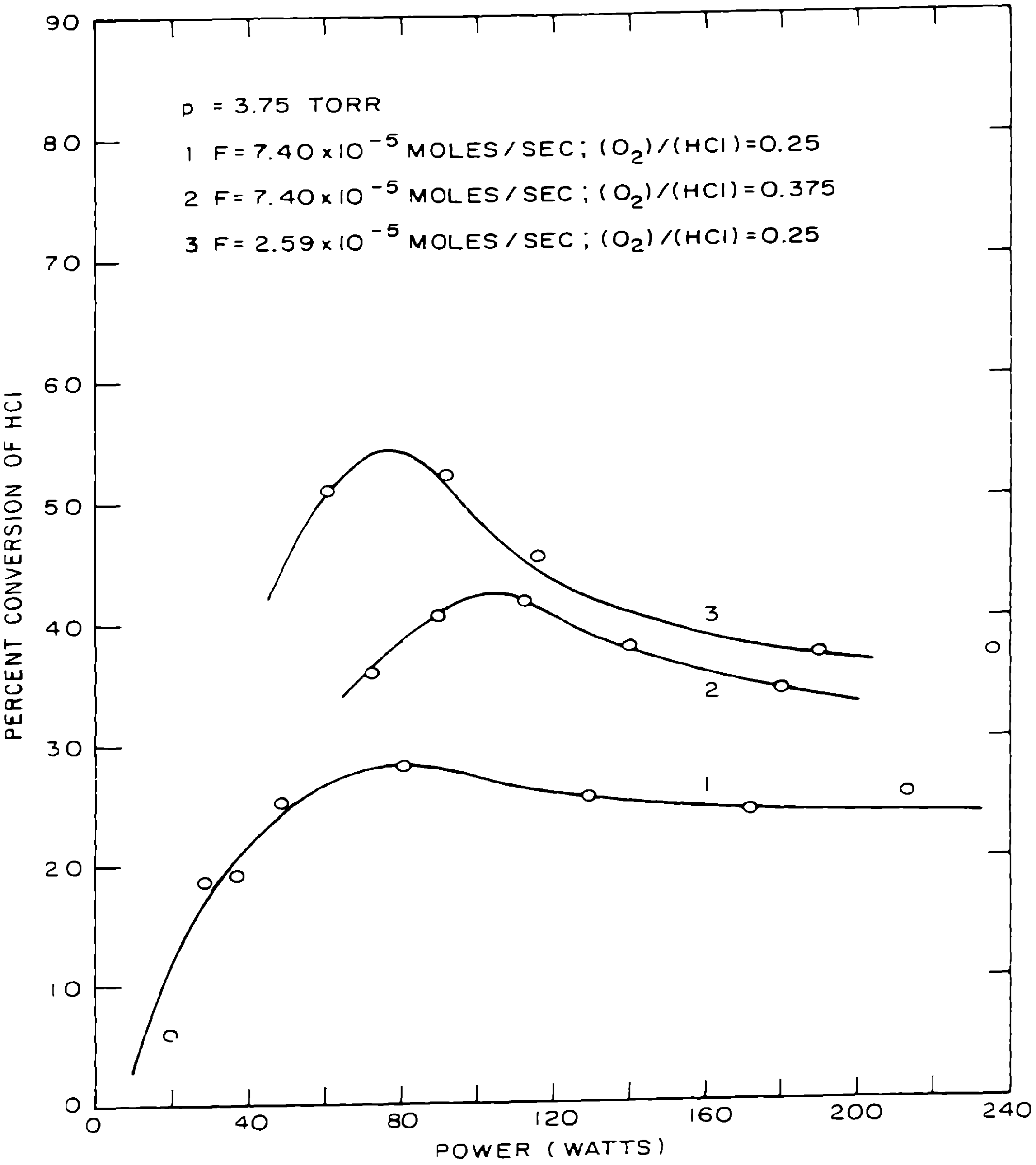

FIGURE 1 PERCENT CONVERSION OF HCl VERSUS POWER

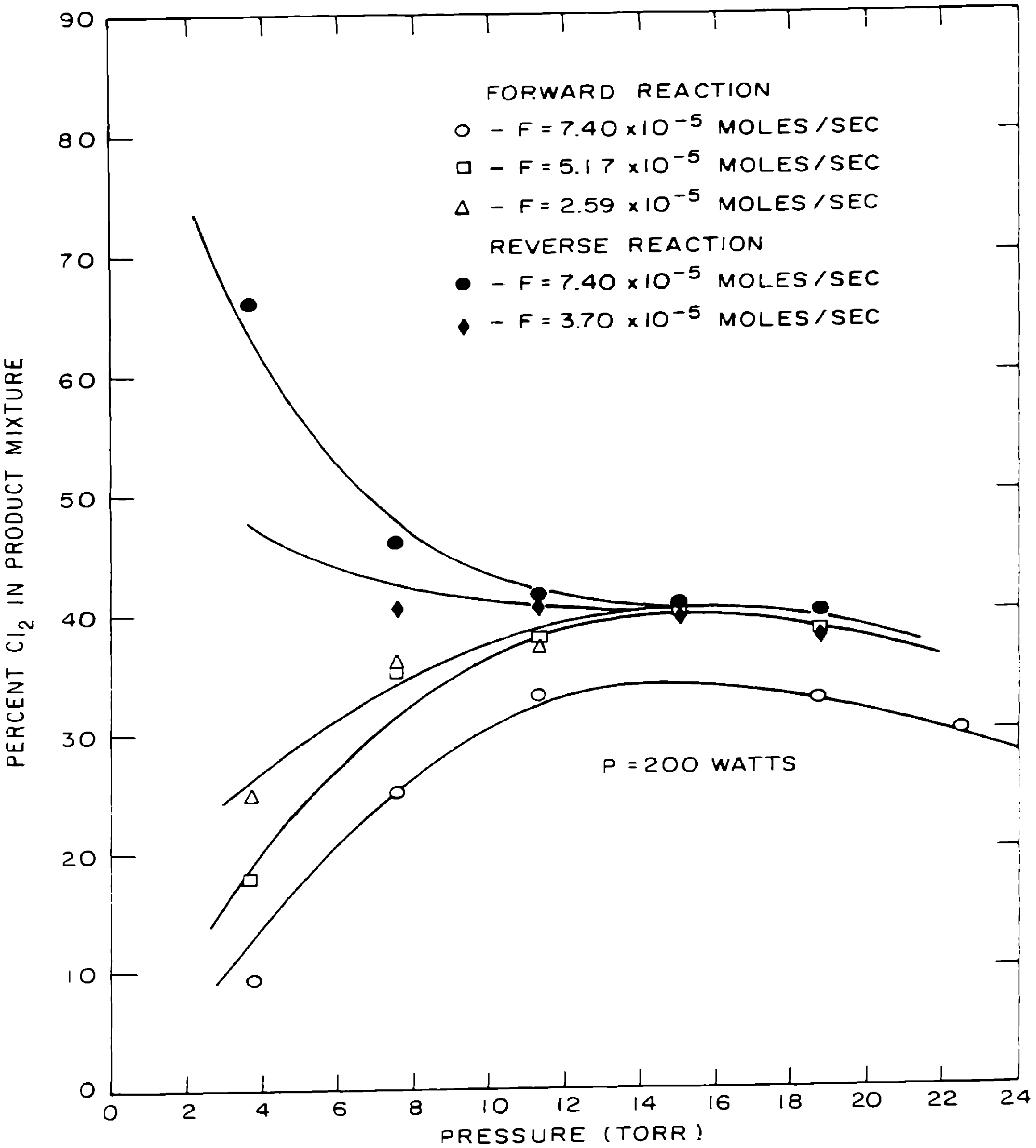

FIGURE 2 THE EFFECT OF PRESSURE ON FORWARD AND REVERSE REACTIONS AT CONSTANT POWER

decreased and the pressure is increased, the separate curves for the forward and reverse reactions begin to merge and approach a common mole percent of chlorine. For pressures above 15 Torr this value begins to gradually decrease as the pressure is further increased.

An interpretation of the steady state concentration of chlorine can be given in terms of a modified theory of chemical equilibrium. Manes (51) and Potapov (52) have shown that for a multitemperature system, such as is found in a glow discharge, an equilibrium constant can be derived in terms of the partition functions for the translational, rotational, vibrational, and electronic degrees of freedom of each reaction partner. Instead of evaluating these at the gas temperature T_g, each partition function of each degree of freedom is evaluated at the excitation temperature for that degree of freedom. The composition expression related to the equilibrium constant retains the conventional form. Consequently, the reaction system continues to respond to the Law of Mass Action, but the equilibrium composition can no longer be determined from a knowledge of the gas temperature and pressure alone. A similar conclusion was arrived at on the basis of experimental evidence by Vasil´ev (28) and by Blaustein and Fu (20). In the present case the steady state conversion was found to decrease as the temperature and pressure of the gas were simultaneously increased and to increase when the ratio of oxygen to hydrogen chloride was increased. Both these trends are in agreement with those predicted by the Law of Mass Action. However, the actual value of the steady state conversion cannot be properly determined from the gas temperature and pressure and the corresponding single-temperature equilibrium constant.

Investigation of the separate introduction of either hydrogen chloride or oxygen into the discharge with the subsequent addition of the second reactant immediately below the discharge showed that the dissociation of either reactant will lead to a conversion of hydrogen chloride. The use of excess oxygen, together with a hydrogen chloride discharge, showed that the yield of chlorine could be improved but that this effect begins to diminish as a greater and greater excess is used. This behavior can be explained by regarding the oxygen molecules as a getter of hydrogen atoms, preventing their recombination with chlorine atoms. Consequently, an upper limit to the yield of chlorine is achieved when all the hydrogen atoms produced as a result of hydrogen chloride dissociation are reacted to form water.

An examination was also made of the relative effects of discharging chlorine and water vapor on the conversion of chlorine to hydrogen chloride. In this case only the use of a water vapor discharge led to significant conversion.

A kinetic mechanism for the forward reaction can be given in terms of the following 14 reaction steps:

1. $HCl + e \rightarrow H + Cl^-$
2. $O_2 + e \rightarrow O + O^-$
3. $H_2O + e \rightarrow OH + H^-$
4. $Cl_2 + e \rightarrow Cl + Cl^-$
5. $O + HCl \rightarrow OH + Cl$
6. $H + O_2 \rightarrow OH + O$

6a. $H + O_2 + M \rightarrow HO_2 + M$

6b. $H + HO_2 \rightarrow 2OH$

7. $OH + HCl \rightarrow H_2O + Cl$
8. $H + Cl_2 \rightarrow HCl + Cl$
9. $2OH \rightarrow H_2O + O$
10. $O + OH \rightarrow O_2 + H$
11. $H + Cl + M \rightarrow Cl_2 + M$
12. $2O + M \rightarrow O_2 + M$
13. $H + OH + M \rightarrow H_2O + M$
14. $2Cl + M \rightarrow Cl_2 + M$

This set of reactions was chosen under the conditions that: a) only those steps be included which lead to the observed final products or the reformation of the reactants; b) only the lowest energy electron collision processes be selected which lead to the dissociation of hydrogen chloride, oxygen, chlorine, and water vapor; c) only homogeneous reaction steps be considered in order to keep the over-all description of the mechanism as simple as possible. Simultaneous consideration of all 14 reaction steps does not lead to a simple expression for the rate of disappearance of hydrogen chloride in terms of the concentrations of the reactants and products. To provide for such a relation, two additional assumptions were made: a) only those steps leading to the formation of chlorine and water vapor would be considered; b) decomposition of the products by electron collisions would be excluded. The eight reaction steps which remain after application of the above restrictions can be grouped so as to yield an expression of the form

$$\frac{d(HCl)}{dt} = - Ak_1(HCl)(e) - Bk_2(O_2)(e)$$

where the values of the numerical constants depend on the choice of the reaction steps. Over the range of variables studied $(B/A)(k_2/k_1) \ll 1$ so that the rate expression can be further simplified.

The following assumptions are used in conjunction with the above rate expression in order to calculate values for the conversion:

a) The electric field strength throughout the discharge is constant and is given by dividing the voltage across the electrodes by the length of the discharge zone.

b) The resistance of the discharge is constant and, over the range of variables studied, is independent of pressure, gas composition, and current.

c) The gas temperature in the discharge is proportional to the power dissipated and is given by

$$T_g = 293 + \Delta T^* P/200$$

where P is the power dissipated in the discharge and ΔT^* is left as an adjustable constant, which is chosen so that the calculated conversions match the experimental ones.

d) The reactor volume is taken as the volume of the discharge zone.

e) The value of the electron temperature T_e can be chosen from a plot of T_e versus E/p' given by Bailey (48) for pure hydrogen chloride.

f) The electron density in the discharge is uniform and is given by

$$n_e = \frac{I}{\pi a^2 e\, v_d}$$

where I is the discharge current. a, the radius of the discharge tube, e, the charge on the electron. and v_d, the electron drift velocity. The value of v_d is determined from a plot of v_d versus E/p' given by Bailey (48) for pure hydrogen chloride.

g) The rate constant k_1 can be calculated from the experimentally determined value of the collision cross section for reaction 1 and the assumption of a Maxwellian distribution of electron energies.

h) The flow pattern through the discharge is either plug flow or well-mixed flow.

i) The constant A appearing the rate expression is left as an adjustable constant.

The theoretical value of the conversion can then be determined from

$$12.8\ k_1 \left(\frac{p}{RT_g}\right) n_e \ \frac{V}{F_{HCl}} = -4\ \ln(1-x) + x$$

for the assumption of plug flow and from

$$16.8\ k_1 \left(\frac{p}{RT_g}\right) n_e \ \frac{V}{F_{HCl}} = \frac{x(5+x)}{(1-x)}$$

for the assumption of well-mixed flow. The conversions calculated from these equations agree very closely with the experimental ones, as can be seen from Figure 3. The

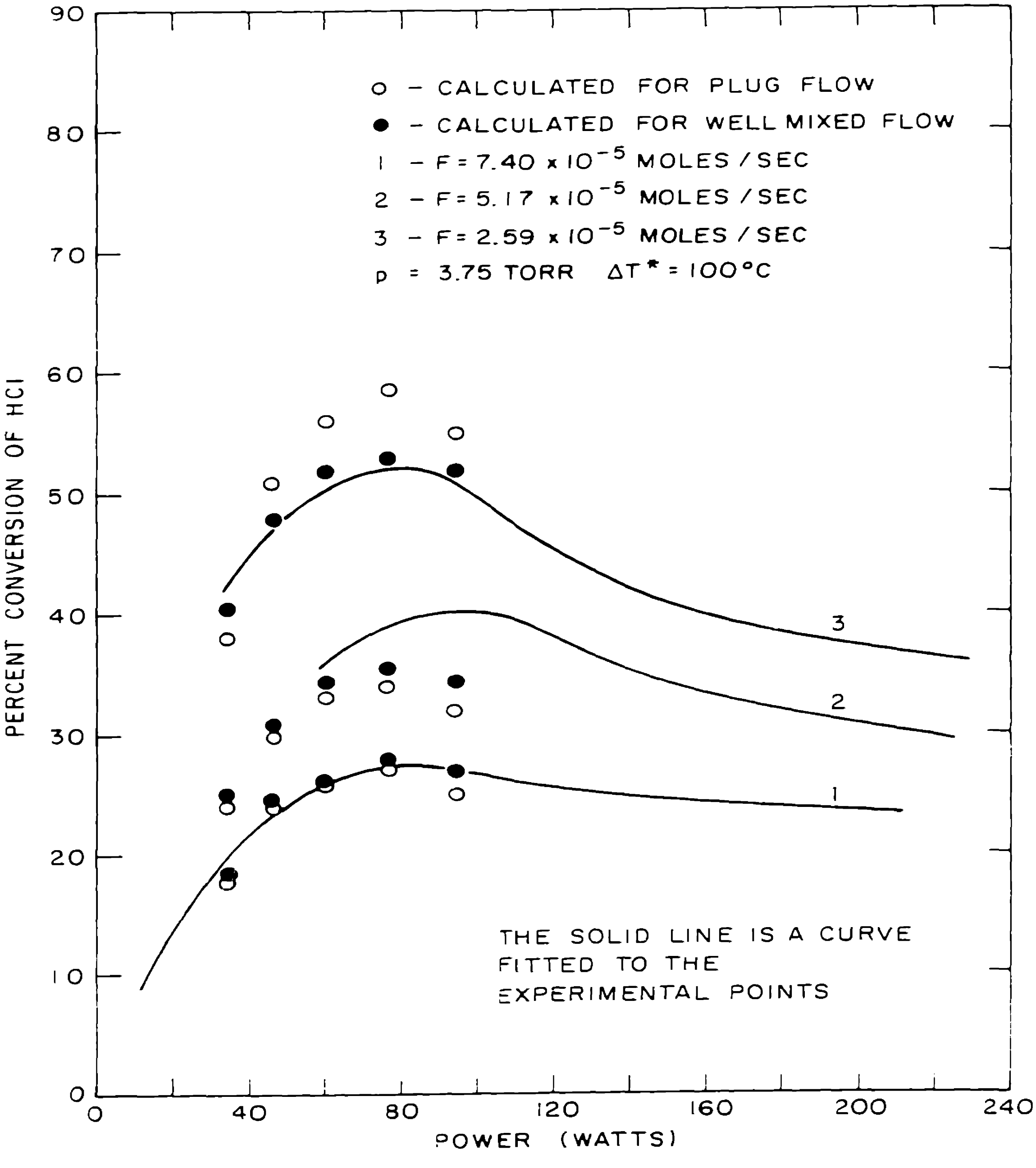

FIGURE 3 CALCULATED CONVERSIONS FOR THE FORWARD REACTION AT 3.75 TORR

model of the reaction system correctly predicts the appearance of a maximum in the plot of percent conversion versus power at constant pressure and the shift of the maximum to higher power as the pressure is increased. Multiplication of the two equations by $\frac{\alpha}{0.25} \frac{1+\alpha}{1.25}$, where $\alpha = (O_2)/(HCl)$, allows the effects of an increase in the ratio of oxygen to hydrogen chloride to be taken into account.

A set of calculations were made to determine the fraction of the total energy supplied to the discharge which was taken up by a particular excitation or loss mechanism. Losses due to diffusion, ionization, dissociative attachment, detachment, and infrared radiation were considered. The following fractional losses could be associated with these processes:

$$F_{diff} = 9.1 \times 10^{-5}$$

$$F_{ion} = 2.7 \times 10^{-4}$$

$$F_{diss} = 7.0 \times 10^{-3}$$

$$F_{det} = 3.9 \times 10^{-2}$$

$$F_{ir} = 1.9 \times 10^{-1}$$

It can readily be seen that only the excitation of infrared emission represents a significant loss. The fractional loss due to excitation of emission in the visible region was not calculated since the cross section for the process was not available. However, in view of the low electron temperatures occurring in the present system (2×10^{13} °K< $T_e < 10^4$ °K), significant excitation of energy levels which might radiate in the visible range is not expected.

Visual observation of the discharge showed that as the pressure was raised above a certain level, the discharge column contracted. This phenomenon can be explained in terms of the effect of negative ions on the diffusion coefficient for electrons and in turn on the radial distribution of electrons.

It was also observed that the discharge in the vicinity of an electrode emitted light of a shorter wavelength than did the volume in the center of the discharge. Such an observation reflects the occurrence of a higher field strength and electron temperature in the vicinity of the electrodes. Perel' and Pinskii (62) offer a theoretical explanation for the presence of such high field strength regions, which are due to nonuniformities in the electric field distribution. The experimental measurements of Dzherpetov *et al.* (64) and Polman (65) substantiate this theory.

D. Conclusions

Over 50% conversion of hydrogen chloride to chlorine and water can be obtained in the oxidation of hydrogen chloride in a radiofrequency discharge operating at 20 MHz. For a fixed pressure and flow rate, the conversion for the forward reaction passes through a maximum when plotted versus power. Increasing the pressure for a constant power causes the conversion to rise to a maximum at ~ 15 Torr and to subsequently decrease. Increases in conversion can also be obtained by reducing the total molar flow rate and by increasing the ratio of oxygen to hydrogen chloride in the feed.

Studies of the reverse reaction showed that the conversion of chlorine does not pass through a maximum as a function of power. Again, an increased conversion can be attained by decreasing the flow rate.

When data for the forward and reverse reactions, taken at constant power, are plotted versus pressure, it is observed that for high pressures and low flow rates the percent of chlorine in the product mixture approaches an asymptotic value. This steady state concentration can be interpreted in terms of a modified theory of chemical equilibrium.

The passage of only one reactant through the discharge with the subsequent addition of the second downstream showed that for the forward reaction either hydrogen chloride or oxygen could provide the necessary reactive species. A similar study on the reverse reaction showed that only the dissociation of water results in a significant conversion of chlorine.

A kinetic mechanism was proposed for the forward reaction. The primary step in this mechanism is a dissociative attachment process involving hydrogen chloride. Values for the conversion derived from the integrated rate expression for the consumption of hydrogen chloride agreed quite well with the experimental values. The proposed kinetic expression properly predicted the appearance of a maximum conversion and the shift of this maximum to higher power for an increase in pressure.

The agreement between the calculated and the experimental values of conversion was found to be better for the assumption of well-mixed flow than for the assumption of plug flow. This observation was attributed to axial dispersion of reactants as a result of molecular diffusion.

A calculation of the manner in which the power fed to the discharge is consumed showed that a large fraction of this power may be used to excite hydrogen chloride to emit infrared radiation.

CHAPTER II

INTRODUCTION

A. Background

The decrease in the cost of electric power which is being made possible by the advent of nuclear power sources has led to a re-examination of chemical processes which depend on electricity for a supply of energy. In the light of these circumstances, attention has turned to the possibility of using an electric gas discharge to promote chemical reactions for industrial production. The electric discharge is of particular interest, because it is capable of producing large quantities of chemically active species. These species, which are usually atoms or free radicals, can be used to promote chemical reactions which are kinetically inhibited in the absence of a catalyst, or they may be used in the formation of thermodynamically unstable compounds, or, alternately, they may be caused to impinge on a solid surface in order to promote a change in the surface characteristics.

Studies on chemical reactions in electric discharges have been carried out in two distinct discharge regimes. The characteristics of these regimes are shown in Table 1. The primary distinction between a hot and a cold discharge, as these are often referred to, is the equivalence of the

Table 1

Characteristics of Hot and Cold Discharges

Hot Discharge

1. $T_e > T_g$ $T_e > 10^3\ {}^oK$ $T_g > 10^3\ {}^ok$

2. $n_e > 10^{14}$ electrons/cm^3 $\overline{P} > 10^3$ watts/cm^3 $p \simeq 1$ atm

3. Can be sustained by:

   A. d.c. arc

   B. d.c. plasma torch

   C. r.f. plasma torch

Cold Discharge

1. $T_e >> T_g$ $T_e \simeq 10^4\ {}^oK$ $T_g \simeq 10^2\ {}^oK$

2. $n_e < 10^{12}$ electrons/cm^3 $\overline{P} < 10^2$ watts/cm^3 $p < 10^2$ Torr

3. Can be sustained by:

   A. d.c. glow discharge

   B. r.f. and microwave glow discharge

electron and gas temperatures in the case of the hot discharge and the disparity between these two temperatures in the cold discharge. It should also be noted that the conditions found in a cold discharge are generally milder from the standpoint of electron density, gas temperature, and power density.

To date, most of the industrially promising work on chemical reactions in an electric discharge has been done in arcs. And of this work most has been limited to hydrocarbon cracking, the synthesis of acetylene from hydro-rbons and from the elements, and the fixation of nitrogen as nitric oxide. The evidence of these investigations has shown that in all cases free radicals are present in the discharge zone and play an important role in determining the yield of product. As an example, in a study of the synthesis of acetylene from the elements in a high intensity carbon arc, Blanchet (1) observed that the volume concentration of acetylene in the products was greatly in excess of that predicted by equilibrium for any temperature obtainable in the arc. An explanation for this observation was based on the supposition that C_2H radicals, present in relatively large concentrations in the arc zone, reacted with H atoms to form more acetylene in the quench step of the reaction.

Despite the interesting results obtained with arcs (1,2,3), the necessity of operating at high gas temperatures is a disadvantage. Since all species must be raised from the ambient temperature to that of the arc, a considerable portion of the electric energy is consumed in heating the reactants, and this energy is then wasted in a quench step. The high temperatures also produce materials problems and require that an arc reactor be cooled. The coolant again drains off energy from the process. Because of these disadvantages it becomes desirable to investigate the possible use of the second discharge regime. In this case it should be possible to carry out reactions at significantly lower gas temperatures, and as a result a larger portion of the discharge energy should become available for chemical activation.

Operation with a cold discharge is not without its own disadvantages. The necessity of operating at low gas pressures decreases the throughput of reactants through a given apparatus cross section and reduces the pressure head available for flow. If an attempt is made to raise the pressure, the rate at which energy is exchanged between electrons and molecules is increased and the gas temperature rises.

Two possible sources yield a discharge with the characteristic of a high ratio of electron to gas temperature. These are the positive column of a d.c. glow discharge and a glow discharge sustained by a high frequency source. The d.c. discharge has two limitations which need to be considered. The first is the presence of electrodes which can become a source contamination for a chemical reaction. The second is that the maximum current which can be passed through the discharge is limited by the cathode area. A high frequency discharge, on the other hand, does not require electrodes within the discharge volume and can be maintained by means of capacitive or inductive coupling between the generator and the discharge. Furthermore, since a high frequency glow discharge does not depend on electrode processes for the generation of new electrons, the current which can be passed is not limited. Thus, for the purposes of chemical reaction, a high frequency glow discharge appears to be more advantageous.

B. Previous Work

Although electric discharge chemistry using high frequency sources has been investigated since about 1930, most of the work reported has been of a qualitative nature. The objective has usually been to identify the composition and yield of the reaction products, but, with the exception of total power, these have not been related to the variables describing the operation of the discharge. Glocker and Lind (4) have given an extensive review of the work done up to 1939, and, more recently, Jolly (5) and Kana'an and Margrave (6) have presented surveys of the work done up to 1961. The latter two works describe the various types of discharge which have been used and the results of their application to different classes of chemical compounds. In view of the availability of these reviews, only a survey of some of the qualitative work will be given here. The last portion of this section will be devoted to a discussion of the work reported in the Soviet literature on the oxidation of nitrogen. These investigations have not been referred to previously and are representative of one of the few instances in which an attempt has been made to relate the discharge parameters, namely the electron density and temperature, to the observed chemical changes.

The most fundamental type of reaction studied is the dissociation of diatomic gases. This area covers the dissociation of hydrogen, nitrogen, oxygen, and the halogens.

Shaw (7) describes a number of experiments done on the dissociation of hydrogen at 3000 MHz. The maximum yield of hydrogen atoms was obtained at a pressure of 0.5 Torr. At this pressure with 100 watts of power dissipated in the discharge and a flow rate of 10^{-5} moles/sec, the hydrogen from the discharge was 90% dissociated. For the same pressure and power, the yield of atoms increased with increasing flow rate, although the extent of dissociation decreased. At low flow rates, the yield of atoms increased linearly with increasing power at low power, but leveled off as the degree of dissociation increased. At higher flow rates, only partial dissociation occurred even at high power. Curiously enough the maximum number of hydrogen molecules dissociated per unit of energy, obtained by Shaw, agreed quite closely with that noted by Poole (8) in a d.c. glow discharge.

Bak and Rastrup (9) have also studied the dissociation of hydrogen by a microwave discharge. Their findings showed that preliminary saturation of the hydrogen stream with water greatly enhanced the yield of hydrogen atoms. Similar observations have been reported by Wood (10) for the process occurring in a d.c. glow discharge and by Shaw (11) for a microwave discharge.

Young et al. (12) describe the formation of nitrogen atoms when molecular nitrogen is introduced into a microwave discharge. Their observations showed that at a pressure of 10 Torr the atomic concentration of nitrogen could be raised from 2×10^{13} atoms/cm^3 to 1.2×10^{15} atoms/cm^3 by the addition of $\sim 5 \times 10^{12}$ molecules/cm^3 of SF_6. Nitric oxide and oxygen were found to have a similar effect; however, larger concentrations were needed to produce the same enhancement.

The dissociation of oxygen has been investigated by Elias et al. (13) and Kaufman and Kelso (14). The latter investigators examined the effects of Ar, He, H_2, N_2, NO, and N_2O as catalysts for the process. The nitrogen compounds were found to be especially effective, yielding 90 atoms of nitrogen per molecule of catalyst.

The yield of halogen atoms from a discharge is usually low because of the high recombination rate of these species. Ogryzlo (15), however, describes the successful dissociation of chlorine, bromine, and iodine by a microwave discharge when the walls of the discharge tube were poisoned to prevent recombination.

The best description of the chemical effects of a microwave discharge is due to McCarthy (16). His work covered the dissociation of hydrogen, nitrogen, and oxygen as well as the synthesis of nitric oxide from oxygen and nitrogen and the formation of acetylene from methane. The increase in yield per unit energy was found to correlate with two variables, α and β, as defined by

$$\alpha = \frac{E^2 p}{\tau Z_s} \qquad \beta = \frac{p Z_s}{E^2 t}$$

where E is the electric field strength, p, the pressure, Z_s, the shunt impedance of the discharge, t, the residence time in the discharge, and τ, the time of flight from the discharge to the point at which the free radical concentration is measured. The variable α was used to correlate the data on dissociation and β that on synthesis. Since the quantity E^2/Z_s is proportional to power, the results of McCarthy showed that as power was increased the yields per unit energy from dissociation increased, but those for synthesis decreased. For the synthesis of nitric oxide, a maximum of 0.75 moles/kwhr was obtained and for the synthesis of acetylene 1.3 moles/kwhr.

A study of the dissociation products of n-hexane passed through a microwave discharge carried out by Coates (17) showed 25 individual components to be present. It was postulated that the dissociation of n-hexane resulted from electron-molecule collisions and from thermal reactions in the discharge zone. The type of products isolated suggested that free radical reactions played an important role in the dissociation and product formation reactions. Over the range of 25 to 125 watts of microwave power, the product distribution was independent of input power.

Streitwieser and Ward (18) have examined the introduction of toluene vapor into a microwave discharge. The major products were benzene, ethylbenzene, styrene and phenlyacetylene. The authors concluded that, since only small amounts of the xylenes and biaryls were present, free radicals were not an important intermediate. Instead it was postulated that molecular anions, formed as a result of electron capture by the reactant, were responsible for the chemical activity. It was felt that had significant fragmentation occurred, tars and noncondensibles would have been observed.

In a more recent study of the dissociation of toluene in a radiofrequency discharge by Dinan (19), a different product distribution was reported from that presented by Streitwieser and Ward. In addition to benzene and ethylbenzene, significant amounts of bibenzyl, diphenylmethane, and biphenyl were observed. It was noted that the presence of the last three products indicates that free radicals are the major reaction intermediates. This particular study is of interest since it points to the possibility of observing a different product composition in a microwave and a radiofrequency discharge.

The formation of hydrocarbons from hydrogen and carbon monoxide in a microwave discharge has been reported by Blaustein and Fu (20). A non-flow reactor was used, consisting of a 20 or 36 cm long tube sealed at one end. The discharge was sustained in a five to one mixture of hydrogen to carbon monoxide at 10 cm from the sealed end. For reaction times of three minutes and longer, it was found that high yields of methane and acetylene were obtained, without the formation of polymers. When the bottom of the reactor was cooled, very large amounts of ethane were formed, but the presence of ethylene was never observed. These results stand in contrast to those of McTaggart (21) who studied the reaction in a flow system using a microwave discharge and a hydrogen to carbon monoxide ratio of 2.5. His observations showed that deposits of carbon were formed in addition to layers of a glassy, yellow polymer with an empirical formula $C_{25}H_{35}O$. The only gaseous products noted were water vapor and traces of carbon dioxide, formaldehyde, methane, and ethane.

In another study of the carbon monoxide-hydrogen system, Hollahan (22) found that a yellowish polymer was formed when mixtures of carbon monoxide, hydrogen, and nitrogen were passed through a radiofrequency discharge operating at 13.56 MHz. At low flow rates of nitrogen, the material occurred as a transparent, tightly adherent film. At higher nitrogen flow rates, the transparency decreased, the amount of nitrogen in the polymer increased, and the strength appeared to decrease. The formation of the polymer was noted to be pressure sensitive. Thus, at 0.3 Torr the polymer would form, but at ~ 1 Torr no polymer was observed.

In the area of sulfur chemistry, Emeleus and Tittle (23) have identified the decomposition products of sulfur hexafluoride in a microwave discharge. Reactions of these fluorides with chlorine in the discharge produced pentafluorosulfur chloride. Their reaction with oxygen led to sulfur oxide tetrafluoride and sulfuryl fluoride.

A recent report by Vastola and Stacy (24) shows that carbon disulfide and hydrogen are the major reaction products when methane or neopentane is added downstream from a radiofrequency discharge in hydrogen sulfide. Under conditions which minimize the back diffusion of the hydrocarbon into the discharge, substantially complete conversion of the hydrogen sulfide and hydrocarbon can be effected.

In the area of heterogeneous reactions, Blackwood and McTaggart (25) have produced oxygen atoms in a radiofrequency discharge and allowed these to impinge on carbon. Carbon monoxide and carbon dioxide are the only two products. A second example of the action of discharge products on carbon is given in the work of Vastola *et al.* (26). Their findings showed that atomic hydrogen reacting with carbon outside a microwave discharge gave negligible results, whereas, if the carbon was placed inside the discharge, small amounts of ethane, propyne, and 1-pentane were formed. An extensive reaction occurred between atomic oxygen and carbon when the carbon was either inside or outside of the discharge, carbon monoxide being the major product. The products of a water discharge reacted with carbon to give principally a hydrogen-carbon monoxide mixture.

The effect of driving frequency on the yield and distribution of products of a chemical reaction occurring in an electric discharge has been discussed in only one work appearing in the literature. Eremin _et al_. (_27_) studied the oxidation of nitrogen to nitric oxide in a discharge at 270 KHz and 50 Hz. For both frequencies the discharge was maintained between two steel electrodes contained within a quartz tube. The following observations were made:

1. A comparison of the yield of nitric oxide as function of the gas flow rate from a 270 KHz and a 50 Hz discharge, both operating at 180 Torr and 70 watts, showed that the high frequency discharge yielded three times as much nitric oxide as did the low frequency one.

2. As the power was varied at a constant pressure and flow rate, an inversion point was observed. At high powers the low frequency discharge was more effective, and at low power the high frequency form gave better results.

3. As the pressure was increased, the power at which the inversion point was observed shifted to lower powers.

4. A comparison of discharges at 270 KHz, 500 KHz, 700 KHz, and 1 MHz showed that identical quantities of nitric oxide were produced.

5. A study of the kinetics showed that the same kinetic expressions were applicable to both high and low frequency discharges.

6. A comparison of an electrodeless high frequency discharge, maintained by two external rings placed around the quartz tube, with a discharge at the same frequency sustained by electrodes showed that both discharges obeyed the same kinetic expression.

7. A comparison of the ultraviolet spectra from discharges operating at 500 KHz and 50 Hz showed no essential differences.

Since the kinetic mechanism did not appear to change with frequency or mode of excitation, it was postulated that the observed yields were solely a function of the electron temperature. It is felt that the last observation is probably a result of a change in the electric field distribution between the electrodes and not, as was proposed by Eremin et al., due to a direct functional relation between the electron temperature and the driving frequency.

A discussion of the interaction between electrons and molecules present in a discharge with relation to the oxidation of nitrogen has been treated by Vasil'ev (28). In this work an expression is derived for the rate at which electrons collide with gas molecules in a manner leading to a specific excitation. This relation has the form

$$r_j = 4.7 \times 10^{17} \frac{d^2}{\sqrt{\delta}} \frac{p}{T_g} J a_j e^{-\epsilon_j/kT_e}$$

where r_j is the rate of reaction j per unit volume, d, the diameter of the target molecule, δ, the fraction of its energy which an average electron looses on collision, p and T_g, the gas pressure and temperature, J, the discharge current density, ϵ_j, the excitation energy of the j-th level, a_j, a pre-exponential constant which is characteristic of the collision excitation function for the j-th process (29), and T_e, the electron temperature. The quantitites T_e and δ can both be determined from $E/p' = E/(p\ 293/T_g)$, the ratio of the electric field strength to the gas pressure evaluated at 293 °K. Thus once the relationship between E/p' and T_e and δ is known (see Chapter III), r_j can be evaluated, if the gas temperature and pressure, the electric field strength, and the current density are known. It is then proposed that the rate at which nitric oxide is produced is directly proportional to r_j so that

$$\frac{d(NO)}{dt} = \chi r_j$$

$$= k_j(T_e) \frac{Ip}{T_g}$$

where χ is the number of molecules of nitric oxide formed per j-th event, k_j is an equivalent reaction rate constant, and I is the discharge current. On the basis of this type of an expression, it is concluded that data on the formation of nitric oxide in a discharge might be correlated in terms of the product Ip.

A series of investigations by Mal'tsev, Eremin et al. (30) on the oxidation of nitrogen was carried out in a static system with a 50 Hz discharge maintained between two electrodes. Their results showed that for various discharge tube diameters and ratios of nitrogen to oxygen, the yield of nitric oxide could, in fact, be correlated with Ip for low values of this parameter. A semi-empirical expression for the concentration of nitric oxide in the products was derived in terms of a proposed kinetic scheme and the product Ip. This expression was found to fit the data but, again, only for low values of Ip. The partial success of this approach shows that the kinetics of the reaction do indeed depend on the variables which govern the rate of electron-molecule collisions.

C. Objective

The objective of the present work has been to investigate the occurrence of a chemical reaction in a radio-frequency electrodeless discharge. Of specific interest was an examination of the reaction under conditions such that it was rate limited. The data obtained under such conditions could be interpreted in terms of a reaction mechanism in which electron-molecule collisions are responsible for the formation of the active species. In this way it would be possible to determine the dependence of the over-all reaction rate and the consumption of energy per pound of product on the discharge variables.

As a second aim of the investigation, it was desired to determine whether a steady state conversion might be attained similar to that reached at equilibrium for thermal reactions. For this purpose, the rates of both the forward and the reverse reactions were studied. If a steady state did exist, then it would have to be examined in the light of chemical equilibrium extended to a multitemperature system.

Finally, it was desired to determine the amount of energy which is dissipated by each excitation process in the discharge. This information should shed light on the major sources of wasted energy and could provide insight on methods for reducing these losses.

The chemical reaction chosen for this study was the oxidation of hydrogen chloride, in which

$$4\ HCl + O_2 = 2\ Cl_2 + 2\ H_2O$$

From the standpoint of thermodynamics, this reaction is favored at low temperatures, but fails to proceed in the absence of a catalyst due to kinetic limitations. An investigation of this reaction by Cooper (31) in a microwave discharge revealed that up to 50% conversion could be obtained when a stoichiometric mixture of hydrogen chloride and oxygen was passed through the discharge at pressures between 4 and 40 Torr. An investigation was also made of the case in which only one of the reactants was discharged and the second one added downstream. These experiments showed that the dissociation of either hydrogen chloride or oxygen was sufficient to cause the reaction to proceed, the former being somewhat more effective. In the present work this reaction was carried out at 20 MHz using external ring electrodes to sustain a discharge in a quartz tube. The lower frequency was chosen for two reasons. First, it allowed a comparison to be made with the work done at the microwave frequency of 2450 MHz in order to determine what effects a severe reduction in frequency might have on the extent of reaction. The second reason for choosing the lower frequency was the ease with which the voltage across the discharge could be measured. This measurement provided a necessary piece of information for the discussion of the reaction kinetics. Such a measurement could not be made at the microwave frequency and, consequently, placed a limitation on the interpretation of the data taken at that frequency.

CHAPTER III

PHYSICAL CHEMISTRY OF AN ELECTRIC DISCHARGE

A. Transfer of Energy

In an electric gas discharge energy is transferred from the electric field by free electrons produced through partial ionization of the gas. This energy is in turn transferred to the atomic and molecular constituents of the gas by means of electron collisions with the heavier particles. As will be seen, it is during the second of these processes that chemical activation occurs.

Consider a single electron which is subjected to an oscillating electric field having a component only along the z axis

$$E = E_o \sin \omega t \qquad (1)$$

A force balance written on the directed motion of the electron will have the form

$$m \frac{dv}{dt} = - e E_o \sin \omega t - mv \nu_m \qquad (2)$$

where v is the directed or drift velocity of the electron brought about by the action of the field, ν_m, the frequency of elastic collisions between electrons and gas molecules, m and e, the mass and charge of the electron. Integration of equation (2) gives

$$v = -\frac{eE_o}{m}\frac{(\nu_m \sin \omega t - \omega \cos \omega t + \omega)}{(\nu_m^2 + \omega^2)} \qquad (3)$$

The work done on the electron in the time increment dt is

$$dW = F\, vdt \qquad (4)$$

$$= -e\, E_o \sin(\omega t)\, v\, dt$$

Substituting equation (3) into equation (4) and integrating from t = 0 to t = $2\pi/\omega$ yields an expression for the work done on the electron in the period of a cycle

$$W = \frac{e^2\, E_o^2\, \pi\, \nu_m}{m\omega(\omega^2 + \nu_m^2)} \qquad (5)$$

The rate at which work is done, i.e., the power, can be obtained by dividing W by t = $2\pi/\omega$, yielding

$$P = \frac{e^2\, E_o^2}{2m\, \nu_m}\left(\frac{\nu_m^2}{\omega^2 + \nu_m^2}\right) \qquad (6)$$

For a discharge in which there are n_e electrons per unit volume, the rate at which energy is absorbed from the field per unit volume will be given as

$$\overline{P} = \frac{n_e e^2 E_o^2}{2m \nu_m} \left(\frac{\nu_m^2}{\omega^2 + \nu_m^2}\right) \qquad (7)$$

It should be noted that if ν_m were zero in equation (7), the electrons would not absorb energy from the electric field. This can be explained physically in the following terms. An electron free from collision will oscillate in an electric field ninety degrees out of phase with the electric field. Under this condition, the electron will absorb and radiate power to an equivalent extent over the period of a cycle. As a result no net power will be absorbed. When elastic collisions are allowed to occur, the phase of the electron velocity with respect of the field is randomized, and work is done as the field attempts to re-establish a collision-free oscillatory motion.

The current density through the plasma can be obtained from the expression

$$\overline{P} = J E_{eff} \qquad (8)$$

where J is the current density and $E_{eff}^2 = \frac{E^2}{2} \left(\frac{\nu_m^2}{\omega^2 + \nu_m^2}\right)$. Substituting equation (7) into equation (8) gives

$$J = n_e e \left[\frac{eE}{m \nu_m \sqrt{2}} \left(\frac{\nu_m^2}{\omega^2 + \nu_m^2} \right)^{1/2} \right] \qquad (9)$$

The factor in the square brackets represents the time averaged drift velocity v_d so that equation (9) can be rewritten as

$$J = n_e e v_d \qquad (10)$$

At this point it should be noted that in the derivation of the power density $\overline{P}$, two important simplifying assumptions have been made. The first is that the elastic collisions are perfectly elastic so that no energy is lost by the electron to the target molecule, and the second is that ν_m is independent of electron energy. Both of these assumptions are idealizations. In fact, a small amount of energy is lost to the target when an electron experiences an elastic collision. The fraction of the initial electron energy which is lost is given by 2m/M where m is the mass of the electron and M is the mass of the target. Again, with the exception of helium and hydrogen, ν_m is usually a function of energy. Consequently, a value for ν_m obtained by averaging over electron energy should be used.

The energy absorbed by the electrons is in turn lost through elastic and inelastic collisions. A discussion of this topic will be given in the next section. At this point it is important to point out that ionization provides a source of new electrons to replace those lost by diffusion from the bulk of the plasma. The electrons which diffuse subsequently recombine with positive ions on the walls of the container. A steady state electron density is achieved when the rates of production and loss balance.

At steady state the spatial distribution of electrons is determined by solution of the continuity equation. The solution for the particular situation in which diffusion and bulk gas flow are simultaneously responsible for electron movement has been presented by Romig (32). The geometry which was considered is shown in Figure 4. Ionization is assumed to occur only in the control volume of length 2L, and the electric field is assumed to be uniform and directed axially. An illustration of the axial distribution as well as the analytic form of the solutions is shown in Figure 4. The radial distribution is given by a zero order Bessel function and is independent of the axial coordinate z. The axial distribution, on the other hand, is symmetric about the center of the discharge for low flow rates, but shifts downstream as the flow rate is increased.

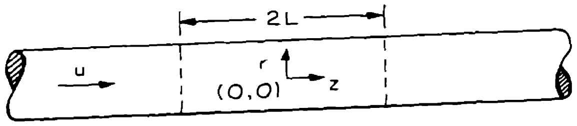

$$-z^* \geq -1 \quad \frac{n_e}{n_{e\max}} = J_0(2.405\, r^*)\, \frac{\Lambda \phi}{L \cos \phi z_0^x}\, \exp\left[\beta(z^* - z_0^*) + \alpha(z^* + 1)\right]$$

$$-1 \leq z^* \leq 1 \quad \frac{n_e}{n_{e\max}} = J_0(2.405\, r^*)\, \frac{\exp\left[\beta(z^* - z_0^*)\right]}{\cos \phi z_0^*}\, \cos \phi z^*$$

$$-z^* \geq 1 \quad \frac{n_e}{n_{e\max}} = J_0(2.405\, r^*)\, \frac{\Lambda \phi}{L \cos \phi z_0^*}\, \exp\left[\beta(z^* - z_0^*) + \alpha(1 - z^*)\right]$$

$z^* = z/L$

$r^* = r/R$

$K = 2.405\, L/R$

$\alpha = (K^2 + \beta^2)^{1/2}$

$\beta = uL/D$

$z_0^* = \tan^{-1}(\beta/\phi)/\phi$

$\phi = (L^2/\Lambda^2 - \alpha^2)^{1/2}$

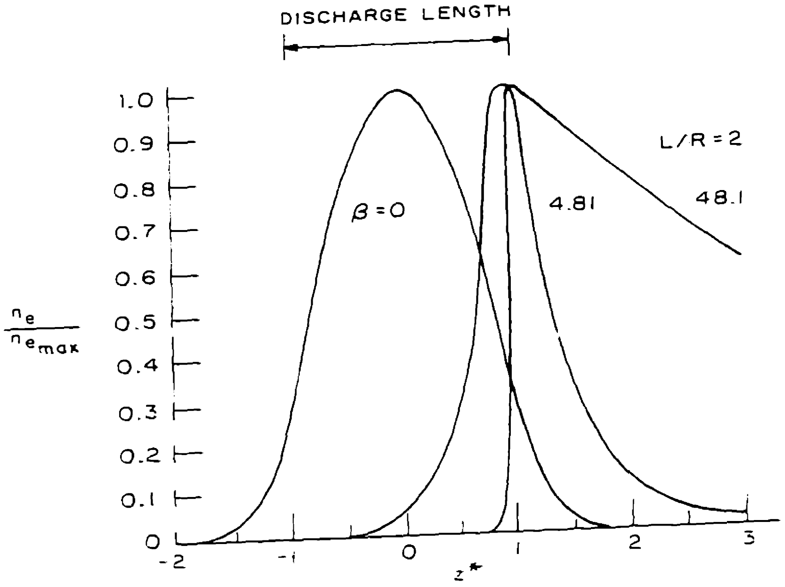

FIGURE 4 ELECTRON DENSITY DISTRIBUTION

The quantity Λ appearing in the equations shown in Figure 4 is called the diffusion length and is a measure of the distance an average electron will travel in a volume before it produces one new charged particle. For a closed cylinder of radius a and length 2L, Λ_c is given by

$$1/\Lambda_c^2 = (\pi/2L)^2 + (2.405/a)^2 \qquad (11)$$

For an open cylinder with $L/a > 8$ and flow Λ is given by

$$1/\Lambda^2 = 1/\Lambda_c^2 + (u/2LD)^2 \qquad (12)$$

where u is the average linear velocity and D is the electron diffusion coefficient.

Brown and MacDonald (33) have shown that all the data on breakdown field strengths for high frequency discharges may be characterized by Λ, ω, and p. This theory has been extended by Rose and Brown (34) to the description of the field necessary to maintain a discharge at any electron density. The results were obtained from a solution of the Boltzmann transport equation under the following assumptions: the electric field strength in the volume considered is spatially uniform; ionization of gas molecules provides a source of new molecules; diffusion of electrons to the container walls and subsequent recombination there provides the only sink for electrons. Figure 5 illustrates the theoretical solution obtained for hydrogen.

For a particular discharge container and gas flow rate, Λ becomes fixed, and lines of constant pressure can be plotted on Figure 5. The intersection of an isobaric line with the line $n_e\Lambda^2 = 0$ represents conditions at breakdown, and the breakdown field strength can be determined from this point. As the electron density increases, lower values of E_{eff} are obtained if a constant pressure is maintained. The value of E_{eff} does not decrease indefinitely for large values of $n_e\Lambda^2$, but instead approaches an asymptotic value. Experimental verification of this behavior is provided by Lathrop (35).

B. Dissipation of Energy

Four types of electron-molecule collisions lead to the dissipation of the energy absorbed by the electrons. These include elastic collisions in which energy is transferred to the translational mode of the target molecule and inelastic collisions which lead to free radical formation, ionization,and excitation to radiative levels. The degree to which any one of these channels is favored is determined by the electron temperature T_e.

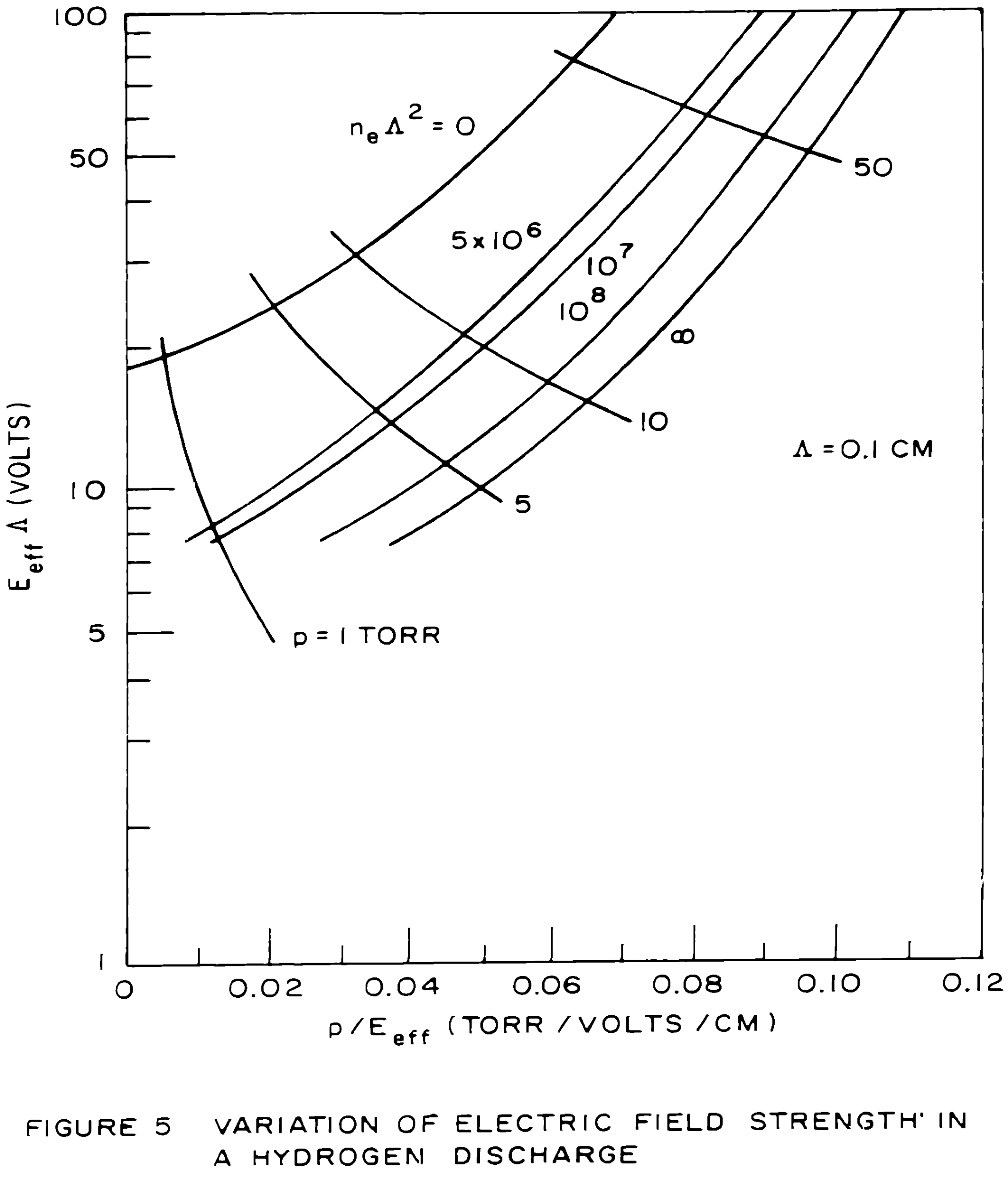

FIGURE 5 VARIATION OF ELECTRIC FIELD STRENGTH IN A HYDROGEN DISCHARGE

The electron temperature T_e is a difficult quantity to measure experimentally, and hence it becomes desirable to establish a relationship between T_e and a more readily measurable experimental variable. This may be done by writing an energy balance between the average energy an electron gains between collisions and the average energy which will be dissipated in the next collision. This leads to

$$\frac{e^2 E_{eff}^2}{m \nu_m} = \delta \frac{3}{2} kT_e \qquad (13)$$

For ν_m we can substitute the approximate expression

$$\nu_m = \bar{v}_r N \bar{Q} \qquad (14)$$

where $\bar{v}_r$ is the average random electron velocity equal to $\sqrt{\frac{8}{\pi} \frac{kT_e}{m}}$, N, the gas density, and $\bar{Q}$, the average elastic collision cross section. Substitution of equation (14) into equation (13) gives

$$(\frac{12}{\pi})(kT_e)^2 \delta = \frac{e^2 E_{eff}^2}{N^2 \bar{Q}^2} \qquad (15)$$

Using the perfect gas law, the gas density may be expressed as

$$N = \frac{6.02 \times 10^{23}}{2.24 \times 10^{4}} \frac{293}{760} \frac{p}{T_g} \qquad (16)$$

where T_g and p are the gas temperature and pressure in the discharge. Equation (15) then becomes

$$T_e = 1.43 \times 10^{-17} \frac{e}{\bar{Q}\ k} \frac{1}{\delta^{1/2}} \frac{E}{p'} \sqrt{\frac{\pi}{3}} \qquad (17)$$

where $p' = p\ 293/T_g$. Thus T_e can be expressed as a function of E_{eff}/p' and δ which is also a function of T_e. Figure 6 illustrates the experimentally determined curves of T_e versus E/p' for hydrogen chloride, oxygen, water, and chlorine. For a discussion of the experimental technique used in determining these curves, see Appendix D.

The total energy transferred by the electrons to the molecules is given by

$$n_e \bar{\epsilon} = n_e\ \delta\ \frac{3}{2}\ kT_e \qquad (18)$$

This transferred energy is shared over all the possible loss mechanisms. Vasil'ev (36) gives a convenient form for the energy balance which ensues

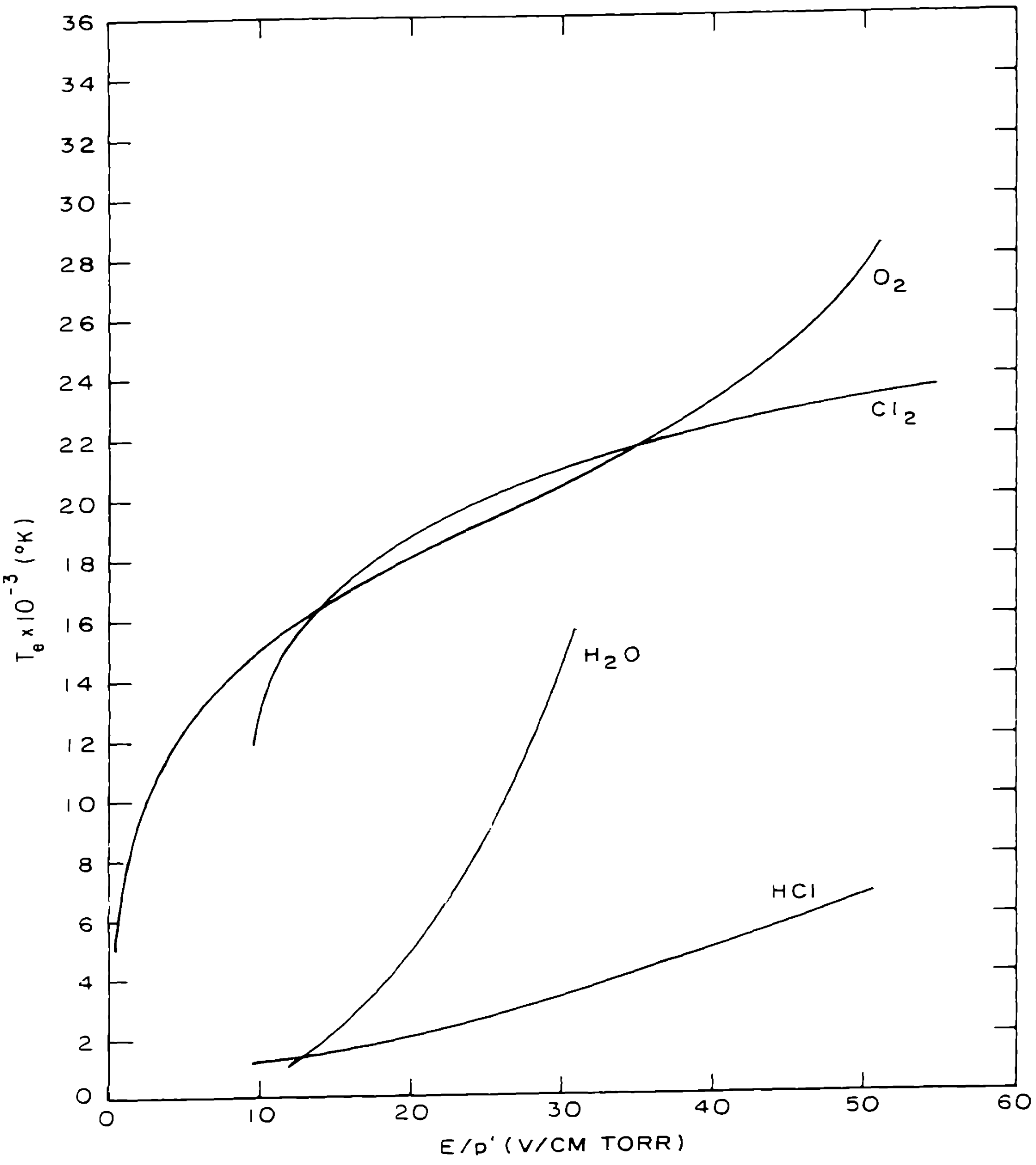

FIGURE 6 ELECTRON TEMPERATURE VERSUS E/p'

$$\bar{\epsilon} = \epsilon_u + \sum_j a_j \epsilon_j e^{-\epsilon_j/kT_e} + \frac{3}{2} kT_e a_+ e^{-\epsilon_+/kT_e} \tag{19}$$

where $\epsilon_u = \frac{2m}{M} \frac{3}{2} kT_e$ is the energy lost at each elastic collision, ϵ_j, the energy of the j-th excitation level, a_j, a pre-exponential factor determined by the characteristics of the excitation cross section for the j-th level (29), a_+ and ϵ_+ correspond to the pre-exponential factor and the energy for ionization. The last term in the balance accounts for the energy that a newly created electron must absorb in order to come to equilibrium with the rest of the free electrons. Substitution of equation (19) into equation (18) shows that δ is solely a function of T_e. Figure 7 shows values of δ versus T_e for hydrogen chloride, oxygen, water, and chlorine.

The fraction of the total energy transferred which goes towards a particular excitation process is given by

$$\Delta_j = \frac{\epsilon_j a_j e^{-\epsilon_j/kT_e}}{\bar{\epsilon}} \tag{20}$$

$$= \frac{\epsilon_j a_j e^{-\epsilon_j/kT_e}}{\delta \frac{3}{2} k T_e}$$

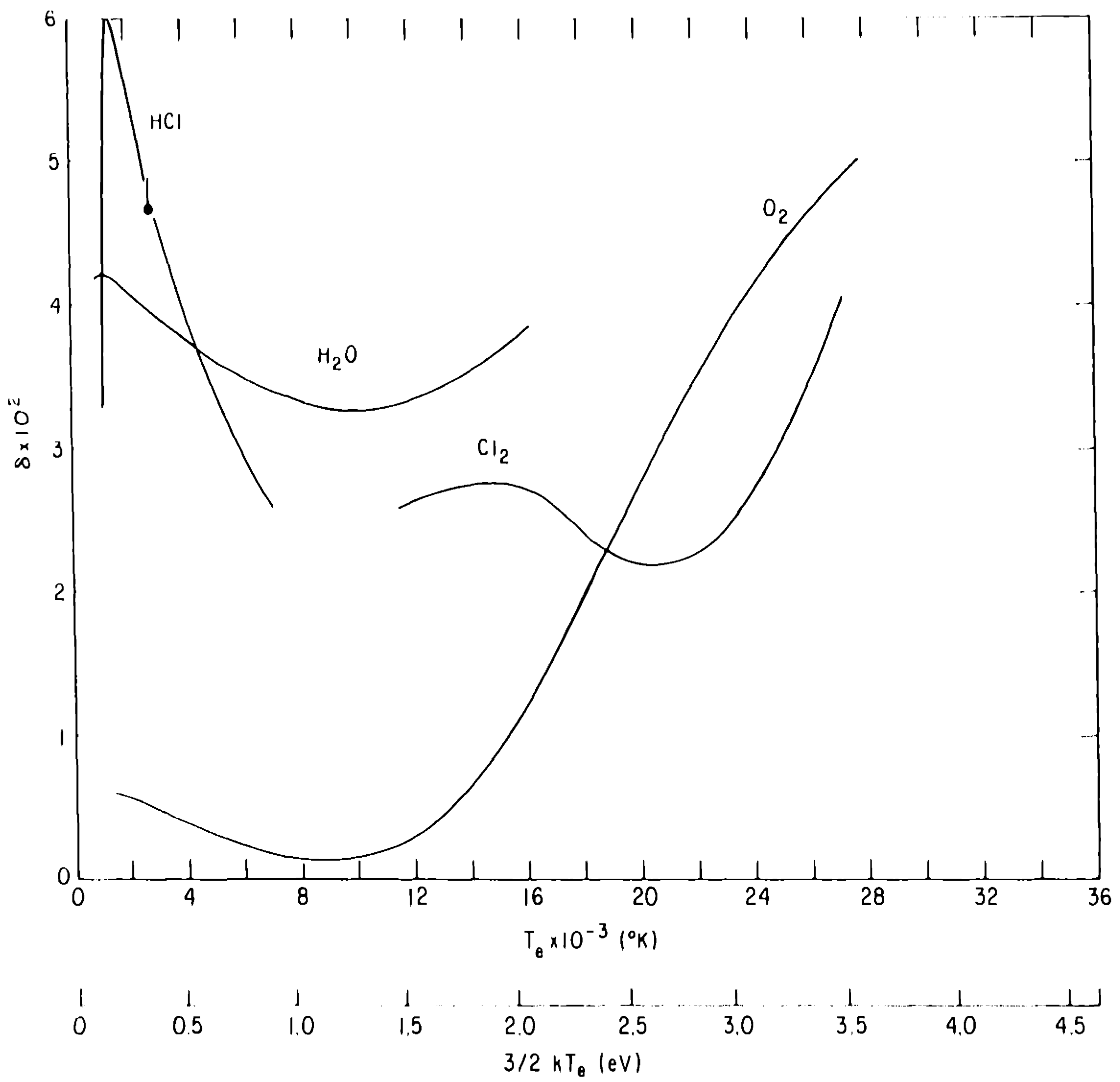

FIGURE 7 FRACTIONAL ENERGY LOSS PER COLLISION VERSUS ELECTRON TEMPERATURE

Thus Δ_j is also simply a function of T_e. But since $T_e = f(E/p')$ for a particular gas, this implies that the distribution of transferred energy is determined by E/p' alone.

A theoretical evaluation of the fractional distribution of energy in a hydrogen discharge used for the production of hydrogen atoms was made by Lunt and Meek (37). The results of their calculations are shown in Figure 8. Four loss mechanisms were investigated: loss through elastic collisions; dissociation, the curves marked $^3\Sigma_u$ and $^3\Sigma_g$; excitation to a radiative level, the curve marked $'\pi_u$; and ionization. It should be noted that elastic collision losses decrease sharply as E/p' is raised. This means that a smaller and smaller fraction of the total energy is being used to heat the gas. On the other hand, the curves for the dissociation of hydrogen each pass through a maximum. This type of behavior indicates that an optimum value of E/p' exists at which the energy usage towards the formation of hydrogen atoms is maximized. If the two dissociation curves in Figure 8 are summed, this leads to a curve with a maximum at E/p' = 30 V/cm Torr. An experimental verification of this prediction was carried out by Poole (8) who observed a maximum yield of atomic hydrogen per unit of energy supplied to the positive column of a d.c. glow discharge at an E/p' = 30 V/cm Torr.

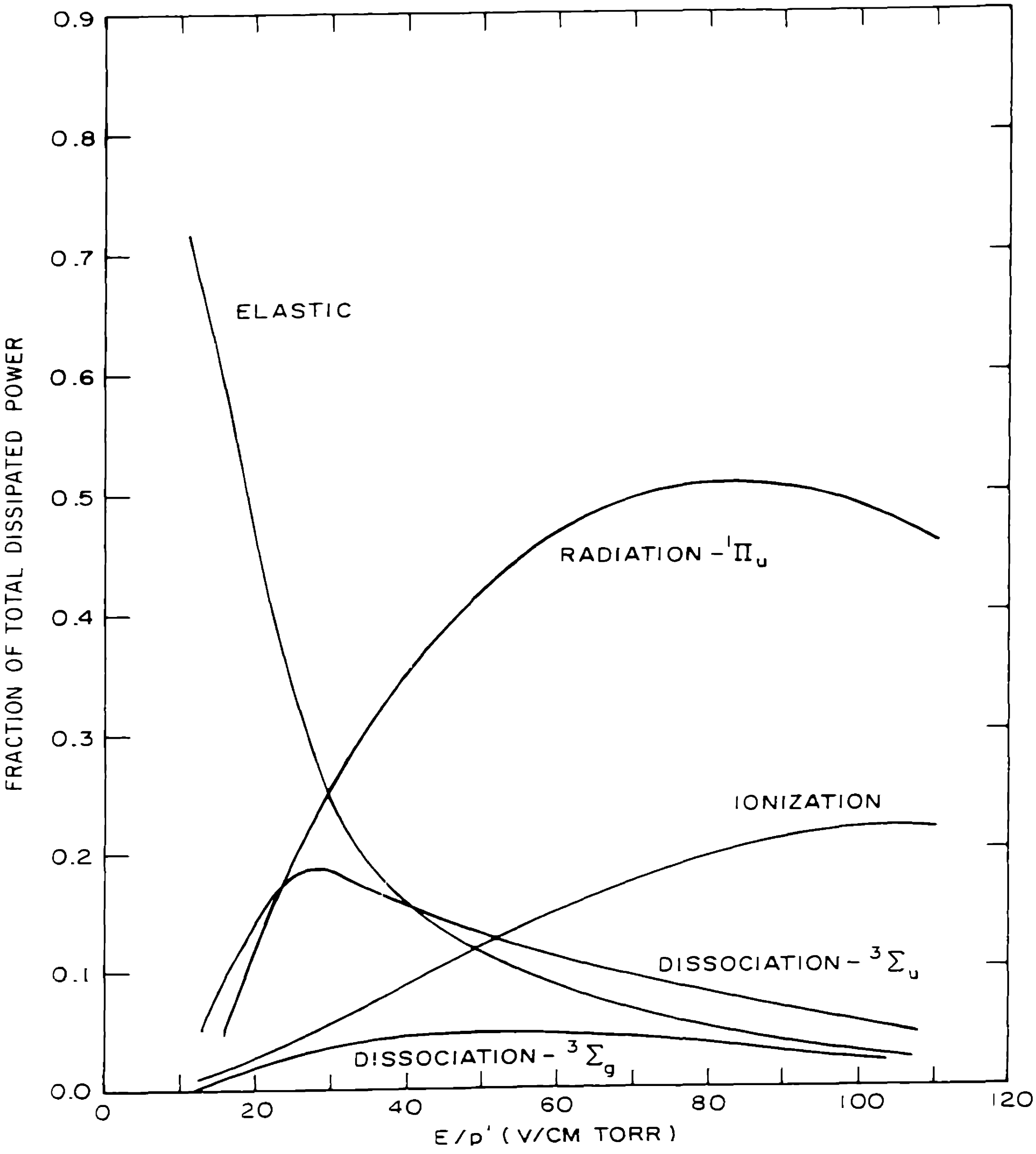

FIGURE 8 DISTRIBUTION OF DISSIPATED POWER IN HYDROGEN

An equivalent maximum value for the atomic yield per unit energy was obtained by Shaw (7) working with a microwave discharge in hydrogen.

From this evidence it can be seen that the electron temperature is the parameter which determines the efficiency of energy usage towards a specific collisional process. Thus a chemical reaction which depends on a free radical precursor should give its highest yields per unit energy supplied to the discharge at the electron temperature which gives the highest yields per unit energy of the necessary free radical. In addition to determining the distribution of transferred energy, the electron temperature should also affect the rate at which free radicals are formed due to electron-molecule collisions. Consequently, those chemical reactions which are rate limited by the formation of free radicals should show a rate dependence on electron temperature when carried out in a discharge.

CHAPTER IV

APPARATUS

A. General Description

The experimental apparatus as shown in Figure 9 consists of three separate systems: an electrical system for the supply of radiofrequency power and the measurement of the voltage across the discharge; a gas handling system for the supply of the reactants and the collection of products; a heat exchange loop for cooling the reactor and for measuring the total power dissipated in the discharge. In order to study the reverse reaction, a separate device is included which provides a constant flow of water vapor. The experimental variables which could be measured were the r.f. power, the voltage across the discharge, the total gas pressure, and the reactant flow rates.

B. Electrical System

Radiofrequency power for the discharge was provided by a Lepel Model T-2.5-1-MC1-J-B generator operating at 20 MHz and capable of supplying a 2 kw. Power from the generator was coupled to the discharge through a transformer consisting of two coils mounted concentrically one inside the other. The outer coil acted as the primary of the transformer and also served as the tank coil for the oscillator circuit in

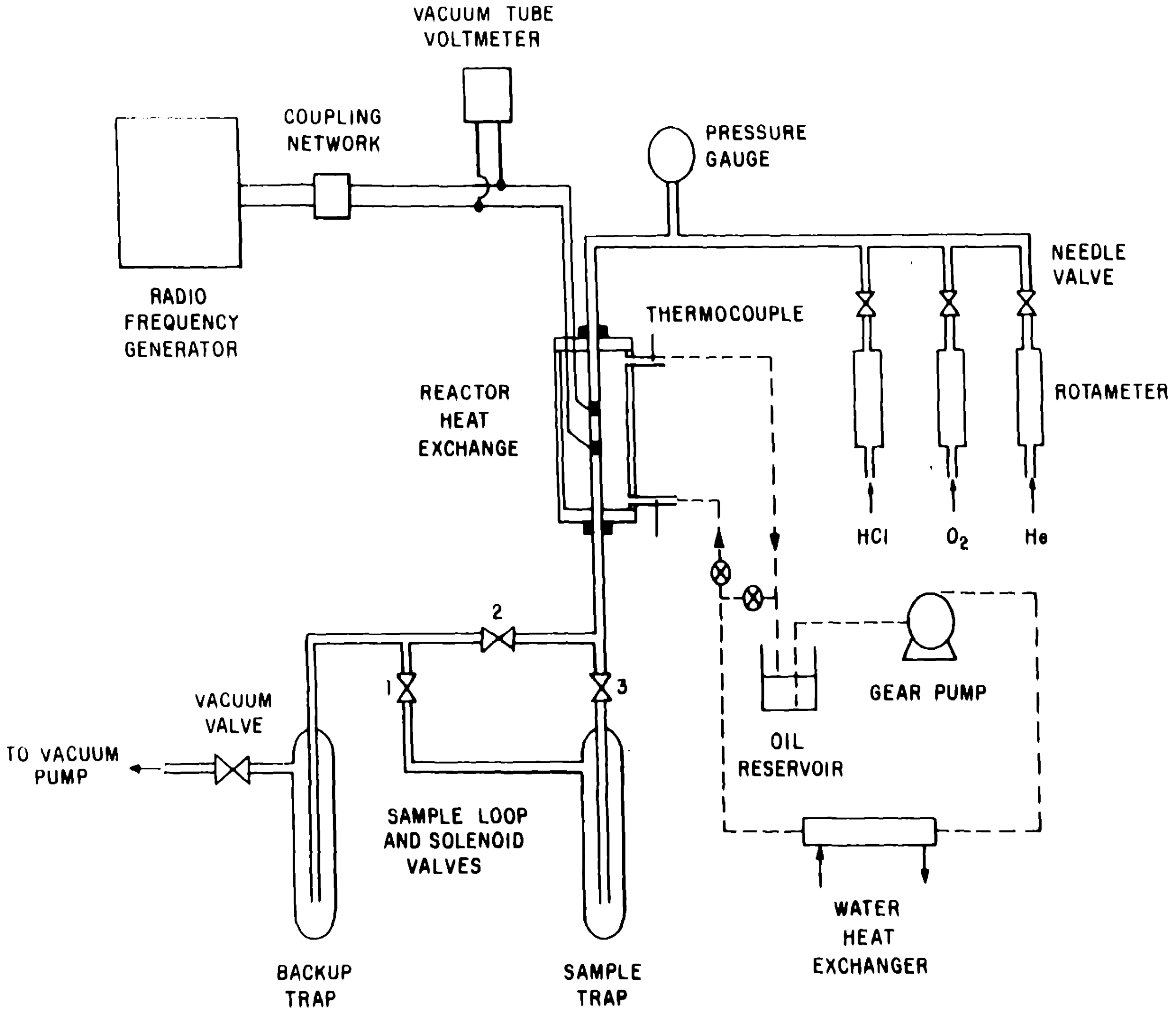

VACUUM TUBE VOLTMETER
COUPLING NETWORK
PRESSURE GAUGE
NEEDLE VALVE
RADIO FREQUENCY GENERATOR
THERMOCOUPLE
REACTOR HEAT EXCHANGE
ROTAMETER
HCl
O_2
He
2
1
3
GEAR PUMP
VACUUM VALVE
TO VACUUM PUMP
OIL RESERVOIR
SAMPLE LOOP AND SOLENOID VALVES
WATER HEAT EXCHANGER
BACKUP TRAP
SAMPLE TRAP

FIGURE 9 SCHEMATIC OF APPARATUS

the generator. The inner coil which acted as the secondary was connected to two copper sleeve electrodes on the outside of the discharge tube.

The voltage applied across the electrodes was measured with a vacuum tube voltmeter designed specifically for operation at high voltages (see Figure 10). The voltage is applied between the plate of the diode and ground. Since the voltage drop across the tube is small, the capacitor charges up to the peak voltage of the signal. This d.c. voltage is then measured by the d.c. voltmeter. The capacitor and choke in the filament supply to the diode prevent possible feedback of r.f. high voltage to the filament transformer.

C. Gas Handling System

The gas feed for the reaction was delivered from a manifold made of 3/8 inch o.d. polyethylene tubing and 3/8 inch Monel Swagelok fittings. Oxygen, hydrogen chloride, and helium could be fed to the manifold. The flow rate of each of these gases was measured by a Matheson 600 series rotameter and controlled by a stainless steel Nupro fine metering valve placed upstream from the rotameter. The inlet pressure of each gas was maintained at slightly above atmospheric as registered by a mercury manometer.

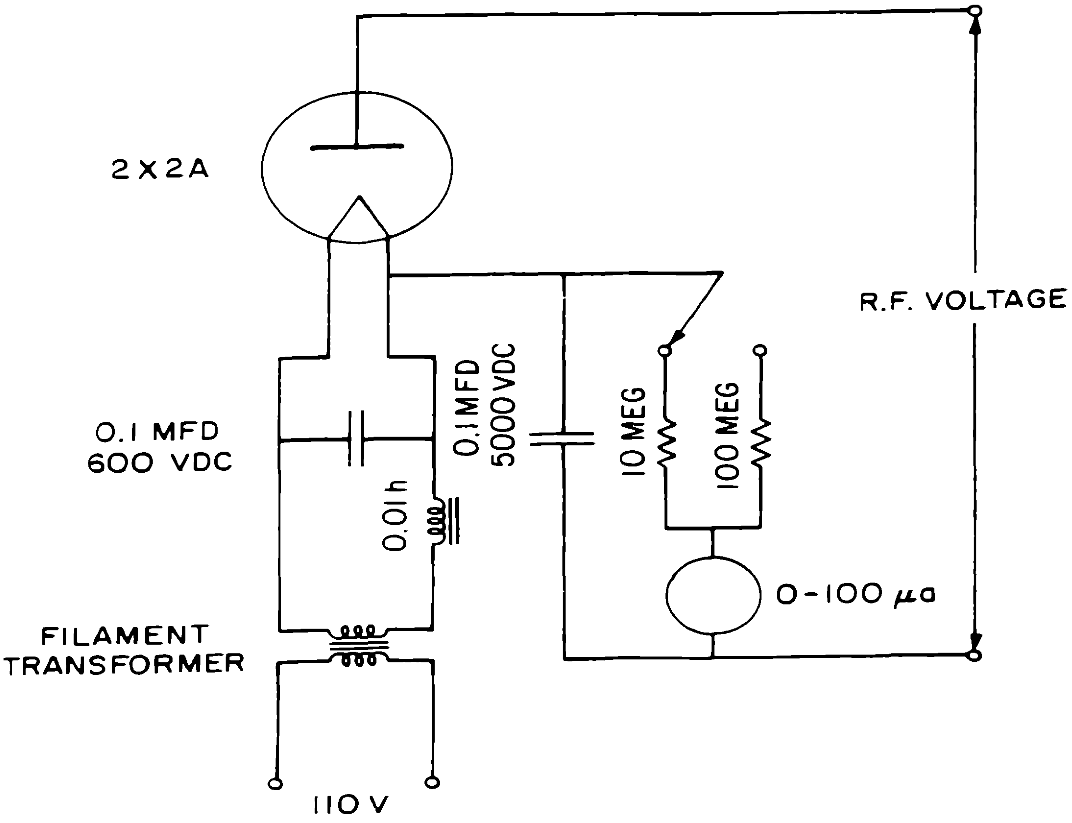
2 X 2A
R.F. VOLTAGE
0.1 MFD
600 VDC
0.1 MFD
5000 VDC
10 MEG
100 MEG
0.01 h
0-100 μa
FILAMENT
TRANSFORMER
110 V

FIGURE 10 CIRCUIT DIAGRAM OF VACUUM TUBE VOLTMETER

A Wallace and Tiernan Model No. FA 141 pressure gauge with a range of 0 to 75 inches of water was used to measure the total gas pressure. The design of this gauge allowed the corrosive mixture to be introduced inside the barometric box and a vacuum to be applied to the case. In this manner the corrosive gas never came in contact with the delicate mechanism inside the case. Unfortunately this design is only available with a calibration in inches of water. All subsequent reports of pressure, however, have been converted to Torr.

The vacuum was produced by a high capacity Kinney vacuum pump. Fine control of the pressure was obtained by use of a 5/8 inch orifice vee stem valve equipped with micrometer threads.

Gaseous products leaving the reactor were trapped in a 19 mm diameter pyrex cold trap immersed in liquid nitrogen at 77 °K. By appropriate switching of the three Asco solenoid valves, the product stream could be made to either pass through the sample trap or bypass it. A second liquid nitrogen trap assured the collection of the gas stream when the sample trap was bypassed and protected the vacuum pump from corrosion.

D. Discharge Tubes

Two discharge tube designs were used in the course of the chemical studies. The first of these consisted of a 12 mm outside diameter quartz tube 61 cm in length. Two copper sleeves, each 2 cm long, could be slipped on the outside of the tube and acted as electrodes. This particular electrode geometry was chosen in order to simulate the axial electric field distribution which was present in the microwave studies of Cooper (31). In the present study no attempts were made to determine what effect a change in the electrode geometry might have on the extent of chemical conversion. The second design, illustrated in Figure 11, was used in the separated feed studies. One of the reactants passed through the central tube and through the discharge zone. The second reactant could then be introduced directly below the discharge zone. The holes in the side of the tube were kept as small as possible so that the second gas could enter at a high velocity and assure good mixing.

A separate discharge tube was constructed for operating a 60 Hz discharge between two cylindrical electrodes. The tube, which is shown in Figure 11, was made of Corning 7052 glass and the electrodes of Kovar. The inner surface of the Kovar electrodes was plated with a 0.0002 inch film of platinum. A quartz thermowell was included so that the

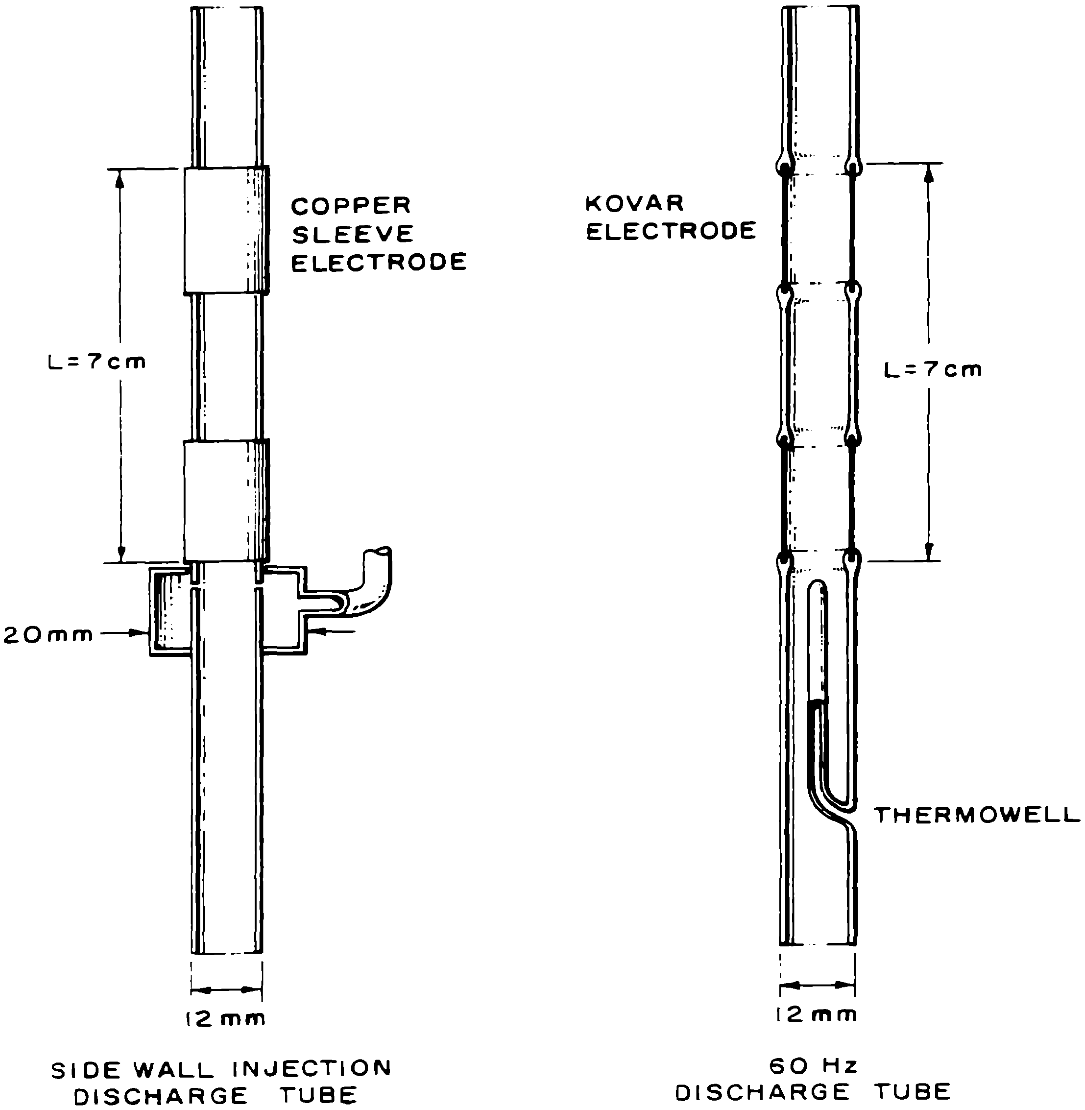
COPPER SLEEVE ELECTRODE
L = 7cm
20mm
12 mm
SIDE WALL INJECTION DISCHARGE TUBE
KOVAR ELECTRODE
L = 7cm
THERMOWELL
12 mm
60 Hz DISCHARGE TUBE

FIGURE 11 DISCHARGE TUBES

gas temperature at the base of the discharge could be measured with a thermocouple.

E. Heat Exchange Loop

A Lucite heat exchanger, illustrated in Figure 9, was placed around the reaction tube in order to cool the walls of the tube and to measure the total power dissipated in the discharge. A description of its latter function will be found in the next chapter. Bayol 35, a paraffinic petroleum distillate marketed by Esso, was used as the heat exchange fluid. This material is non-polar and consequently does not absorb power from the r.f. field. The oil leaving the reactor heat exchanger was in turn heat exchanged with cold water and returned via a constant displacement gear pump. A portion of the flow from the pump could be made to bypass the reactor heat exchanger, and this technique was used to regulate the oil flow rate to the latter. Two metal encased iron-constantan thermocouples were used to measure the temperature difference across the reactor heat exchanger.

F. Water Injection System

In order to study the reverse reaction, it was necessary to feed water vapor as one of the reactants. This was achieved with the apparatus shown in Figure 12. Distilled water is displaced from the syringe at a uniform rate by a

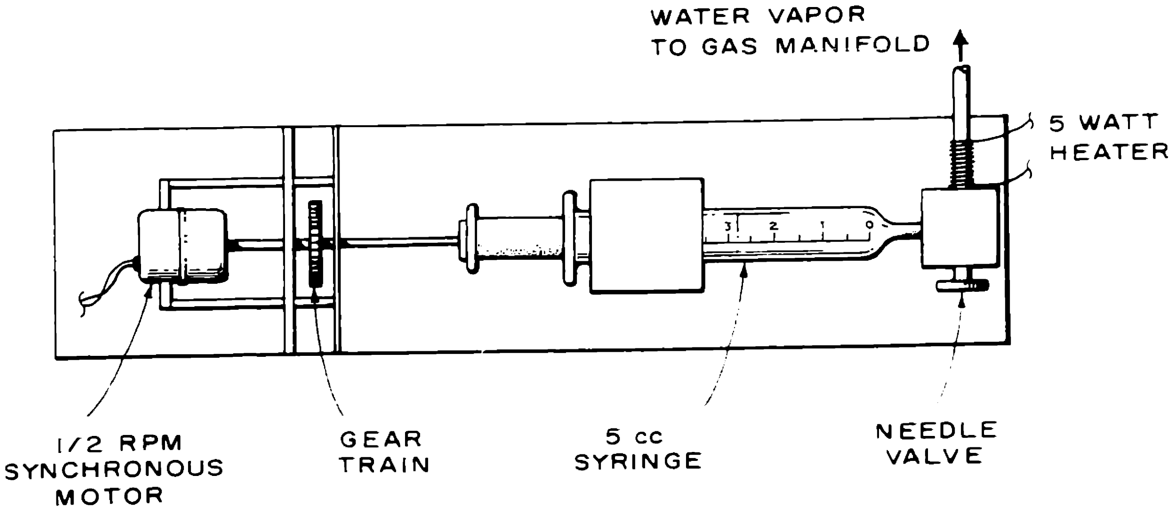
WATER VAPOR
TO GAS MANIFOLD
5 WATT
HEATER
3
2
1
0
1/2 RPM
SYNCHRONOUS
MOTOR
GEAR
TRAIN
5 cc
SYRINGE
NEEDLE
VALVE

FIGURE 12 APPARATUS FOR FEEDING WATER VAPOR

synchronous motor which drives the piston, through a set of gears. The liquid water is then vaporized across the very fine orifice in the needle valve. A small 5 watt heater wrapped around the valve assures that the heat of vaporization is supplied and that ice does not form in the valve. In this manner liquid flow rates of 0.04 ml/min could be achieved.

CHAPTER V

PROCEDURE

A. Mixed Feed

To begin an experimental run the solenoid valves to the sample trap were opened, and the gas manifold, discharge tube, and traps were evacuated. At this point the sample trap was lowered into a Dewar containing liquid nitrogen. Helium was then introduced from the manifold and the pressure brought up to the value desired for a particular run. The r.f. generator was turned on, and a discharge was initiated in the volume between the electrodes by using a Tesla coil. After about 10 minutes the valves to the sample trap were closed, and the reactant gases were introduced at the same time as the helium flow was gradually shut off. When the desired reactant flow rates and pressure had been established, the power control setting on the generator was increased till the voltage across the electrodes attained the desired level. The solenoid valves to the sample trap were then opened, and the reaction products were collected as a solid at liquid nitrogen temperature. The collection time was determined so that the solid when vaporized would produce a pressure of one atmosphere or less in the volume of the trap. At the end of the collection time, the sample trap was again isolated from the vacuum system, and the gas manifold was evacuated in order to remove any traces of the reactants. Finally with the valve to the vacuum pump closed off, the gas system and sample trap were brought up to one atmosphere by backfilling with helium. The trap was then disconnected from the gas system, stoppered, and carried, while still in the Dewar, to the analysis equipment.

Chemical analysis of the reaction products was done by gas chromatography using a twelve foot stainless steel column 1/4 inch in diameter filled with 30-60 mesh Haloport-F (a Teflon-6 material sold by the F & M Corp.) on to which had been deposited a 10% loading of D.C.-11 silicone grease. The column was used in a Model 154 Perkin Elmer chromatograph operating at 35 °C with a helium carrier gas flow rate of 1.14 cm^3/sec. This arrangement allowed for the separation of hydrogen chloride and chlorine.

The analysis procedure was begun by connecting one end of the sample trap to a vacuum manifold and placing a septum over the other end. The septum was made by drilling a hole to within 1/8 inch of the end of a solid rubber stopper. With the trap still under liquid nitrogen, the backfill of helium was pumped off. The line to the vacuum pump was then closed off and the trap removed from the Dewar. As the solid vaporized, the progress of the vaporization was observed by the increase in pressure shown by a manometer. When the pressure was within 80% of one atmosphere, the trap was lowered into an ice bath. This part of the procedure ensured that the water collected as one of the products did not vaporize. This was desired since a water peak would have eluted in the small space between the hydrogen chloride and chlorine peaks, thereby ruining the resolution of these two peaks. After all the product material, except the water, had vaporized the final trap, pressure was adjusted to one atmosphere by bleeding in helium from a carrier gas tank. Aliquots of 0.15 to 0.25 cm^3 in size were drawn from the trap with a syringe, inserted through the septum, and injected into the chromatograph.

B. Separated Feed

Under conditions in which only one of the reactants was passed through the discharge and the second one added downstream, the procedure for the runs and the subsequent analysis remained the same as that for mixed reactants feeds. The distance between the lower edge of the bottom electrode and the point of introduction of the second gas was always maintained at one centimeter.

C. Measurement of Power Consumption

The power dissipated in the discharge was measured by using the reactor heat exchanger as a calorimeter. Preliminary studies showed that the entering and exiting gas temperatures were about equal. Consequently, all the electrical energy consumed by the plasma is either transferred to the cooling oil or escapes as visible light. Although no measurement of the flux of radiation in the visible range was made, it is not felt that this represents a significant part of the total energy. The temperature increase in the oil is due to the energy dissipated by the discharge plus a small amount of energy released by the exothermic forward reaction. The latter amounts to about 2% of the total measured power. Hence, from a knowledge of the oil properties, the oil flow rate, and the temperature difference across the heat exchanger, the power dissipated in the discharge can be calculated. A sample of this calculation appears in Appendix A.

CHAPTER VI

RESULTS

A. Mixed Feed

1. Forward Reaction

The effect of power supplied to the discharge on the conversion of hydrogen chloride to chlorine was investigated over the pressure range of 3.75 to 22.50 Torr. The data are shown in Figures 13 and 14 as percent conversion of hydrogen chloride as a function of power for a constant molar flow rate of 7.40×10^{-5} moles/sec and an oxygen to hydrogen chloride ratio equal to 0.25.

For each curve the conversion at a constant pressure at first increases with power to a maximum and then proceeds to decrease very gradually. The maximum in the conversion is more noticeable at low pressures and is seen to broaden as the pressure is raised. Concurrent with the broadening of the maximum there is a shift of its position to higher power. At a constant power the conversion at first increases with pressure but then begins to gradually decrease as the pressure is raised above 11.25 Torr.

Figures 15, 16, and 17 illustrate the effect of decreasing the total molar flow rate while maintaining an oxygen to hydrogen chloride ratio equal to 0.25. At a pressure of 3.75 Torr the effect of decreasing the molar flow rate

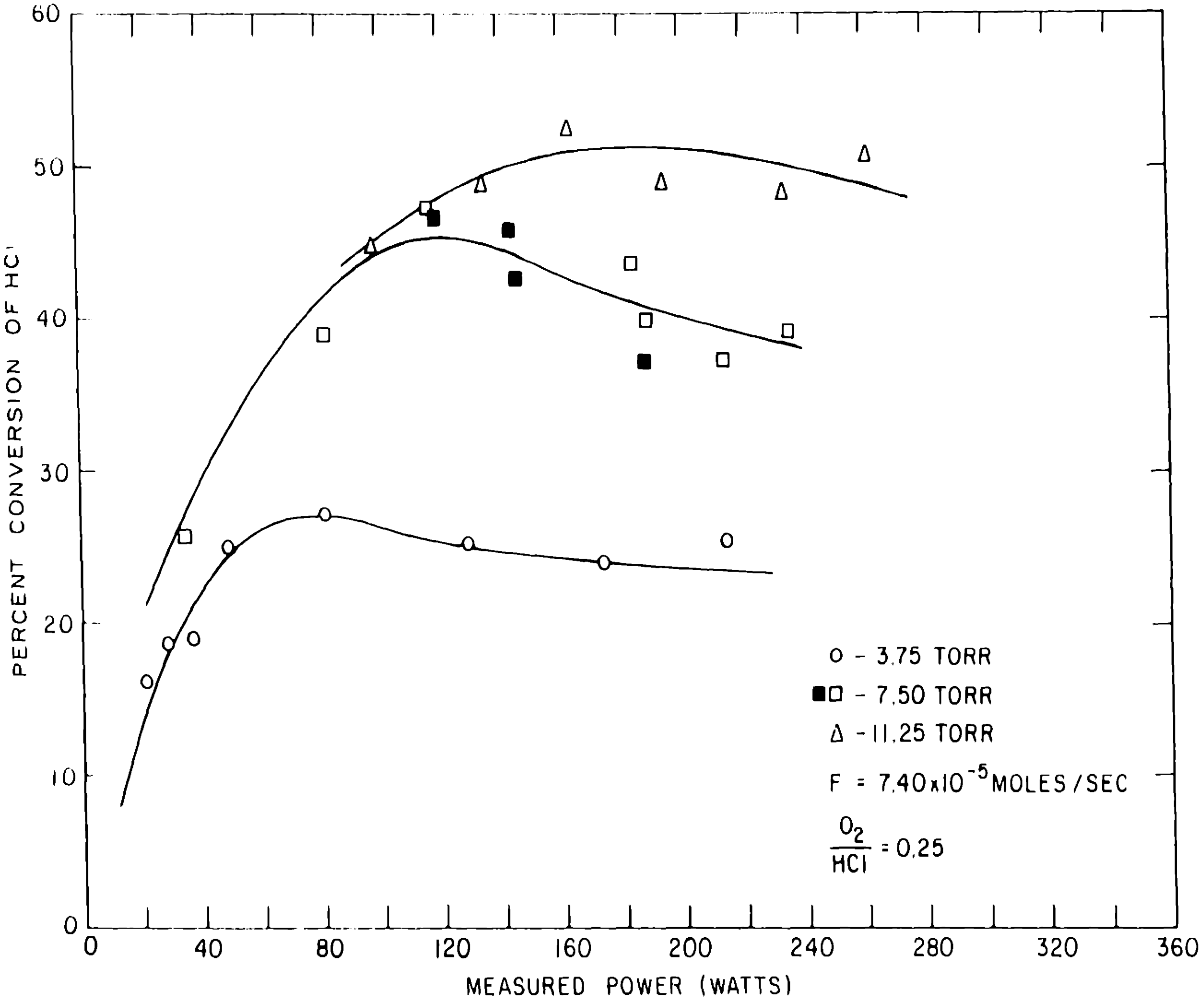

FIGURE 13 THE EFFECT OF PRESSURE ON CONVERSION VERSUS POWER FOR F - 740 $\times 10^{-5}$ MOLES / SEC

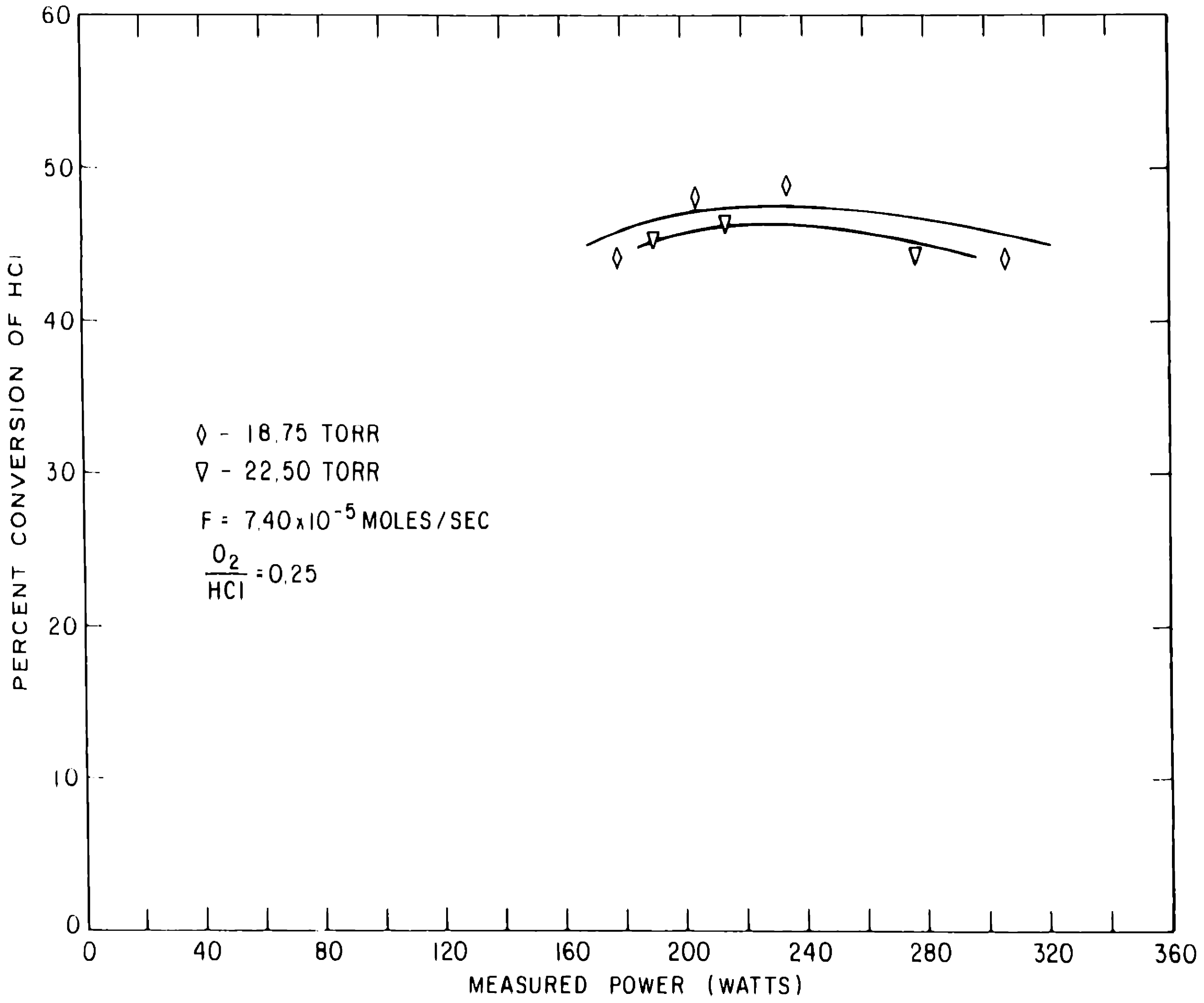

FIGURE 14 THE EFFECT OF PRESSURE ON CONVERSION VERSUS POWER FOR $F = 740 \times 10^{-5}$ MOLES/SEC

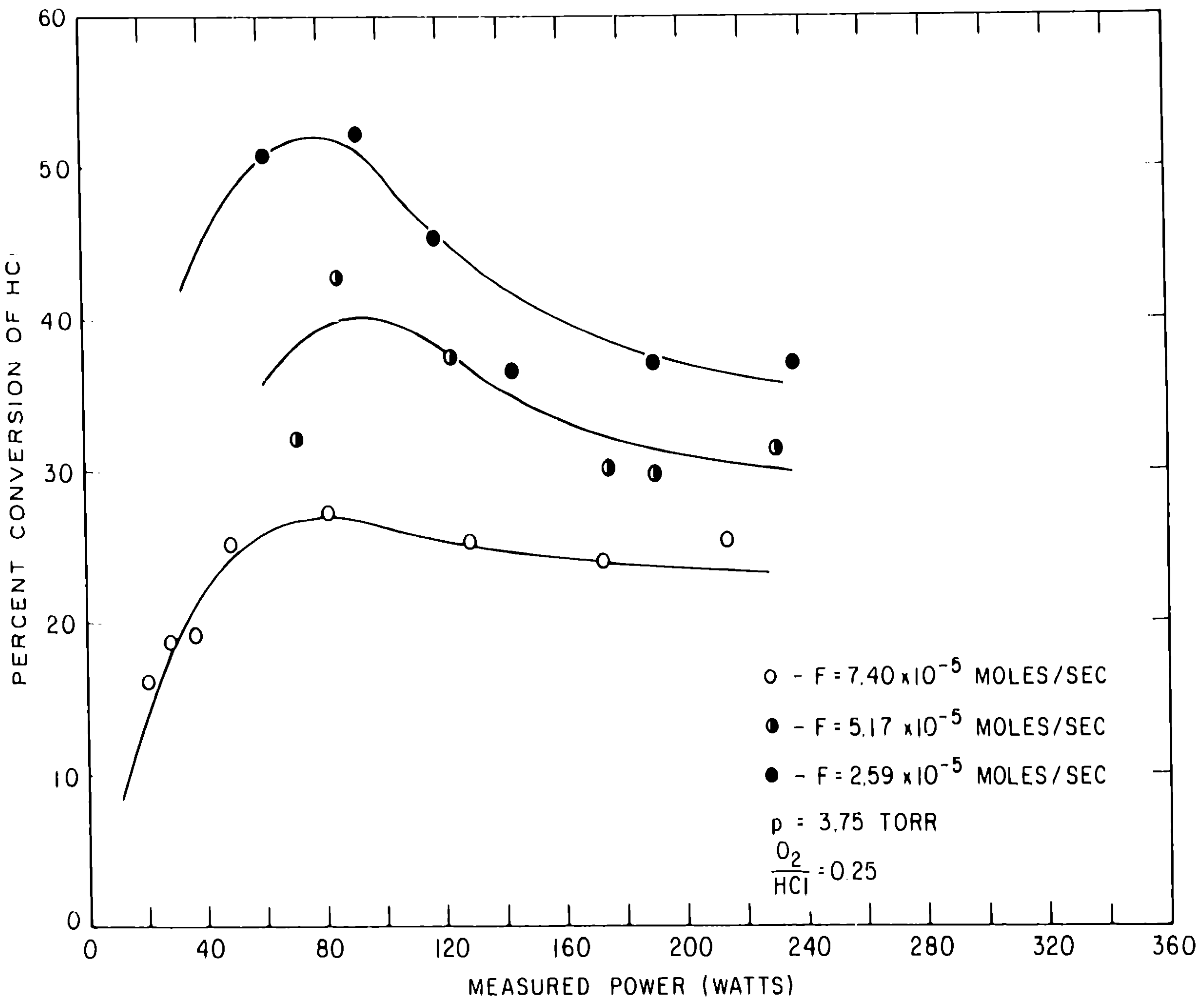

FIGURE 15 THE EFFECT OF TOTAL MOLAR FLOW RATE ON CONVERSION VERSUS POWER FOR 3.75 TORR

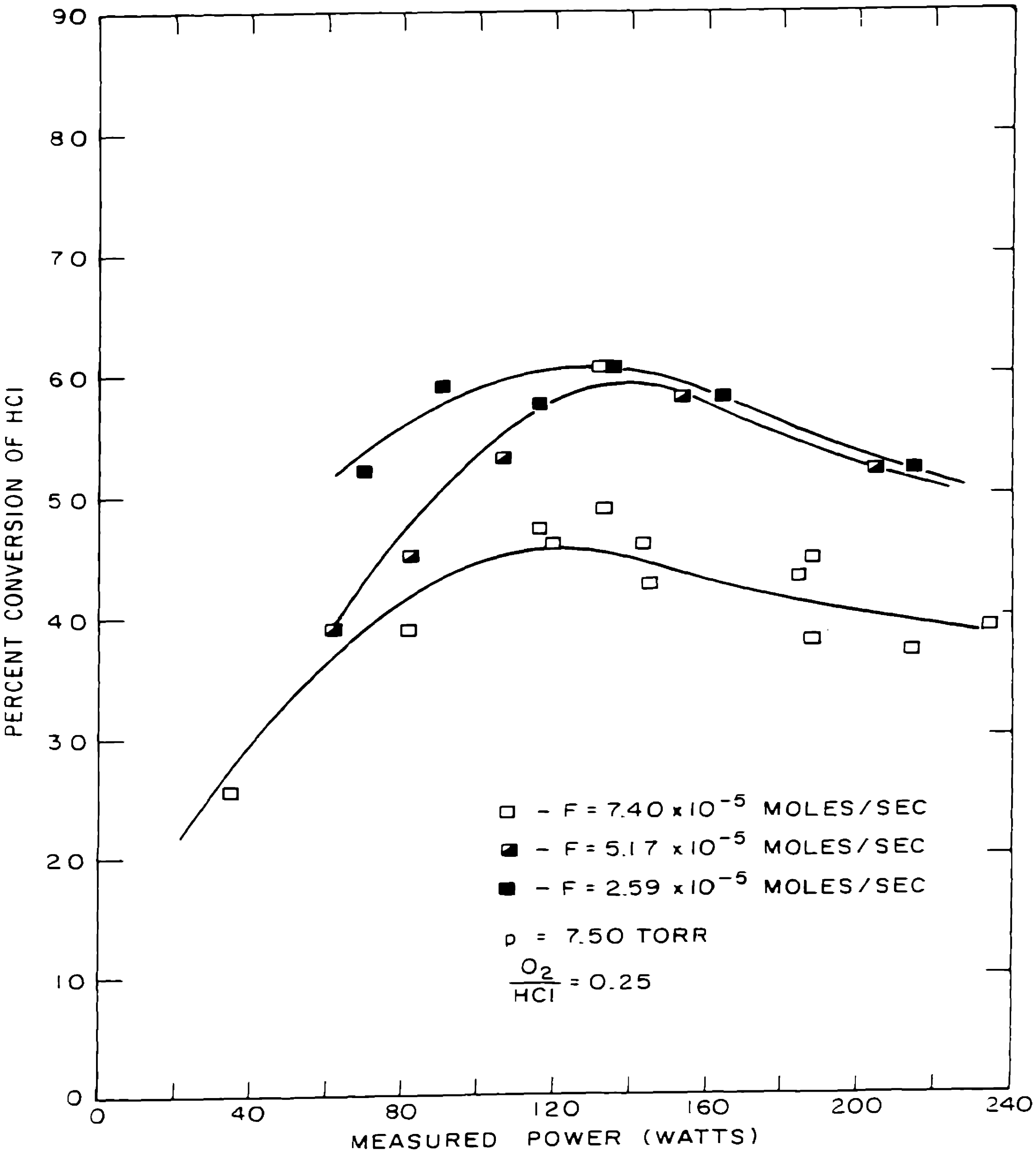

FIGURE 16 THE EFFECT OF TOTAL MOLAR FLOW RATE ON CONVERSION VERSUS POWER FOR 7.50 TORR

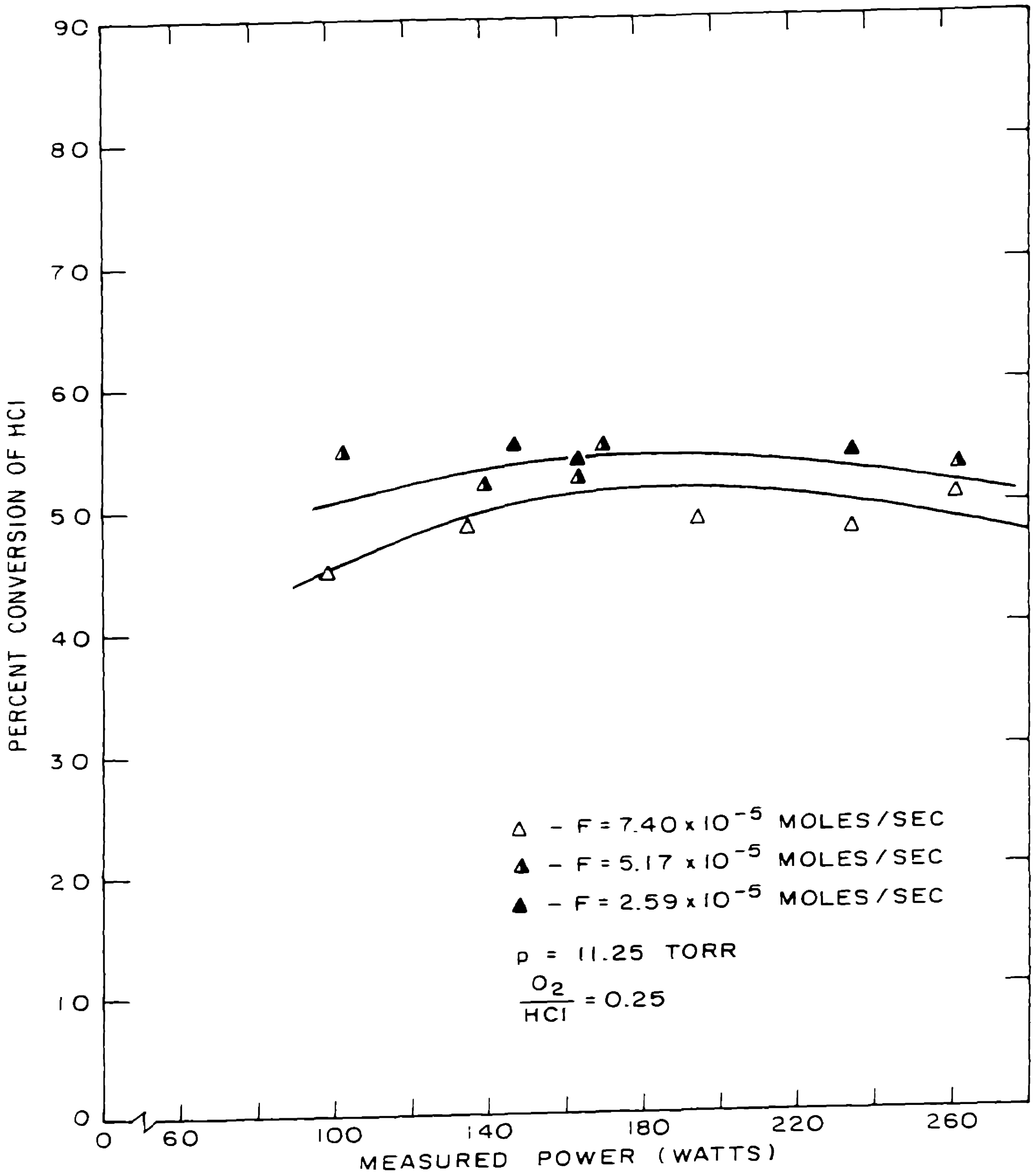

FIGURE 17 THE EFFECT OF TOTAL MOLAR FLOW RATE ON CONVERSION VERSUS POWER FOR 11.25 TORR

is quite pronounced for each change. For the two higher pressures only the first decrease in flow rate produces a major change in conversion, the second one leading to a negligible increase. It should be noted that in each figure the position of maximum conversion is essentially unaffected by the decrease in total molar flow rate.

Figure 18 shows the change in conversion which occurs as a result of an increase in the oxygen concentration in the reacting gas mixture. The total molar flow rate is maintained at 7.40×10^{-5} moles/sec while the oxygen content is varied from stoichiometric to twice stoichiometric. A shift in the position of maximum conversion is observed here as the amount of excess oxygen is increased. However, because the positions of the maxima for the curves corresponding to $(O_2)/(O_2)_s$ equal to 1.5 and 2.0 coincide, it is felt that the observed shift is not due to the presence of excess oxygen but may in fact be the result of a constant discrepancy in the measurement of the discharge power.

Mass spectra were taken of the reactants and products using a CEC 21-614 mass spectrometer. These results are shown in Figure 19. The group of peaks at masses 70, 72, and 74 are due to the three combinations of chlorine isotopes 35 and 37. No peak at mass 66 is observed in the reaction products so that ClO_2 cannot be considered as one of the products. A very slight increase in the peak at mass 51 might, however, be attributed to ClO.

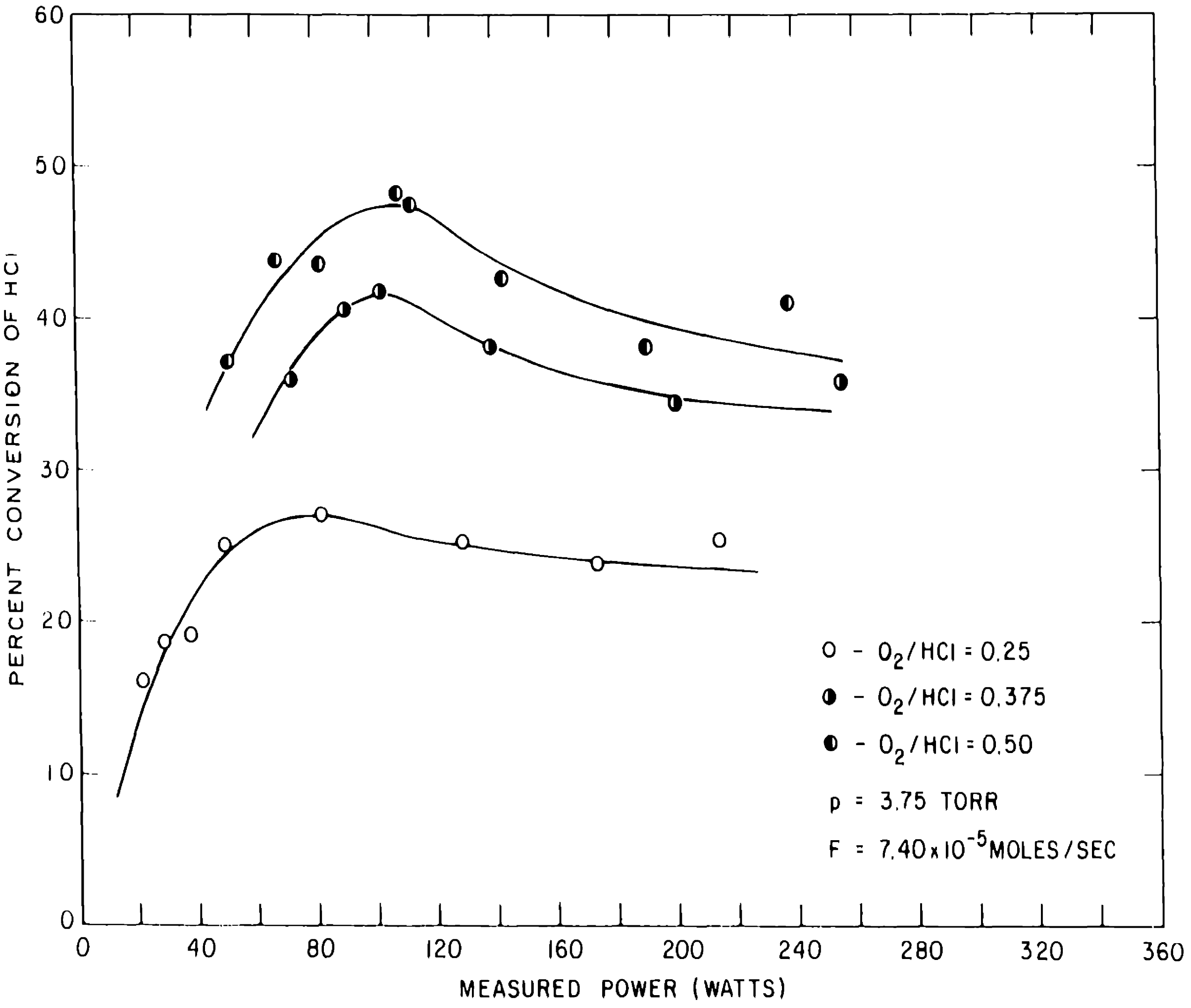

FIGURE 18 THE EFFECT OF OXYGEN TO HYDROGEN CHLORIDE RATIO ON CONVERSION VERSUS POWER FOR 3.75 TORR

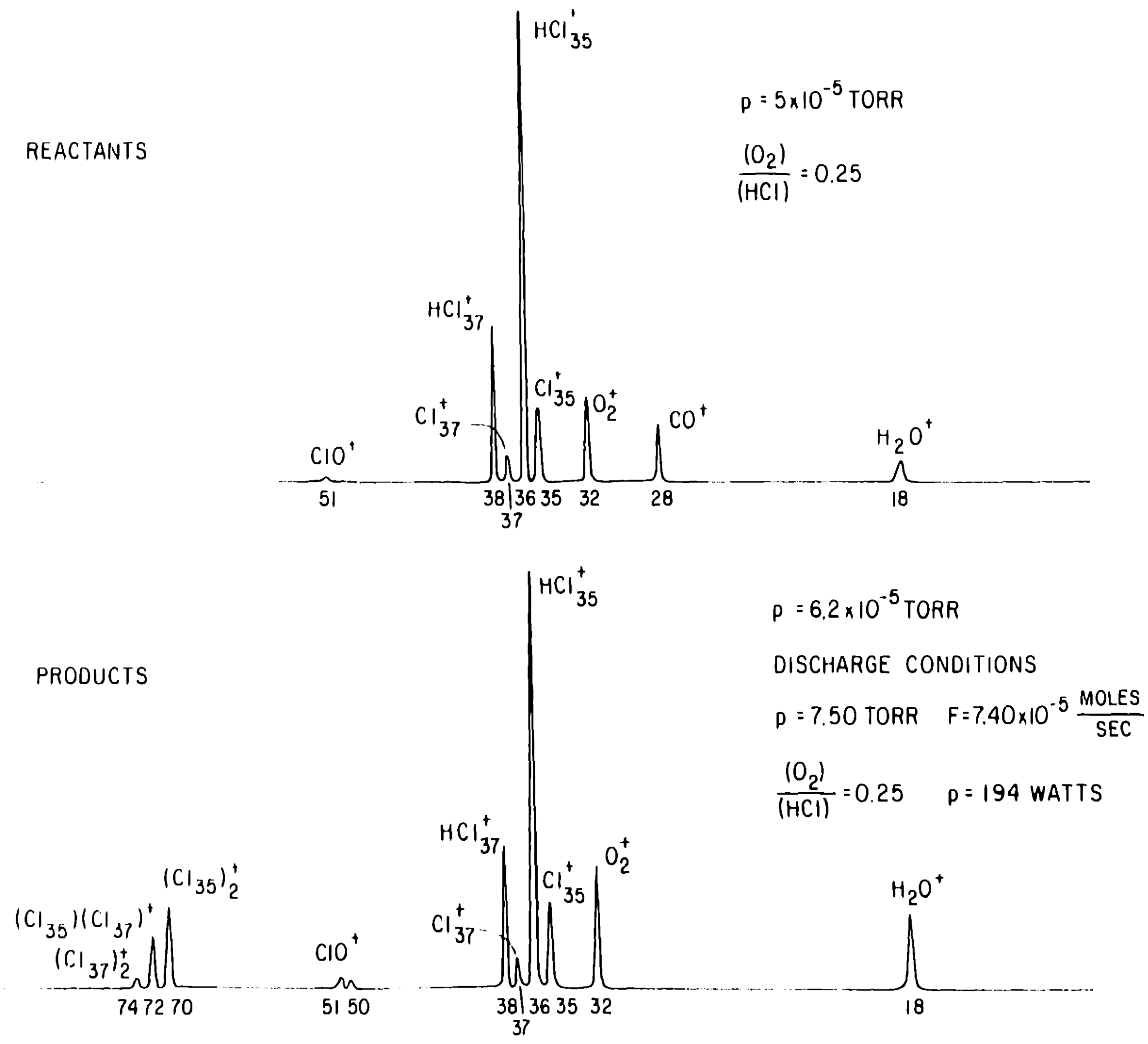

FIGURE 19 MASS SPECTRA OF REACTANTS AND PRODUCTS

2. Reverse Reaction

A plot of the conversion of chlorine to hydrogen chloride via the reverse reaction is shown in Figure 20. The pressure range from 7.50 to 18.75 Torr was investigated for a constant total molar flow rate of 7.40×10^{-5} moles/sec and a water vapor to chlorine ratio equal to one. Attempts to obtain data at higher pressures were not successful because the discharge constricted severely and subsequently went out. For the power available, it was not possible to maintain a stable discharge above 18.75 Torr.

It is seen from Figure 20 that the conversion increases continuously with power and that a maximum conversion such as is characteristic of the forward reaction does not occur. An increase in pressure at constant power also does not lead to a maximum conversion but rather causes a continuing increase.

In order to illustrate the effect of pressure on conversion, at constant power, for both the forward and reverse reactions, a plot is presented in Figure 21 of the mole percent of chlorine in the chlorine-hydrogen chloride product mixture as a function of pressure. The separate curves represent different total molar flow rates. It is seen that for the forward reaction the curves pass through a maximum for all three flow rates. A similar curve was obtained by Cooper (31) using a microwave discharge

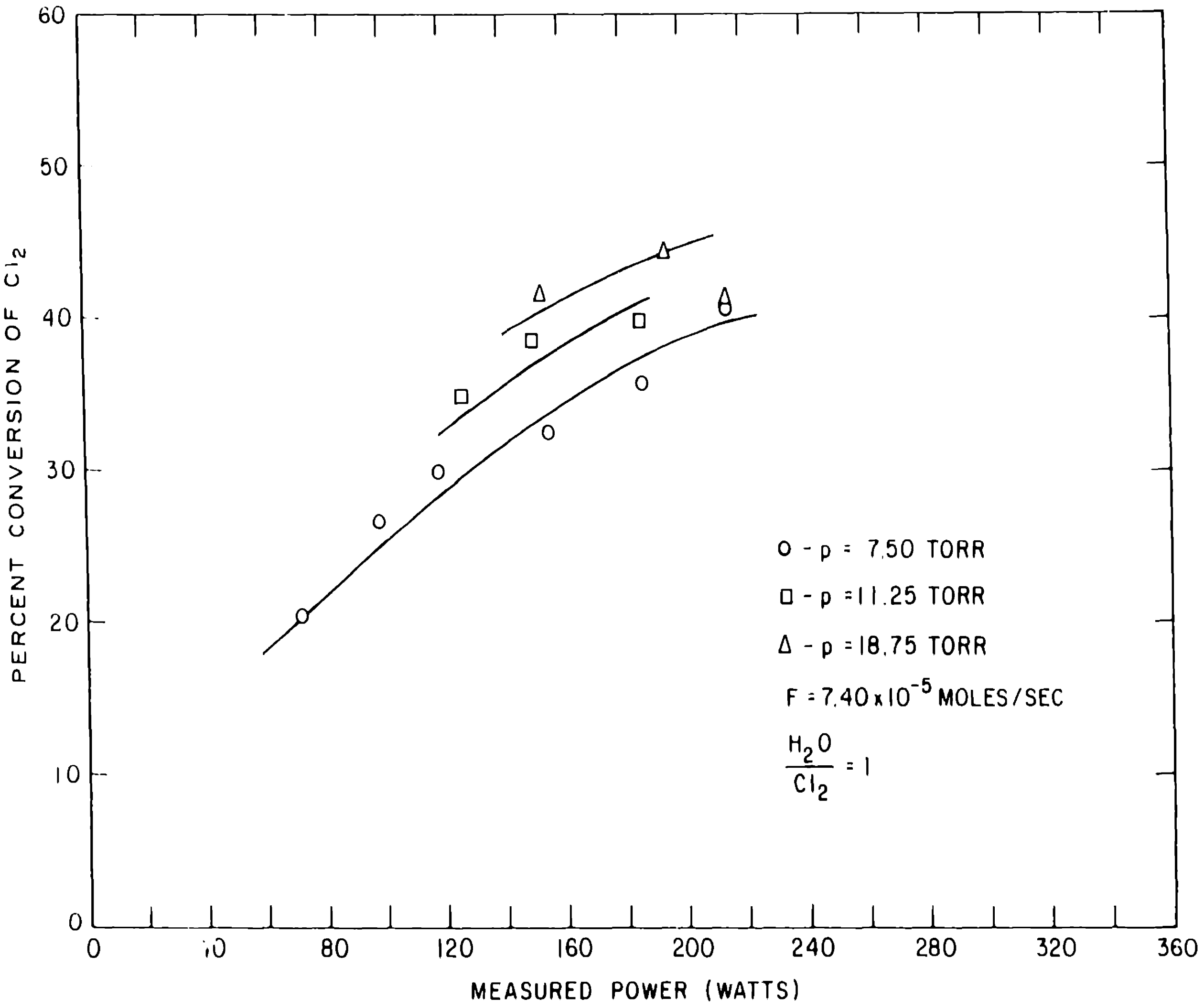

FIGURE 20 THE EFFECT OF PRESSURE ON CONVERSION VERSUS POWER FOR THE REVERSE REACTION

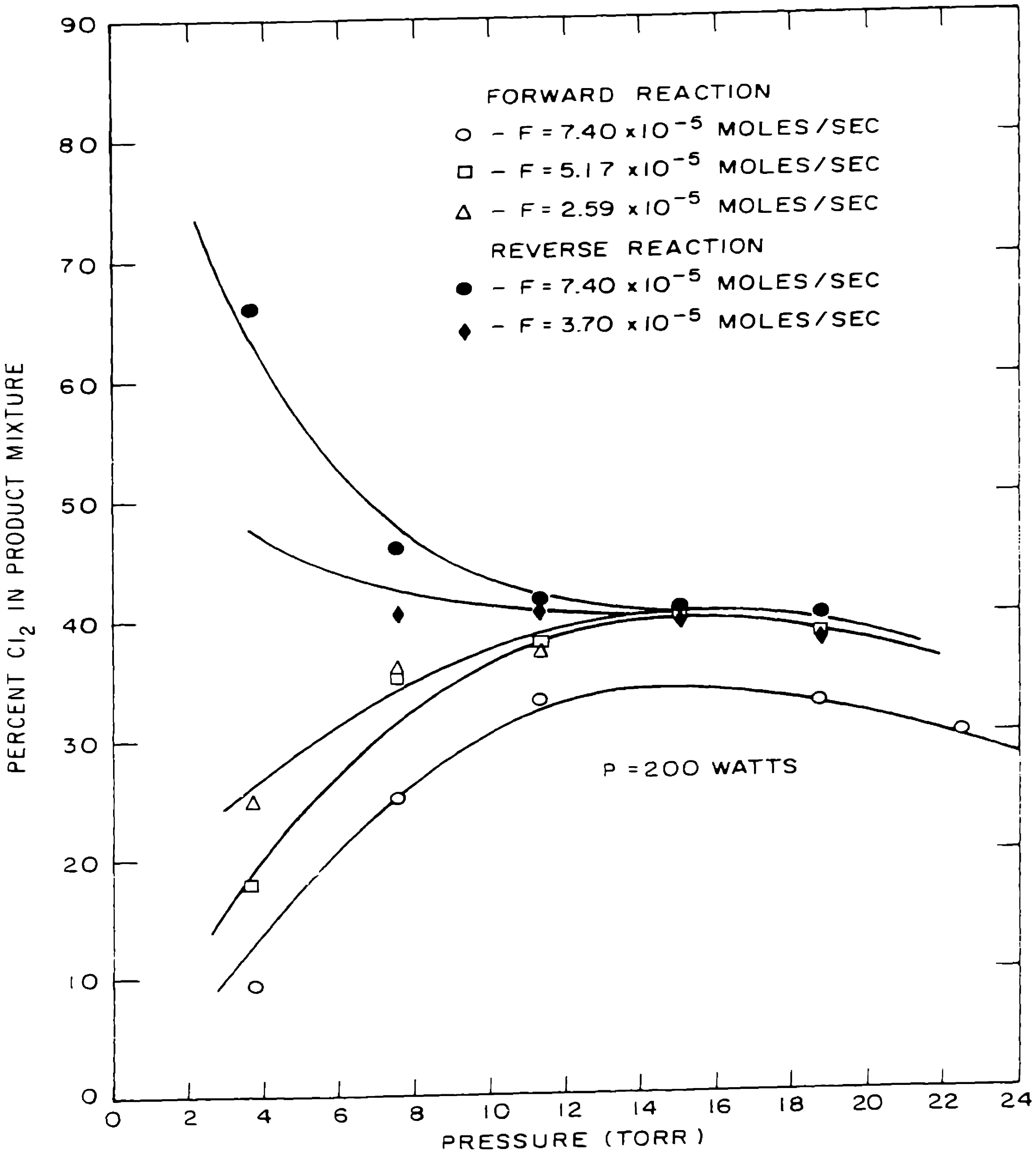

FIGURE 21 THE EFFECT OF PRESSURE ON FORWARD AND REVERSE REACTIONS AT CONSTANT POWER

operating at 200 watts. It would therefore appear that this behavior is characteristic of the chemical system rather than the manner in which the discharge is sustained. On the other hand, both curves for the reverse reaction show a continuously decreasing percent of chlorine in the product as the pressure is increased. A decrease in the total molar flow rate for the forward reaction causes an increase in the percent of chlorine. This effect, however, begins to diminish as lower flow rates are used, particularly at higher pressures. For pressures above 11.50 Torr the curves drawn for the forward reaction for $F = 5.17 \times 10^{-5}$ moles/sec and $F = 2.59 \times 10^{-5}$ moles/sec merge into one. In the case of the reverse reaction the curves for $F = 7.40 \times 10^{-5}$ moles/sec and $F = 3.70 \times 10^{-5}$ moles/sec begin to converge for pressures above 11.50 Torr. Finally, it should be noted that at sufficiently low molar flow rates and pressures above 15.00 Torr the results for both forward and reverse reaction converge.

B. Separated Feed

Studies were made on both the forward and reverse reactions in which only one of the reactants was passed through the discharge, the second one being added one centimeter below the discharge. In all these studies the side wall injection reactor tube, described in Chapter IV, was used.

The change in conversion as a function of power for the forward reaction is shown in Figures 22 and 23. From Figure 22 it is seen that activation of either hydrogen chloride or oxygen will lead to the formation of chlorine. The curve for the activation of oxygen is not as sensitive to a change in power as the one for the activation of hydrogen chloride. However, at low powers the activation of oxygen gives rise to a slightly greater conversion than for the activation of hydrogen chloride. This effect is reversed for higher powers.

The introduction of excess oxygen to the products of a hydrogen chloride discharge leads to an increase in the conversion, as is seen from Figure 23. This increase does not continue indefinitely but, rather, appears to approach an upper limit for greater and greater excesses of oxygen. The onset of this limit can be seen from the curves for $(O_2)/(O_2)_s$ equal to 1.5 and 2.0.

The addition of chlorine to a stoichiometric amount of oxygen leads to a decrease in the conversion of hydrogen chloride. In order to examine the possibility that the chlorine served only as a diluent for the oxygen but did not react with the products of the hydrogen chloride discharge, several runs were made in which equivalent amounts of helium were substituted for chlorine. This procedure showed that helium did not affect the conversion of hydrogen chloride and consequently that the interaction with chlorine is indeed a chemical one.

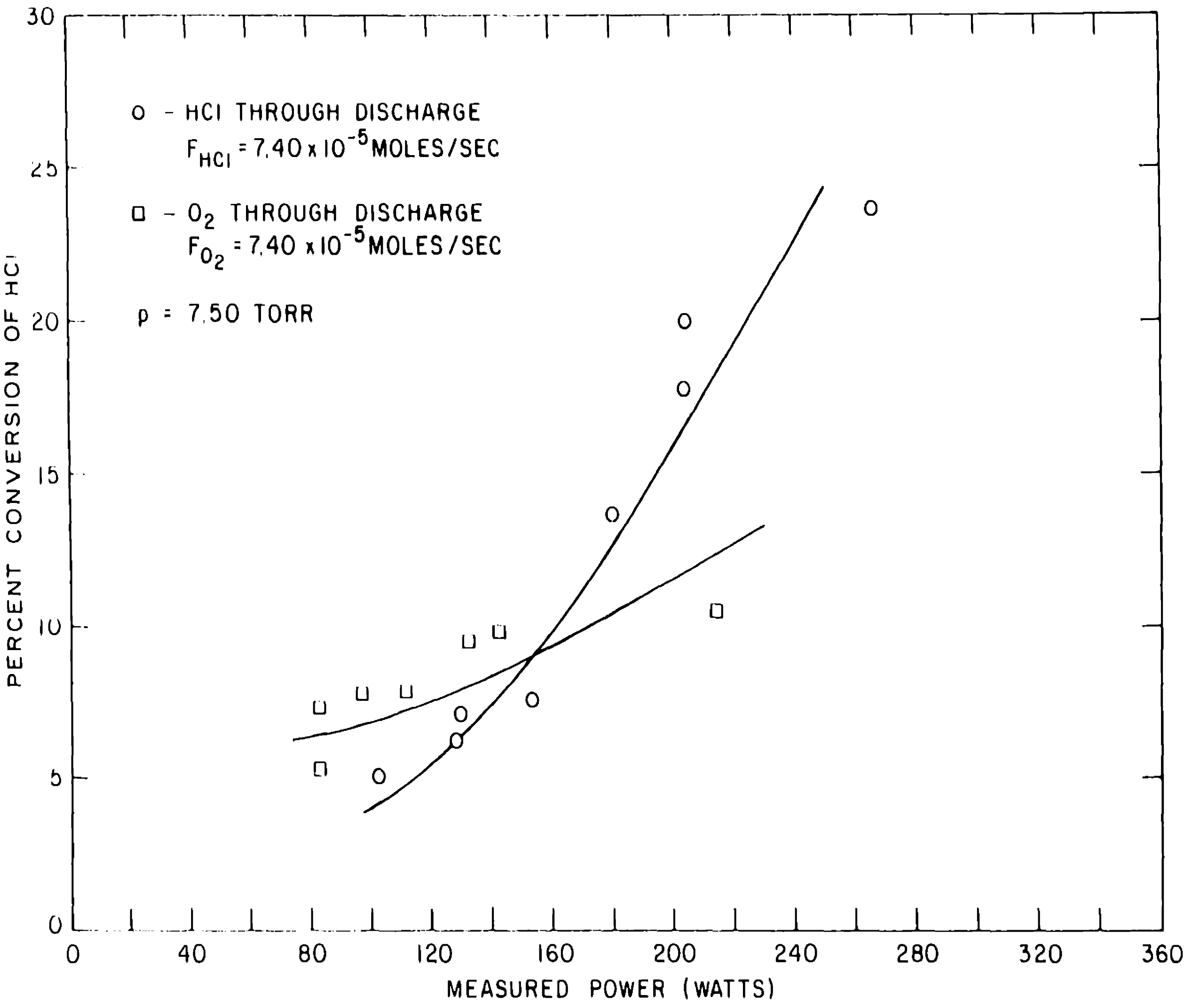

FIGURE 22 THE EFFECT OF DISCHARGING HYDROGEN CHLORIDE OR OXYGEN WITH THE SUBSEQUENT ADDITION OF THE SECOND REACTANT DOWNSTREAM

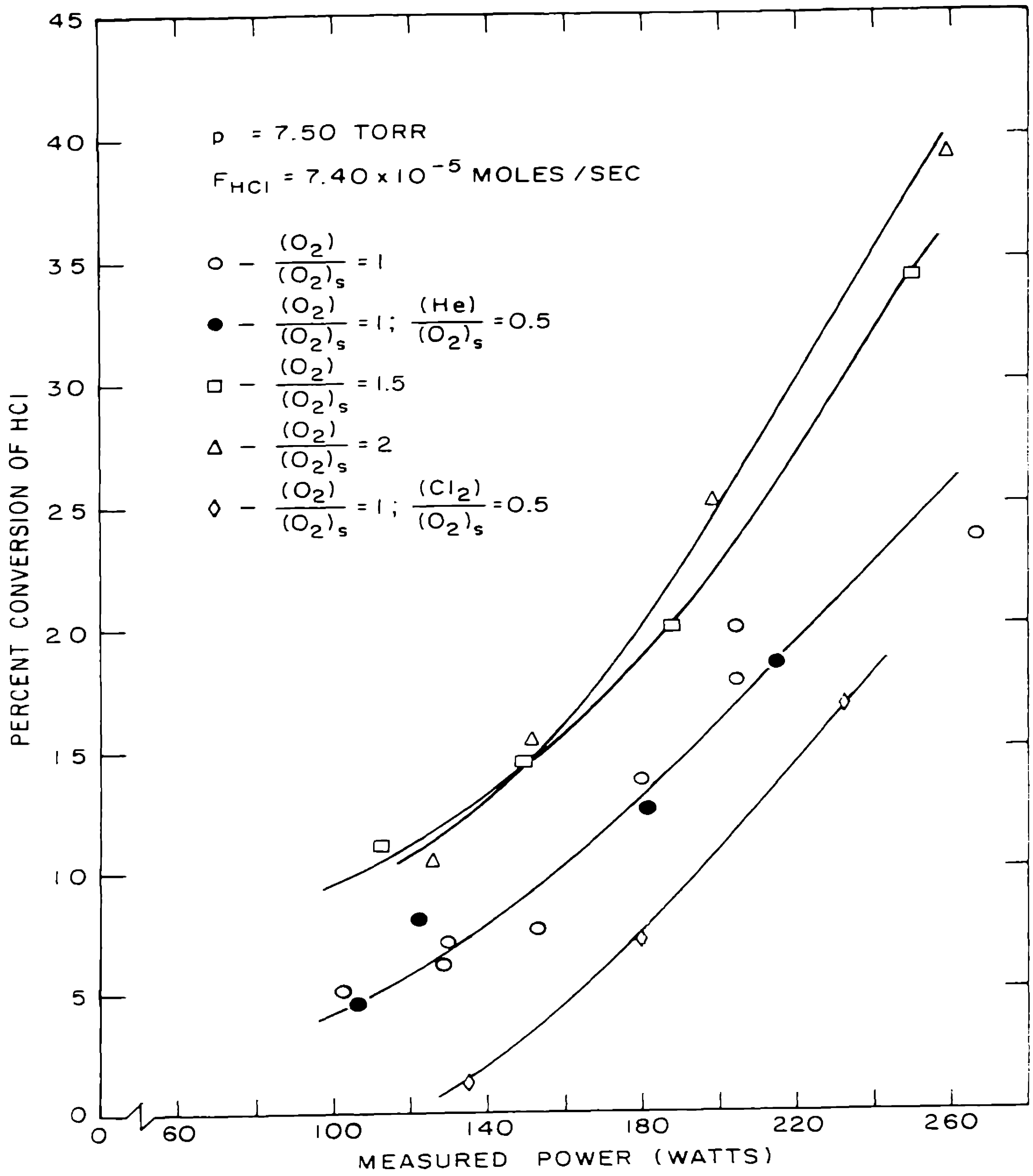

FIGURE 23 THE EFFECT OF ADDING EXCESS OXYGEN OR CHLORINE TO THE PRODUCTS OF A HYDROGEN CHLORIDE DISCHARGE

Investigations of the reverse reaction showed that less than 4% of the chlorine was converted to hydrogen chloride when chlorine was passed through the discharge. On the other hand up to 29% conversion was obtained when water vapor was passed through the discharge and chlorine was added downstream. These results are shown in Figure 24.

C. Physical Measurements and Visual Observations

In the course of the experimental runs, measurements were made of the voltage across the discharge and the power dissipated in the discharge. From these measurements a plot of the voltage-current characteristics of the discharge could be obtained. An example of such a plot is shown in Figure 25 for a discharge in a stoichiometric mixture of hydrogen chloride and oxygen operating at 7.50 Torr. The curve has only a slight positive curvature. If a straight line is drawn through the points, an equivalent resistance of 1.13×10^4 ohms is obtained. Changes in the pressure, molar flow rate, or the ratio of oxygen to hydrogen chloride in the feed produce very little effect on either the curvature of the plot or the value of the straight line resistance.

Attempts were made to measure the gas temperature at the base of the r.f. discharge by means of an iron-constantan thermocouple placed inside a quartz thermowell located concentrically within the discharge tube. These measurements,

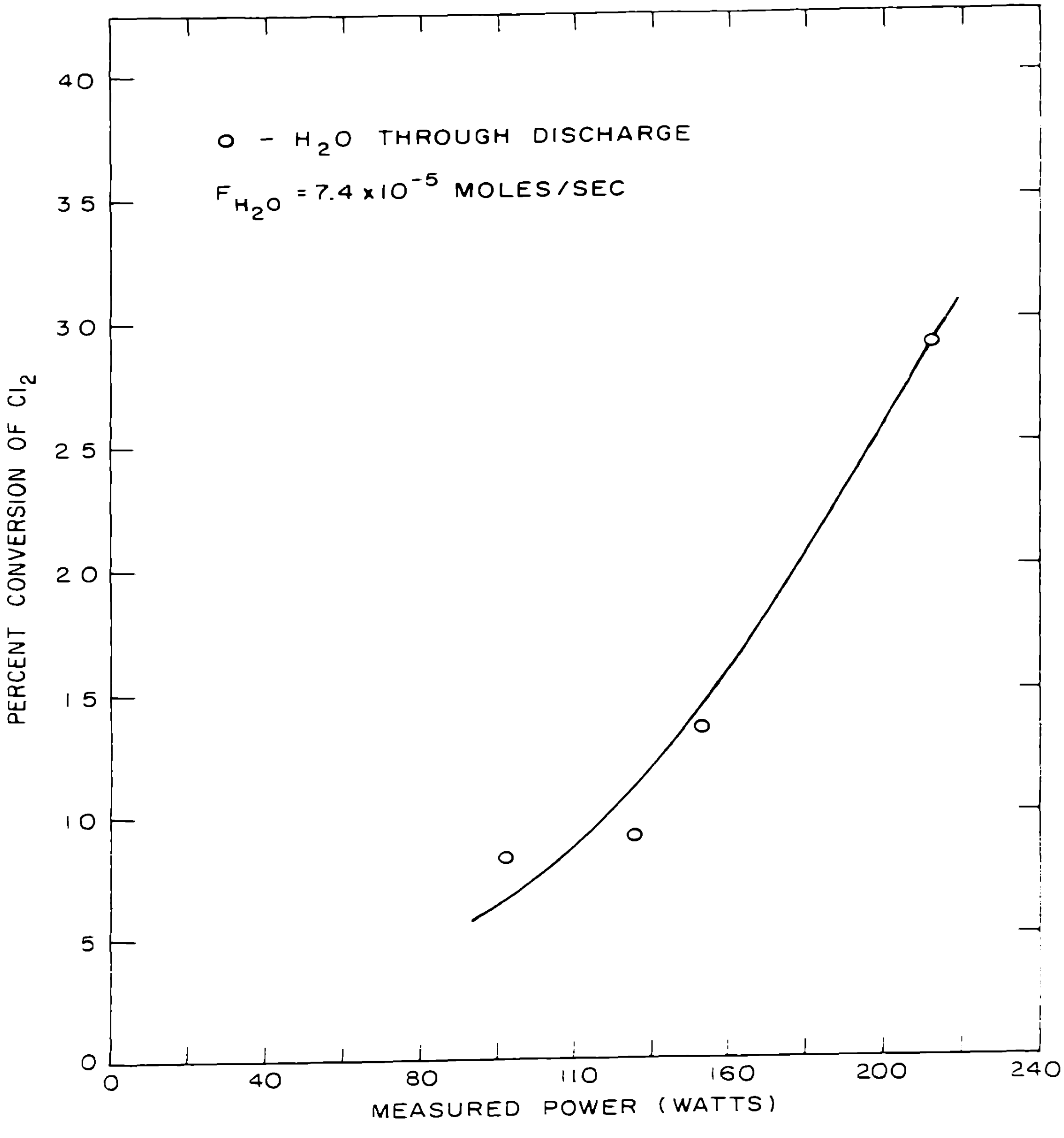

FIGURE 24 THE EFFECT OF DISCHARGING WATER VAPOR WITH THE SUBSEQUENT ADDITION OF CHLORINE DOWNSTREAM

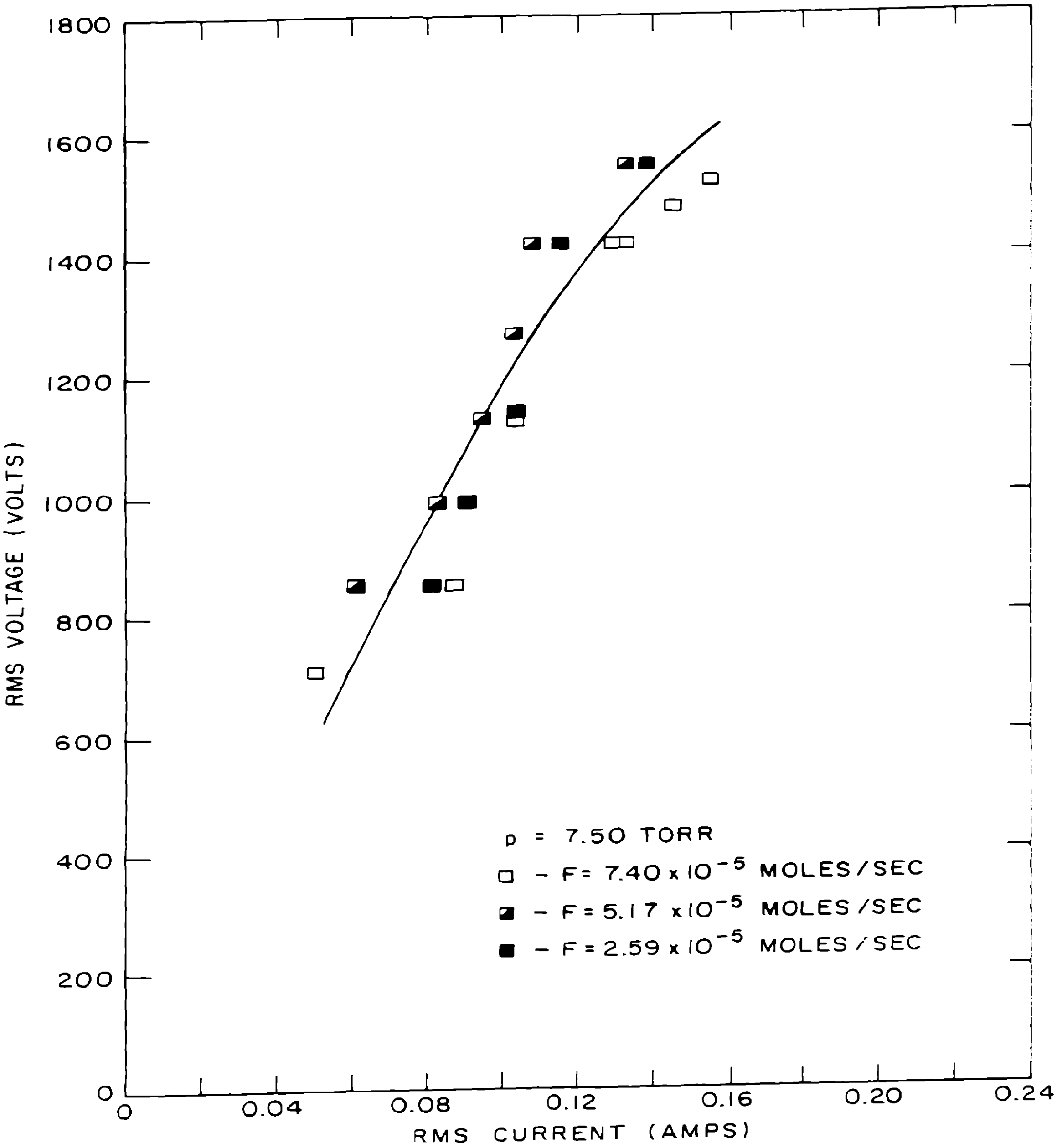

FIGURE 25 VOLTAGE VERSUS CURRENT FOR A 20 MHz DISCHARGE

however, could not be made successfully because it was found that the thermocouple absorbed r.f. energy from the electric field. Thus, even in the absence of a discharge but with the r.f. source turned on, the thermocouple gave a positive reading. In order to avoid this problem and to obtain a related estimate of the temperature, it was decided to measure the temperature in a 60 Hz discharge operated with cylindrical electrodes. The construction of this tube has been described in Chapter IV. Figure 26 shows that the temperature of the gas leaving the discharge tube is found to increase linearly with power at the rate of 0.75 ^{o}C/watt.

Visual observations of the discharge showed that under proper operation the discharge appeared as a uniform glow which filled the radius of the discharge tube and was almost totally contained within the outer boundaries of the two sleeve electrodes. Two regions of distinctly different color were usually observed, one characteristic of the glow contained within the electrode region and the other of the volume between the electrodes. The colors of these regions for each reactant and product gas are listed in Table 2.

Further observations showed that when helium was discharged the glow extended well beyond the volume contained between the electrodes. As the pressure was raised at constant power for such a discharge, the only noticeable effect was a slight decrease in the intensity of light

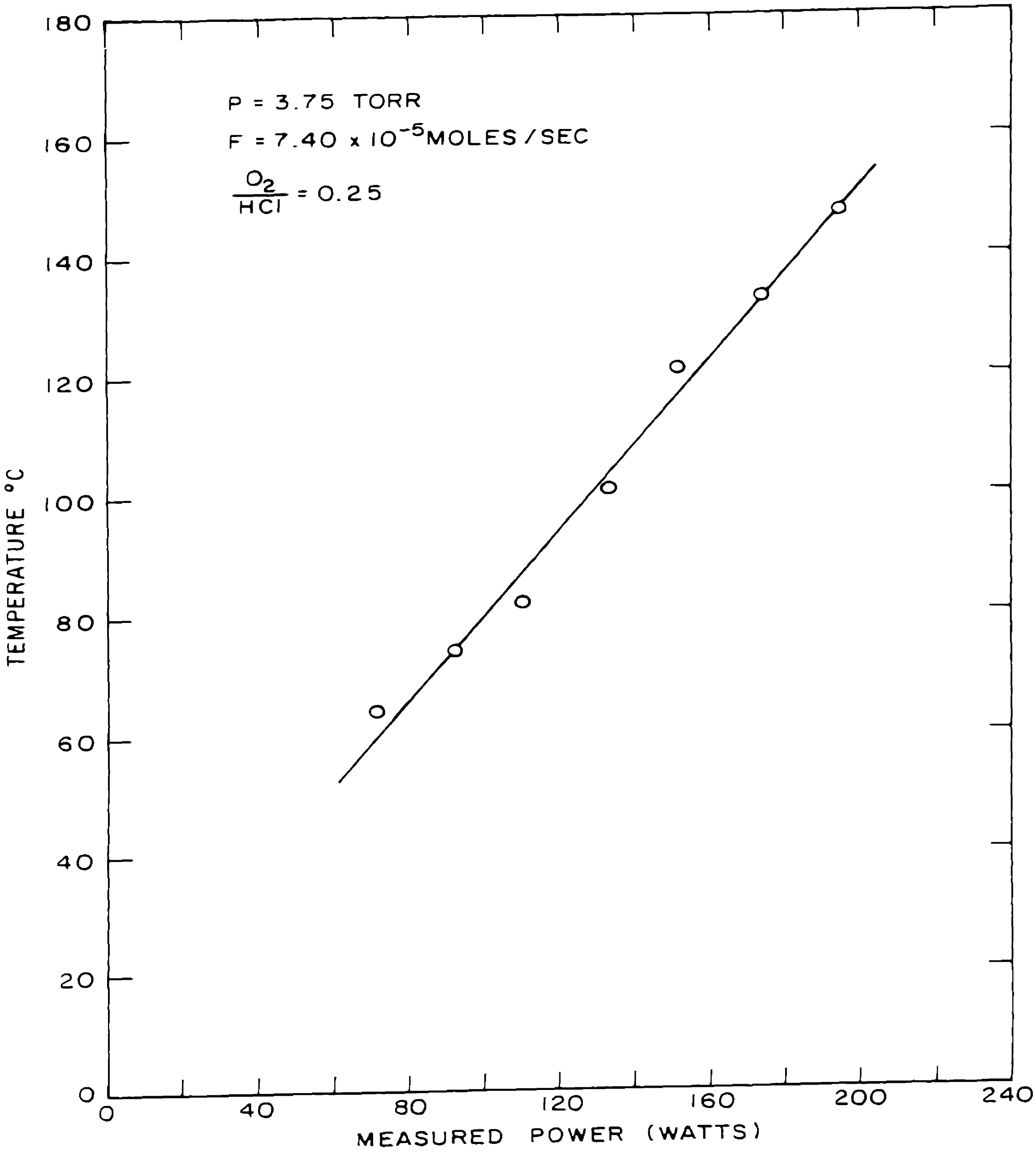

FIGURE 26 GAS TEMPERATURE VERSUS POWER FOR 60 Hz DISCHARGE

Table 2

Color of Emitted Light from Electrode and Central Discharge Volumes

Gas	Electrode Volume	Central Volume
HCl	blue	red
O_2	greenish-white	light red
H_2O	light red	bright red
Cl_2	light blue	blue
80% HCl, 20% O_2	blue	red
50% H_2O, 50% Cl_2	blue	red

output and a decrease in the amount of glow extending outside the electrode regions. When one of the electronegative gases was used, the behaviour with pressure became quite different. In this case there was a tendency for the glow to contract radially with the strongest contraction occurring at a position half-way between the electrodes. At sufficiently high pressures (> 25 Torr), this led to a collapse of the uniform glow and the discharge went out or transformed to a thin streamer, several millimeters in diameter. The effect of contraction was most severe in the case of chlorine and is responsible for the impossibility of obtaining data on the reverse reaction at pressures above 18.75 Torr.

CHAPTER VII

DISCUSSION OF RESULTS

A. Mixed Feed

1. Forward Reaction

a. Effect of Power on Conversion at Constant Pressure

An examination of Figures 15, 16 and 17 shows that a decrease in the total molar flow rate leads to an increase in the conversion of hydrogen chloride, the effect being most evident at the lower gas pressures. This type of behaviour is characteristic of a reaction system which is rate limited by kinetics. Under this limitation it should be possible to determine the final extent of conversion from a knowledge of the reaction kinetics, the flow model which the reactor obeys, and the physical conditions inside the reactor.

A possible reaction mechanism for both the forward and reverse reactions can be given in terms of the following 14 reactions steps:

1. $HCl + e^- \longrightarrow H + Cl^- \qquad \epsilon_1 = 0.66 \text{ eV}$
2. $O_2 + e^- \longrightarrow O + O^- \qquad \epsilon_2 = 4.7 \text{ eV}$
3. $H_2O + e^- \longrightarrow OH + H^- \qquad \epsilon_3 = 5.6 \text{ eV}$
4. $Cl_2 + e^- \longrightarrow Cl + Cl^- \qquad \epsilon_4 = 0.0 \text{ eV}$

5. $O + HCl \longrightarrow OH + Cl$

6. $H + O_2 \longrightarrow OH + O$

6a. $H + O_2 + M \longrightarrow HO_2 + M$

6b. $H + HO_2 \longrightarrow 2\ OH$

7. $OH + HCl \longrightarrow H_2O + Cl$

8. $H + Cl_2 \longrightarrow HCl + Cl$

9. $2\ OH \longrightarrow H_2O + O$

10. $O + OH \longrightarrow O_2 + H$

11. $H + Cl + M \longrightarrow HCl + M$

12. $2\ O + M \longrightarrow O_2 + M$

13. $H + OH + M \longrightarrow H_2O + M$

14. $2\ Cl + M \longrightarrow Cl_2 + M$

This set of reactions represents the minimum number of elementary steps necessary for the formation of those reaction products observed in the mass spectrogram (Figure 19). Steps for the formation of ClO_2, which was not present in the mass spectrogram, and ClO, which is present in only trace amounts, have been excluded. Two other restrictions were placed on the selection of the primary reaction steps. The first was to select only the lowest energy electronic collision process which would lead to the dissociation of hydrogen chloride, oxygen, chlorine, and water vapor. The second restriction was that only homogeneous reaction steps should be considered so that the over-all description of the reaction mechanism might be kept as simple as possible.

The first of these two restrictions leads to the selection of a dissociative attachment process in which one of the products is a negative ion (reactions 1-4). For each of the four molecular constituents, the energy required for such a process is less than the bond dissociation energy of the molecule. Consideration of electron collision dissociation of the molecules into uncharged fragments shows that an excitation to a repulsive electronic state is necessary. This type of excitation always requires more energy than the bond dissociation energy. Thus, for oxygen the energy for dissociation by electron collisions is 8 eV as opposed to 5.1 eV for the bond energy. As a result the dissociative attachment mechanism requires less energy than straightforward dissociation of the molecule into uncharged fragments.

A discussion of the manner in which the electrons are detached from the negative ions is given in Appendix B. In Appendix C it is shown that the form of the over-all rate expression for the appearance of hydrogen chloride will not be affected by the choice of a particular detachment process.

Two alternatives have been described for the reaction between hydrogen atoms and oxygen molecules. These are represented by steps 6 and 6a, 6b. Reaction 6 is described by Foner and Hudson (38) as being responsible for the formation of hydroxyl radicals when the products of a hydrogen discharge operated at a few Torr are allowed to react with an oxygen stream. At several tens of Torr these authors report that hydroxyl radicals cease to be observed but that instead the HO_2 radical is now formed as a result of reaction 6a. Since the experiments described in the present work overlap both pressure regimes, both of these possibilities will be considered.

Reaction 5 has been included on the basis of observations by Harteck and Kopsch (39) and Cooper (31). These authors have shown that oxygen atoms produced by an oxygen discharge are capable of oxidizing hydrogen chloride to chlorine and water.

Although reaction 7 has not been reported in the literature, it is felt that the rate of reaction might be appreciable since the reaction is exothermic and has a $\Delta F_{298} = -14.94$ kcal. The reaction rate constant for the related step

$$OH + H_2 \longrightarrow H_2O + H$$

is reported as $2.3 \times 10^{13} \exp(-5200/RT)$ cm^3/mole sec (40).

Del Greco and Kaufman (41) have reported that reactions 9 and 10 are very rapid. These reactions are responsible for the decay of hydroxyl radicals in a water discharge and explain why the major products of such a discharge are hydrogen atoms and oxygen molecules.

A summary of the information on reaction rate constants available from the literature is given in Table 3.

As is shown in Appendix C, simultaneous consideration of all 14 reaction steps will not lead to a simple expression for the rate of disappearance of hydrogen chloride in terms of the concentrations of hydrogen chloride, oxygen, chlorine, and water vapor. A simple form for this expression is desired, because this would facilitate the testing of its validity in describing the over-all reaction. In order that such an expression might be obtained, the following assumptions were made: a) for the purpose of testing the proposed reaction mechanism on data for the forward reaction, only those reaction steps leading to the formation of the final products, chlorine and water vapor, would be included; b) decomposition of the products by electron collision would be excluded. These restrictions eliminate reactions 3,4,8,10,11, and 12, and the remaining eight reaction steps can be grouped so as to yield an expression of the form (see Appendix C)

Table 3

Reaction Rate Constants

Reaction Rate Constant	Reference
k_1 k_2 k_3	See Equation (27) and Figures 27 and 28
$k_6 = 1.3 \times 10^{14} \exp(-18800/RT) cm^3/mole\ sec$	(42)
$k_{6a} = 8.65 \times 10^{14}\ cm^6/mole^2\ sec$	(42)
$k_8 = 3 \times 10^{14} \exp(-3000/RT)\ cm^3/mole\ sec$	(43)
$k_9 = 1.5 \pm 0.4 \times 10^{12}\ cm^3/mole\ sec\ (300^\circ K)$	(41)
$k_{10} = 1 \times 10^{13}\ cm^3/mole\ sec\ (300^\circ K)$	(41)
$k_{12} = 1 \times 10^{15}\ cm^6/mole^2\ sec$	(44)
$k_{14} = 2.7 \times 10^{16}\ cm^6/mole^2\ sec$	(45)

$$\frac{d(HCl)}{dt} = - Ak_1(HCl)(e) - Bk_2(O_2)(e)$$

where the values of the numerical constants depend on the choice of the reaction steps in the following manner:

A	B	Reaction Steps
4	4	1,2,5,6,7,14
4/3	4/3	1,2,5,6,13,14
4	4	1,2,5,6,9,14
2	4	1,2,5,6a,6b,7,14
1	2	1,2,5,6a,6b,13,14
2	4	1,2,5,6a,6b,9,14

Two reactor flow patterns were chosen for examination, well mixed and plug flow. At the low Reynolds Numbers ($<$ 5) encountered in the experiments described here, a parabolic rather than a flat velocity profile is to be expected. Since the introduction of the actual profile precludes analytic integration of the rate expression, it was decided to use the two proposed flow models and to test their appropriateness by their ability to describe the experimental data.

Taking a mass balance around a differential slice of the reactor in the case of the plug flow model and around the whole reactor in the case of the well-mixed mode, the following two equations are obtained:

$$- Ak_1 \left[1 + \frac{B}{A} \frac{k_2}{k_1} \left(\frac{O_2}{HC_l}\right) \right] (HCl)(e) = - F_{HCl} \frac{dx}{dV} \qquad (21a)$$

$$- Ak_1 \left[1 + \frac{B}{A} \frac{k_2}{k_1} \left(\frac{O_2}{HCl}\right) \right] (HCl)(e) = - F_{HCl} \frac{x}{V} \qquad (21b)$$

Limiting oneself for the moment to the case of a stoichiometric ratio of oxygen to hydrogen chloride, in which case the ratio of oxygen to hydrogen chloride remains constant, equation (21) can be rewritten in terms of x, the fractional conversion of hydrogen chloride, as

$$- Ak_1 \left[1 + \frac{B}{A} \frac{k_2}{k_1} 0.25 \right] \frac{4(1-x)}{(5-x)} \frac{p}{RT_g} \cdot n_e = - F_{HCl} \frac{dx}{dV} \qquad (22a)$$

$$- Ak_1 \left[1 + \frac{B}{A} \frac{k_2}{k_1} 0.25 \right] \frac{4(1-x)}{(5-x)} \frac{p}{RT_g} n_e = - F_{HCl} \frac{x}{V} \qquad (22b)$$

Equation (22a) can be integrated from zero to x, and this integral and equation (22b) can be expressed as

$$4Ak_1 \left[1 + \frac{B}{A} \frac{k_2}{k_1} 0.25 \right] \frac{p}{RT_g} n_e \frac{V}{F_{HCl}} = y_1 \qquad (23a)$$

$$4Ak_1 \left[1 + \frac{B}{A} \frac{k_2}{k_1} 0.25 \right] \frac{p}{RT_g} n_e \frac{V}{F_{HCl}} = y_2 \qquad (23b)$$

where p and T_g are the pressure and gas temperature in the discharge zone, n_e the electron density, V the discharge volume, and y_1 and y_2 are given by

$$y_1 = - 4 \ln(1-x) + x \qquad (24a)$$

$$y_2 = x(5-x)/(1-x) \qquad (24b)$$

Plots of y_1 and y_2 are shown in Figure A-2. Thus, once the terms on the left hand side of equations (23a) and (23b) have been evaluated, a value of x can be found from Figure A-1.

On the basis of Cooper's results (31) on the decay of free radicals with distance from the base of a microwave discharge, it is estimated that significant recombination of these species would have occurred within one centimeter from the base of the discharge for the highest flow rates used in the present study. Since new atomic species are not created by electron collisions in this region, the reaction will cease to operate. Consequently the volume of the reactor can be taken to coincide with the volume of the discharge as determined by the product of the cross sectional area for flow and the length L between the outer edges of the two electrodes (see Figure 11).

As has been mentioned earlier the gas temperature in the r.f. discharge could not be measured directly and, as a result, there is no direct knowledge of how it varies with gas pressure and discharge power. The evidence from the measurements made at 60 Hz indicate, however, that at constant pressure the gas temperature will increase linearly with power. Based on this information the gas temperature variation with r.f. power at constant pressure is taken to be described by the following equation:

$$T_g = 293 + \Delta T^* P/200 \qquad (28)$$

where ΔT^* represents the temperature rise when 200 watts of power are supplied to the discharge. In the subsequent development ΔT^* will be left as an adjustable constant, and the value of the constant will be chosen at each pressure so as to obtain the best fit between the calculated conversions and the experimental ones.

The reaction rate constants k_1 and k_2 for dissociative attachment in hydrogen chloride and oxygen were calculated from the experimental collision cross sections presented by Buchel'nikova (46) and Schulz (47). For an electron with energy ϵ with respect to a molecule the reaction collision frequency per unit gas density is given by

$$\nu_1(\epsilon)/N = v\, Q_1(\epsilon) \tag{26}$$

where $\nu_1(\epsilon)$ is the collision frequency for electrons of energy ϵ, N is the gas density, v is the speed of the electron, and $Q_1(\epsilon)$ is the collision cross section for electrons with energy ϵ. In general, the electron energies will be distributed, only a fraction of them having energies within $\epsilon \pm \frac{1}{2} d\epsilon$. This can be taken into account by rewriting equation (26) as

$$\frac{d\left[\nu_1(\epsilon)\right]}{N} = v\, Q_1(\epsilon) f(\epsilon) d\epsilon \tag{27}$$

where $f(\epsilon)$ is the energy distribution function for electrons. The exact form of $f(\epsilon)$ is not known for electrons interacting with most gases; however, for the present development it will be assumed to be Maxwellian. This allows the introduction of an electron temperature T_e which is of great convenience in describing the average electron energy. An evaluation of the assumption of a Maxwellian distribution is given in Appendix E. With the form of $f(\epsilon)$ chosen, equation (27) can be integrated and the integral set equal to $k_1(T_e)$:

$$k_1(T_e) = \frac{\nu_1(T_e)}{N} = 2\sqrt{\frac{2}{\pi m}}\,(kT_e)^{-\frac{3}{2}} \int_0^\infty \epsilon\, Q_1 e^{-\epsilon/kT_e}\, d\epsilon \tag{28}$$

A description of the computer program used to evaluate this integral numerically is given in Appendix A.

Figures 27 and 28 illustrate the variation of k_1 with electron temperature T_e for dissociative attachment occurring in hydrogen chloride, oxygen, and water vapor. In each case the rate constant is small until a temperature is reached which is in the vicinity of the excitation energy necessary for the particular process. As this energy is approached the reaction rate constant passes through a maximum. It should be noted that in the region where k_1 attains a maximum the values of k_2 and k_3 are essentially zero.

From the plot of discharge voltage against current, given in the last chapter, it was seen that this characteristic is nearly linear and can be fitted by a straight line representing a resistance of about 10^4 ohms. This approximation will be used for the purpose of modeling the discharge. As a result, for each value of V_{rms} chosen the power dissipated in the discharge and the real current passing through it are given by

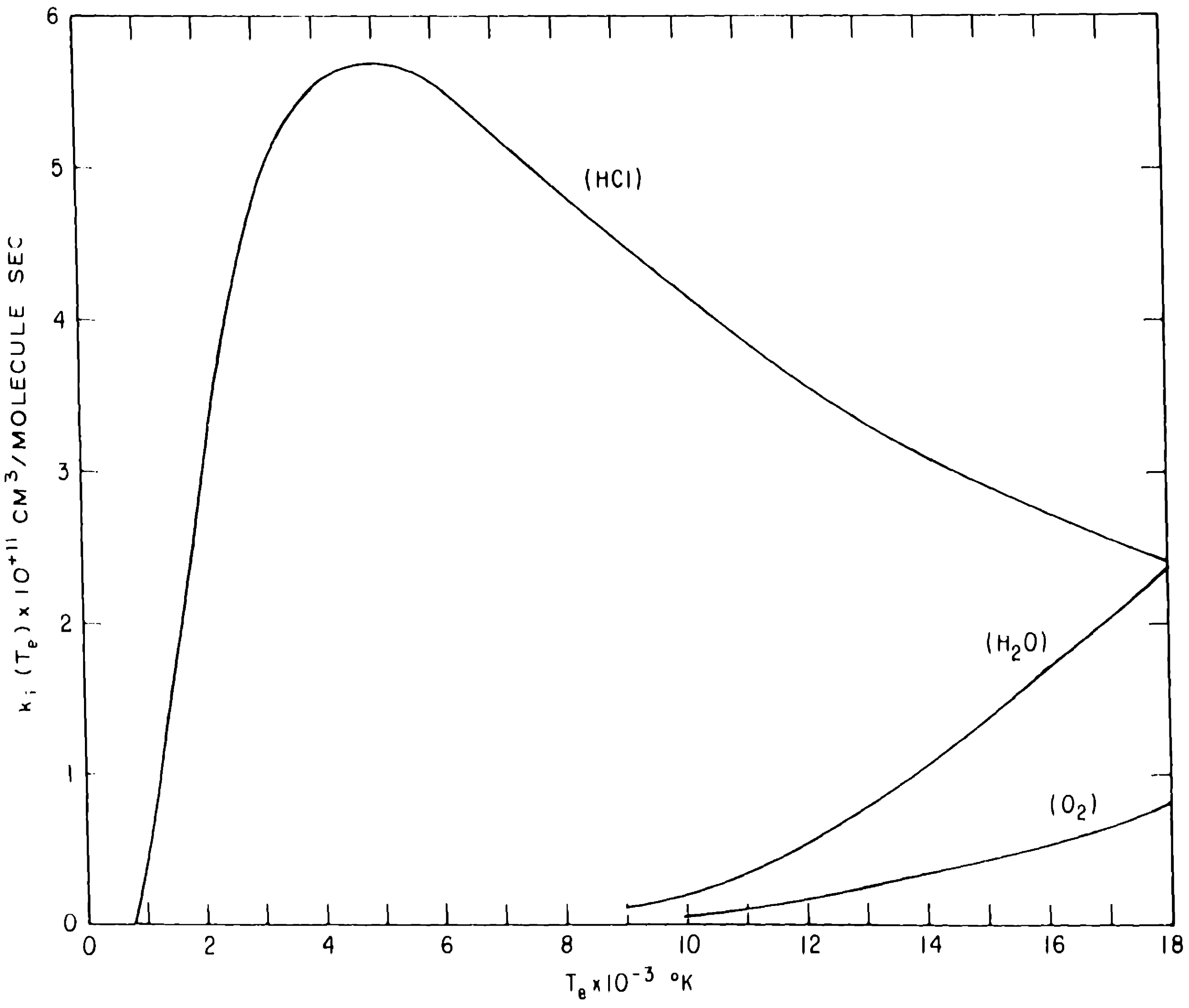

FIGURE 27 DISSOCIATIVE ATTACHMENT RATE CONSTANTS FOR HYDROGEN CHLORIDE, OXYGEN, AND WATER VERSUS ELECTRON TEMPERATURE

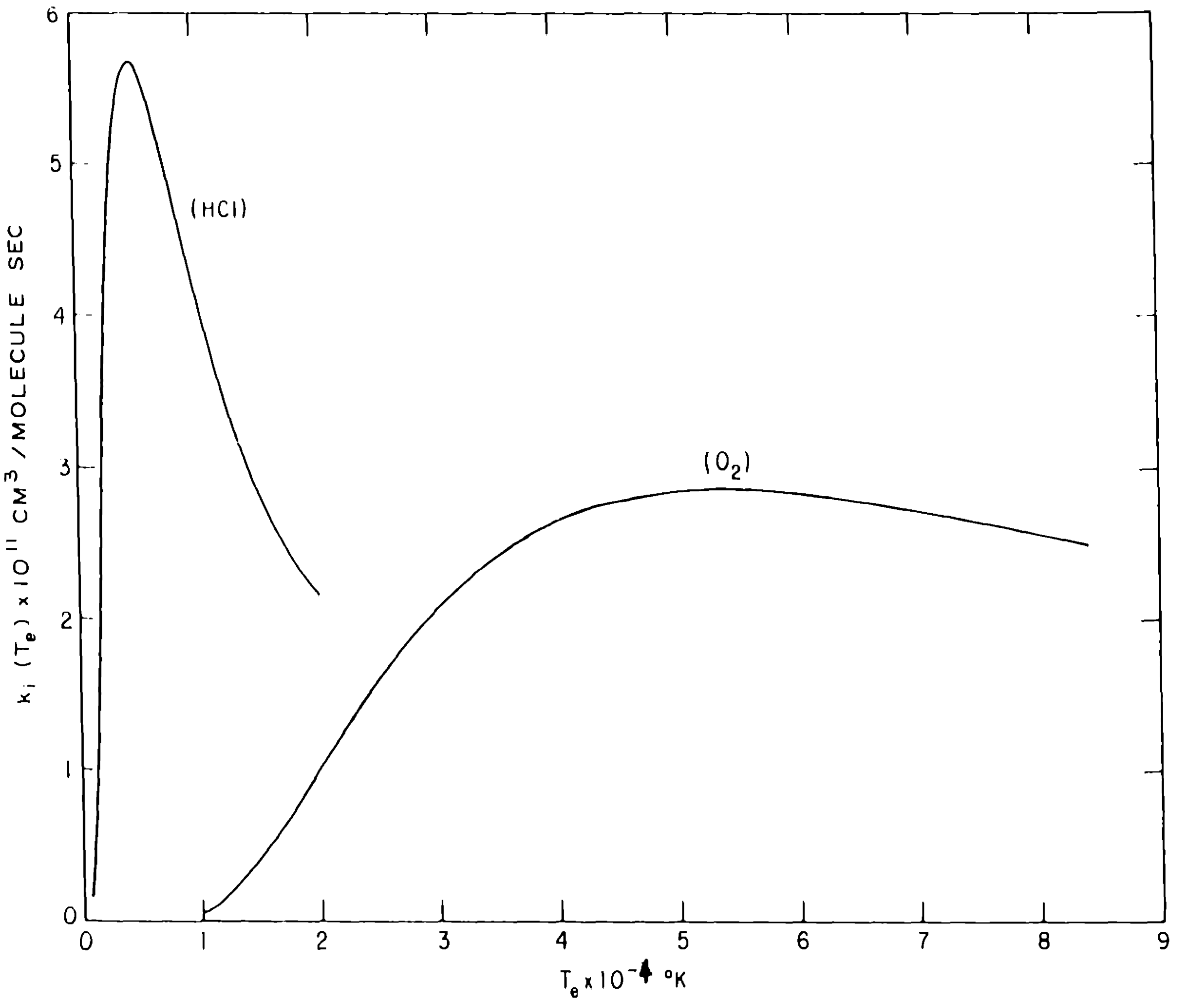

FIGURE 28 DISSOCIATIVE ATTACHMENT RATE CONSTANTS FOR HYDROGEN CHLORIDE AND OXYGEN VERSUS ELECTRON TEMPERATURE

$$P = V_{rms}^2/R \tag{29}$$

$$I_{rms} = V_{rms}/R$$

In addition it is assumed that the potential drop through the discharge is uniform and that the field strength is equal to V_{rms}/L, where L is the discharge length.

In order to choose a value of k_1 from Figure 27 or 28, it is necessary to know the value of T_e corresponding to the examined experimental conditions. The latter can be evaluated from Figure 6 of Chapter III if E/p' is known. For a given rms voltage this parameter can be approximated as V_{rms}/L (p 293/T) . The curves given in Figure 6 are for the pure materials, whereas here we are interested in finding T_e for a reacting gas mixture. This difficulty is gotten around by noting that hydrogen chloride always predominates in the system and consequently choosing the values of T_e from the corresponding curve. When this procedure is adopted and a few rough estimates of T_e are made, it is found that T_e lies in the range of 1500 to 10000 °K. As is seen from Figure 28 the value of k_2 over this range is very small and, as a result, the term $(B/A)(k_2/k_1)$ in equations (23a) and (23b) will be much less than one. For this reason the subsequent kinetic analyses are carried out neglecting the activation of oxygen in the case where oxygen and hydrogen chloride are both present in the discharge.

The electron density is taken to be uniform throughout the discharge zone and is expressed as

$$n_e = J/ev_d = \frac{V_{rms}}{R\pi a^2 \; ev_d} \qquad (30)$$

The value of the drift velocity is chosen from a plot of experimental values of v_d as a function of E/p' given by Bailey (48) and reproduced here in Figure 29.

The procedure for calculating a theoretical curve of the conversion of hydrogen chloride as a function of power at a constant pressure begins with the choice of a set of rms voltages such that the desired power range might be covered. For each of these values the power is computed from equation (29). Next, a value of ΔT^* is chosen and the ratio $T_g/293$ as well as the reduced pressure $p' = p\ 293/T_g$ are computed for each value of V_{rms}. Once p' is known E/p' can be evaluated, and the values of T_e and v_d can be chosen from Figures 6 and 29. The value of k_1 is now chosen from Figure 27 and the gas and electron densities are evaluated. Finally the product

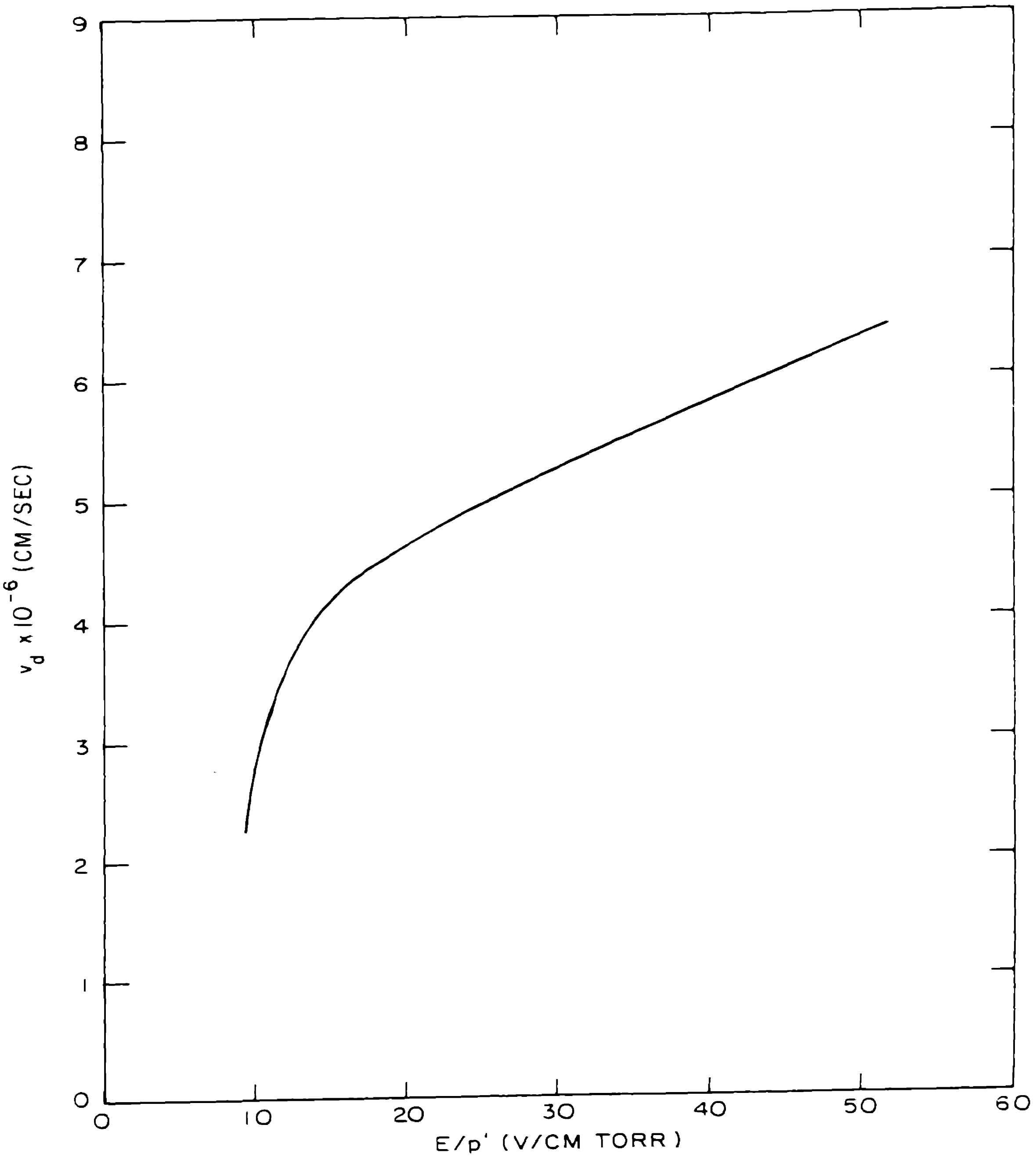

FIGURE 29 DRIFT VELOCITY VERSUS E/p'

$$k_1 \frac{p}{RT_g} n_e V/F_{HCl} = y_i/4A_i = C_i y_i \quad (i = 1,2) \qquad (31)$$

is determined where F_{HCl} is the molar flow rate of hydrogen chloride corresponding to the value for which the experimental data, being simulated, were taken.

The constant C_i in equation (31) is evaluated by setting the value of x_{calc} equal to x_{exp} at a particular power and then finding the value of y_i for this conversion from a plot of y_i versus x (Figure A-2). This procedure is carried out for the data taken at p = 7.50 Torr and F_{HCl} = 5.91 x 10^{-5} moles/sec. Once the value of C_i is found the other values of x_{calc} can be evaluated.

A comparison of the experimental and calculated values of conversion after one iteration shows that, although the calculated values pass through a maximum, the position of this maximum does not necessarily occur at the same power as does that for the experimental values. In order to rectify this a new value of ΔT^* is chosen so as to shift the position of the maximum. Smaller values will shift the maximum to higher powers and larger values to lower powers. The computational procedure described above is repeated, and the new values of x_{calc} are compared to the data. The iteration is continued until the position of the computed maximum and the value of the maximum conversion agree with the experimental ones. A sample calculation is given in Appendix A.

The procedure described above was used to fit the data for p = 7.50 Torr and F_{HCl} = 5.91 x 10^{-5} moles/sec, and the values of C_1 and C_2 thus obtained were taken to be a constant of the reaction system, independent of gas pressure and molar flow rate. Computations were then carried out for p = 3.75 Torr, F_{HCl} = 5.91 x 10^{-5}, 4.13 x 10^{-5}, and 2.07 x 10^{-5} moles/sec; p = 7.50 Torr, F_{HCl} = 4.13 x 10^{-5} moles/sec; p = 11.25 Torr, F_{HCl} = 5.91 x 10^{-5} moles/sec. For each pressure a new value of ΔT^* was chosen so as to best fit the data at that pressure. The results of these computations are shown in Figures 30, 31 and 32. In these figures the theoretical values of conversion are shown as points, whereas the solid lines represent a visual curve fit to the experimental data.

From Figure 30 it is seen that for p = 3.75 Torr and F_{HCl} = 5.91 x 10^{-5} moles/sec both the well-mixed and the plug flow model closely follow the experimentally observed conversions. As the molar flow rate is lowered, it becomes evident that the values predicted by the well-mixed flow model are in closer agreement with the experimental ones than those calculated from the assumption of plug flow. At a pressure of 7.50 Torr, Figure 31 shows that, again, for F_{HCl} = 5.91 x 10^{-5} moles/sec both flow models yield

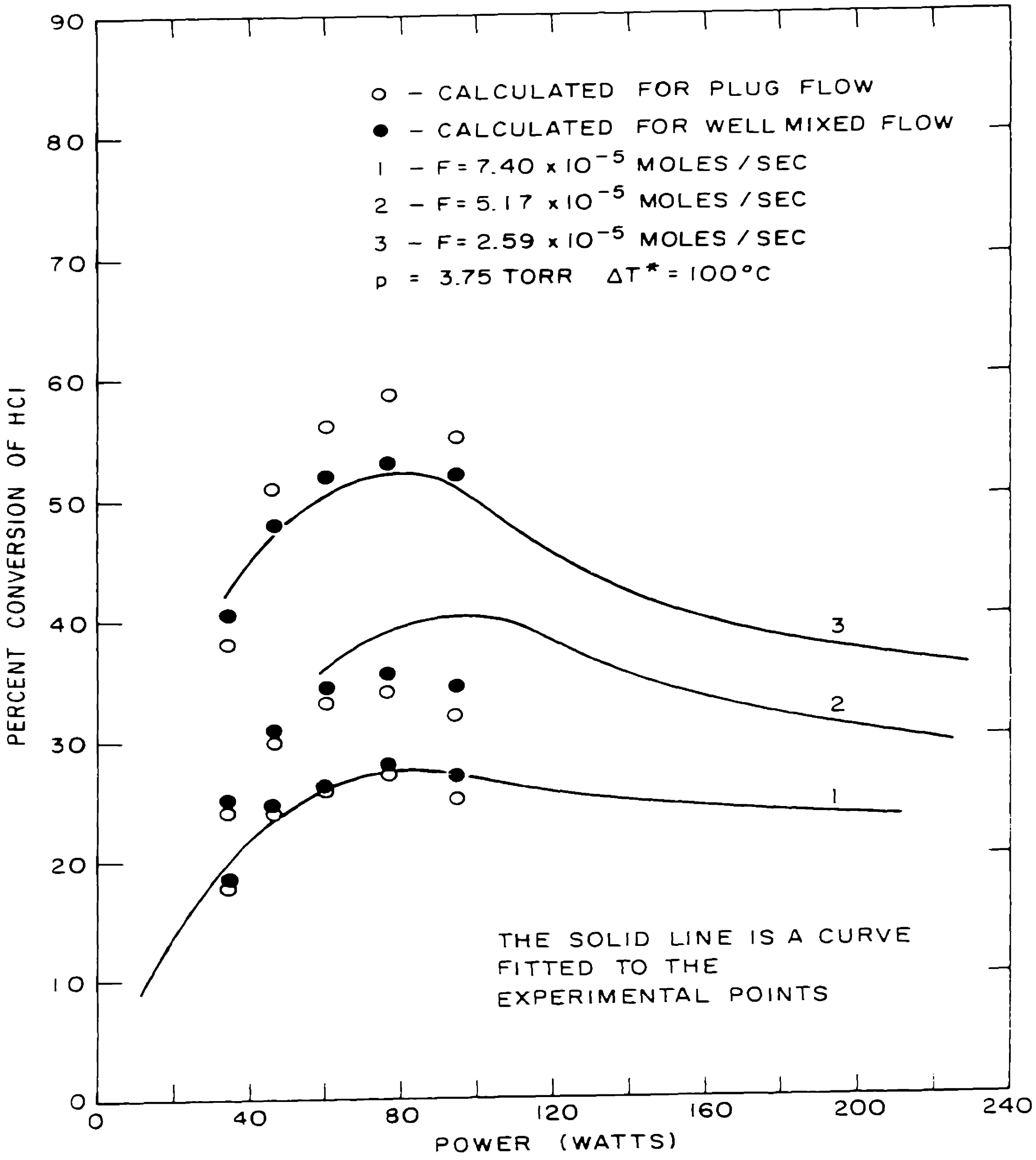

FIGURE 30 CALCULATED CONVERSIONS FOR THE FORWARD REACTION AT 3.75 TORR

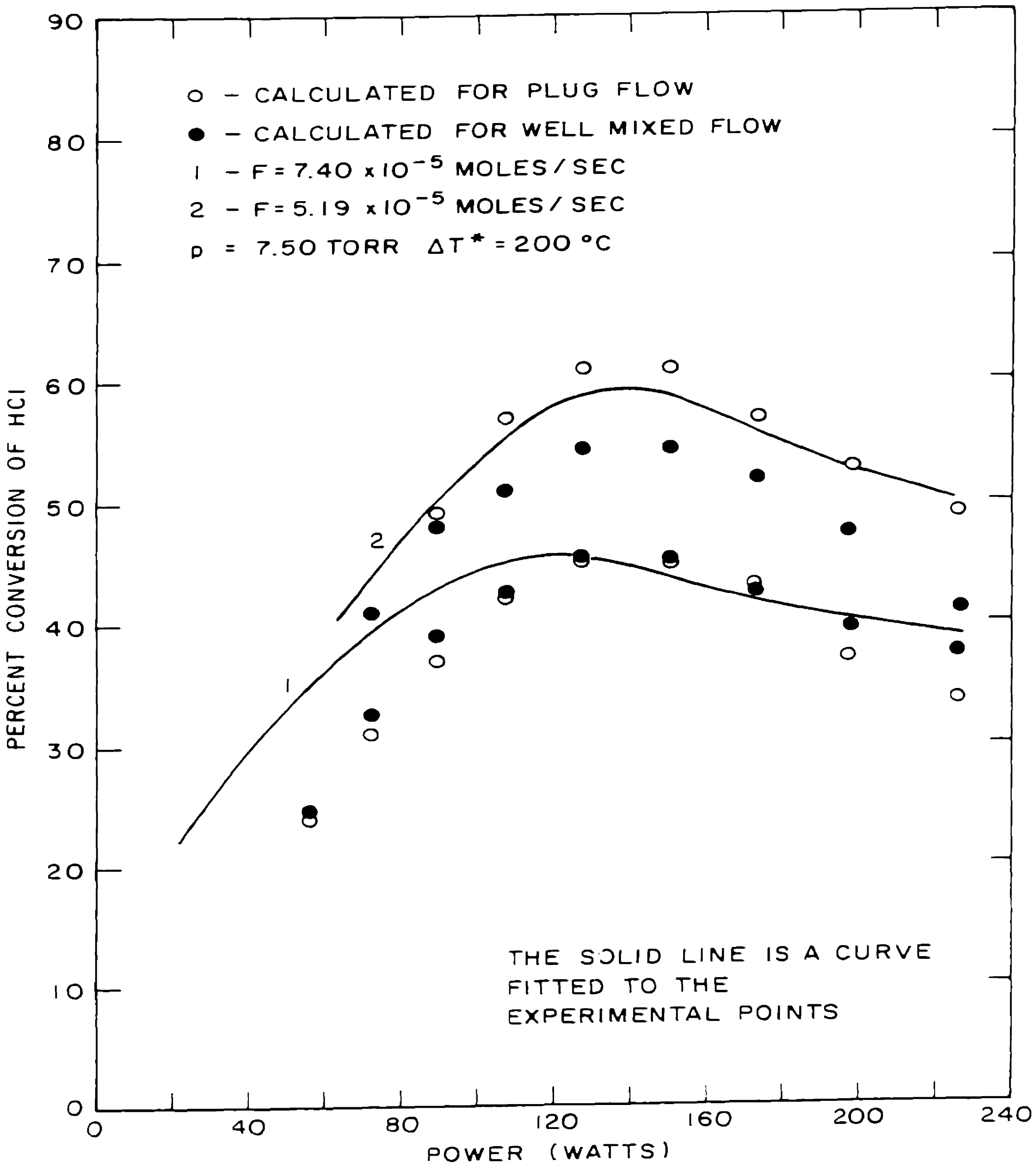

FIGURE 31 CALCULATED CONVERSIONS FOR THE FORWARD REACTION AT 7.50 TORR

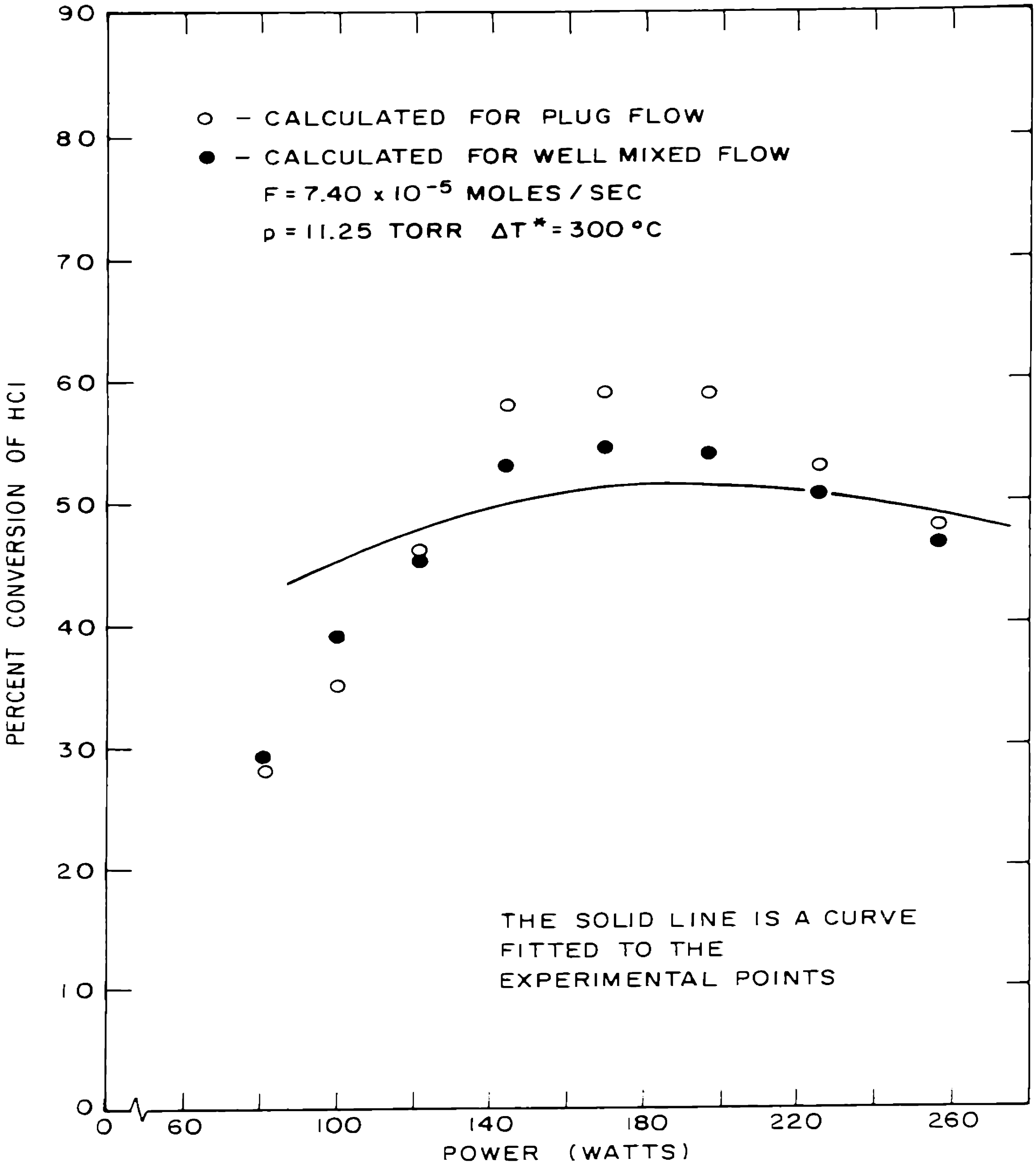

FIGURE 32 CALCULATED CONVERSIONS FOR THE FORWARD REACTION AT 11.25 TORR

practically identical results. However, in this case for F_{HCl} = 4.13 x 10^{-5} moles/sec, the plug flow results follow the experimental curve more closely than those for the assumption of well-mixed flow. Finally, for a pressure of 11.25 Torr and F_{HCl} = 5.91 x 10^{-5} moles/sec (Figure 32), the assumption of well-mixed flow gives a closer representation of the experimental conversion of hydrogen chloride.

An examination of Figures 30, 31, and 32 shows that the well-mixed flow model gives a slightly better fit to the experimental data than does the assumption of plug flow. At the low flow rates used in the present experiments, axial dispersion is predominantly due to molecular diffusion. A calculation of the variance (see Appendix A) gives a value of 0.49. This value is sufficiently large so that deviations from plug flow should, in fact, become noticeable.

In the calculation of the theoretical conversions shown in Figures 30, 31, and 32, the values of C_1 and C_2 have been held constant for all sets of conditions. These values result in A_1 = 3.2 and A_2 = 4.2, which are in close agreement with the value of A which results from an examination of the over-all forward reaction kinetics. As a result the constant A can be considered to be a unique characteristic of the reaction mechanism and not simply an adjustable parameter. In view of the fact that the derived values of A are close to four, it would appear that the assumption of step 6 in the reaction mechanism is more nearly correct than the assumption of steps 6a and 6b.

The proposed rate expression coupled with the assumption of complete mixing in the reactor is found to predict a maximum in the conversion hydrogen chloride as a function of power. Moreover, the model shows that the width of this maximum will broaden, and its position will shift to higher powers as the pressure is increased. This behaviour is a direct consequence of the variation of the rate constant k_1 with T_e.

The assumption that reaction 1 might be replaced by a thermal dissociation process is incorrect. Fishburne (49) has reported a thermal dissociation rate constant for hydrogen chloride equal to $1.92 \times 10^{11} \exp(-69700/RT)$ cm^3/mole sec. In order that this expression give a value comprable to that for k_1 at its maximum, i.e., 3.36×10^{13} cm^3/mole sec, the gas temperature would have to be above 4×10^4 °K. A temperature of this magnitude is certainly outside the range of values considered in the present work, and consequently it can be concluded that thermal collisions cannot be responsible for the dissociation of hydrogen chloride.

Over the range of electron temperatures considered, the term $B/A\ k_2/k_1$ (0.25) appearing in equation (23) is much less than one, so that the ratio of oxygen to hydrogen chloride does not appear explicitly in equations (23a) and (23b). As a result, these equations will respond to a change in the ratio of oxygen to hydrogen chloride indirectly. For a constant molar flow rate, $F_{HCl} = F_{HCl})_s \frac{1.25}{1 + \alpha}$ where $F_{HCl})_s$ is the molar flow rate of hydrogen chloride for a stoichiometric ratio of the reactants and $\alpha = (O_2)/(HCl)$. The total number of moles of gas is slightly changed when α is increased. Thus the term 5 appearing in the denominator of equations (22a) and (22b) becomes $4(1+\alpha)$. If the form of equations (21) through (23) is not altered, except to introduce the value of those terms affected by a change in α, a slight decrease results in the conversion of hydrogen chloride as α is increased. This behaviour is not consistent with the experimental data which show a marked increase in conversion as α is increased. An empirical correction can be introduced which allows the experimental data to be fit by the theoretical model. The empiricism consists in multiplying the left hand side of equations (23a) and (23b) by $\alpha/0.25$ and letting $F_{HCl} = F_{HCl})_s \frac{1.25}{1 + \alpha}$. The curves of y_1 and y_2 to be used with these conditions remain unchanged and are not corrected for variations in α. The calculated conversions, using the proposed corrections, are shown in Figure 33. It is seen that the empirical adjustment of equation (23)

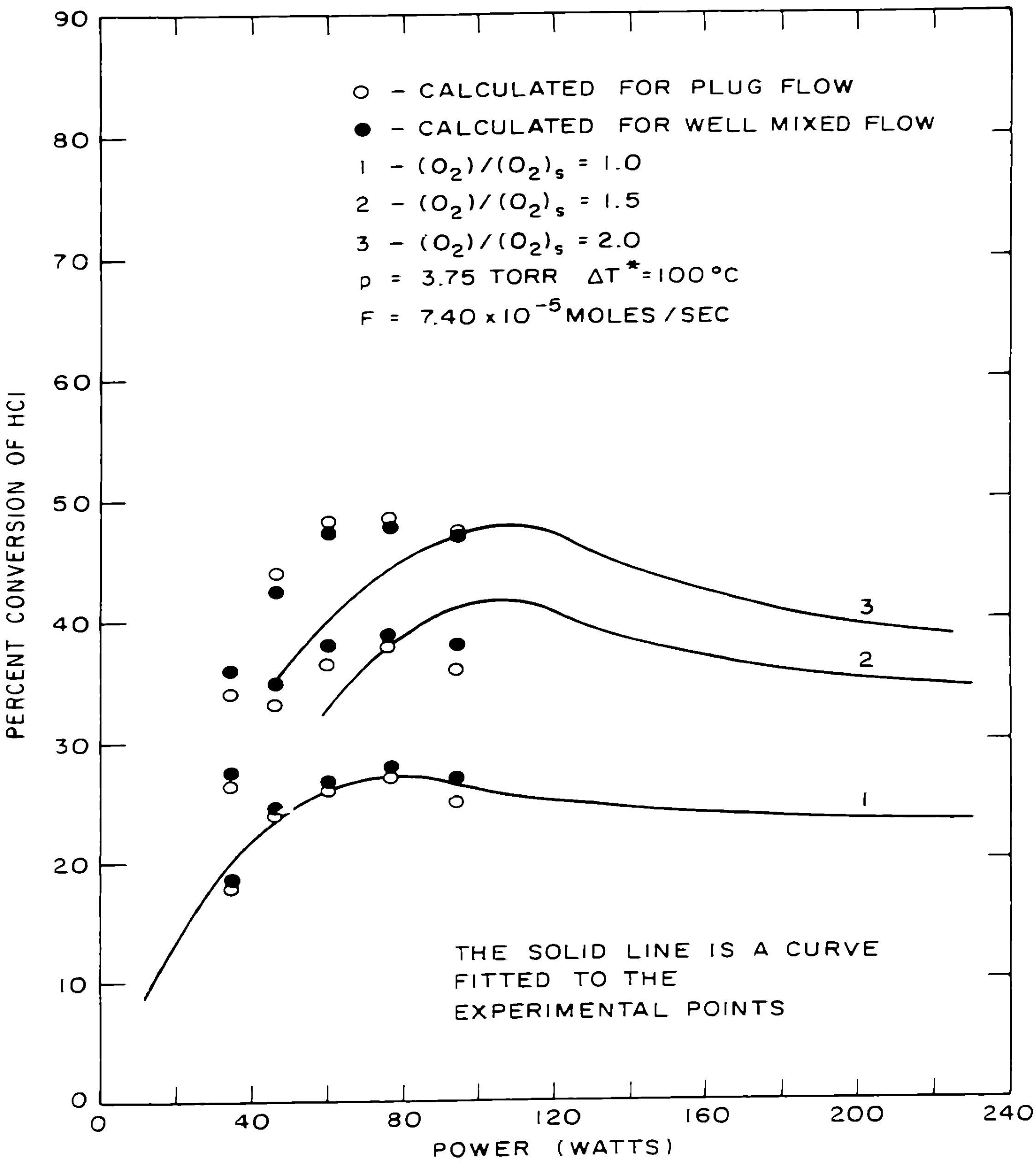

FIGURE 33 CALCULATED CONVERSION FOR THE FORWARD REACTION AT 3.75 TORR TAKING INTO ACCOUNT VARIATIONS IN O_2/HCl

predicts the correct magnitude of increased conversion for an increase in α. The lack of correspondence between the calculated points and the curves marked 2 and 3 is probably due to a persistent error in the measured values of the power for the experimental data associated with these curves. If curves 2 and 3 are shifted by ~ 40 watts to the left, the agreement with the calculated points would be comparable to that obtained in Figures 30, 31 and 32.

b. Power Consumption

The rate of hydrogen chloride consumption per unit power supplied to the discharge is defined as η. Experimentally this parameter is determined from the expression

$$\eta_{exp} = \frac{x_{exp} F_{HCl}}{P} \qquad (32)$$

Since it was shown in the previous section that a theoretical model of the reaction mechanism and reactor flow pattern could be made to predict the conversion of hydrogen chloride, it will be of interest to extend this model to see how well it will predict η.

At any point within the reactor we can write

$$\eta(x) = \frac{Ak_1 \frac{p}{RT_g} \frac{4(1-x)}{(5-x)} n_e}{n_e \, ev_d \, E} \tag{33}$$

$$= \frac{A(k_1/RT_s) \frac{4(1-x)}{(5-x)}}{ev_d \, E/p'}$$

where $T_s = 293\ ^oK$. The numerator in equation (33) is the rate of hydrogen chloride consumption per unit discharge volume as given by equation (22). Looking at equation (22b) we see that we can also set

$$\eta(x) = \frac{x \, F_{HCl}}{\overline{P} \, V} \tag{34}$$

Then equating equations (33) and (34) we find

$$\eta^* = \frac{k_1/RT_s}{e \, v_d \, E/p'} = \frac{F_{HCl}}{P} \frac{(5-x)x}{4A(1-x)} \tag{35}$$

The parameter η^* is solely a function of E/p', and, thus, the right hand side of equation (35) must also be a unique function of E/p'. If the rate of the over-all chemical reaction is governed by the dissociative attachment of hydrogen chloride, then the experimental data should correlate on a plot of η^* versus E/p'. Figure 34 shows that η^* calculated on the basis of Bailey's data (48)

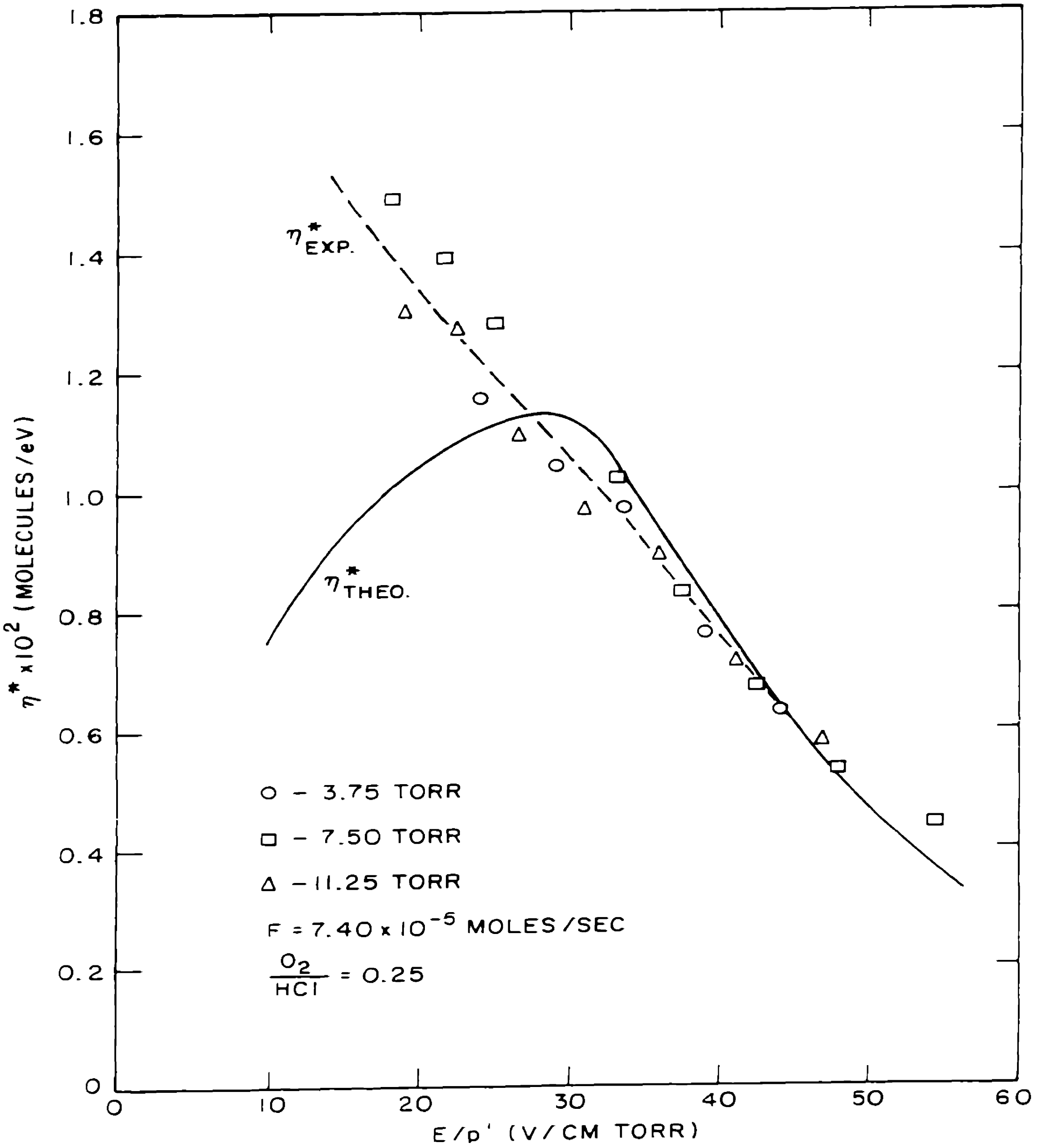

FIGURE 34 THE NUMBER OF HYDROGEN CHLORIDE MOLECULES DISSOCIATED PER UNIT OF ENERGY

for hydrogen chloride and the derived values of k_1 passes through a maximum of 1.13×10^{-2} molecules of HCl dissoc./eV at E/p' = 28.5 V/cm Torr. The points shown in Figure 34 were calculated by evaluating the right hand side of equation (35) for the experimental values of x. The value of E/p' associated with each point was determined from the measured voltage and the expression $p' = p\ 293\ ^{\circ}K/T_g$. The gas temperature T_g was evaluated from equation (25) using the value of ΔT^* appropriate for each pressure.

The experimental points are seen to correlate quite well with each other and with the theoretical curve for E/p' greater than 30 V/cm Torr. Below this value the experimental points still correlate with each other, but the theoretical curve sharply diverges from the experimental points, dropping off to lower values of η^*. It is believed that the discrepancy between the theoretical curve of η^* and the one represented by the experimental points is due to the sensitivity of k_1 for low values of E/p' (see Figure 25). If the value of k_1 had risen more rapidly in the region of $10 < E/p' < 25$ V/cm Torr, the maximum in the curve of η^* would have occurred at a lower value of E/p'. Unfortunately, the experimental data could not be extended to sufficiently low values of E/p' to determine whether the experimental values of η^* would finally pass through a maximum. The fact that data for different pressures can be represented by a single line, however, does indicate that the reaction proceeds by an electron collision process which can be correlated in terms of E/p'.

In order to evaluate the performance of the discharge reactor, the inverse of equation (35) has been evaluated from the experimental data and plotted in Figures 35 and 36 in terms of the power consumed per pound of chlorine produced. At a fixed pressure the power consumption rises linearly at first and then with increasing rapidity as the power is increased further. For a particular pressure the best performance, as measured by $1/\eta$, is obtained near the point of extinction of the discharge. This roughly corresponds to the first experimental point on each constant pressure curve. An increase in pressure produces a decrease in the power consumption, but this method of improving performance finally yields a minimum value of $1/\eta$ for a particular power. Further increase in pressure leads to an increase in P/x as can be seen from Figure 21 and would cause $1/\eta$ to increase again. Figure 36 shows that the power consumption also decreases for an increase in the total molar flow rate or an increase in the ratio of oxygen to hydrogen chloride in the feed. The available experimental data showed that the best performance was obtained for 7.50 Torr, $P = 40$ watts, $F = 7.40 \times 10^{-5}$ moles/sec, $O_2/HCl = 0.25$ at which point $1/\eta = 8.4$ kwhr/lb Cl_2 produced. This

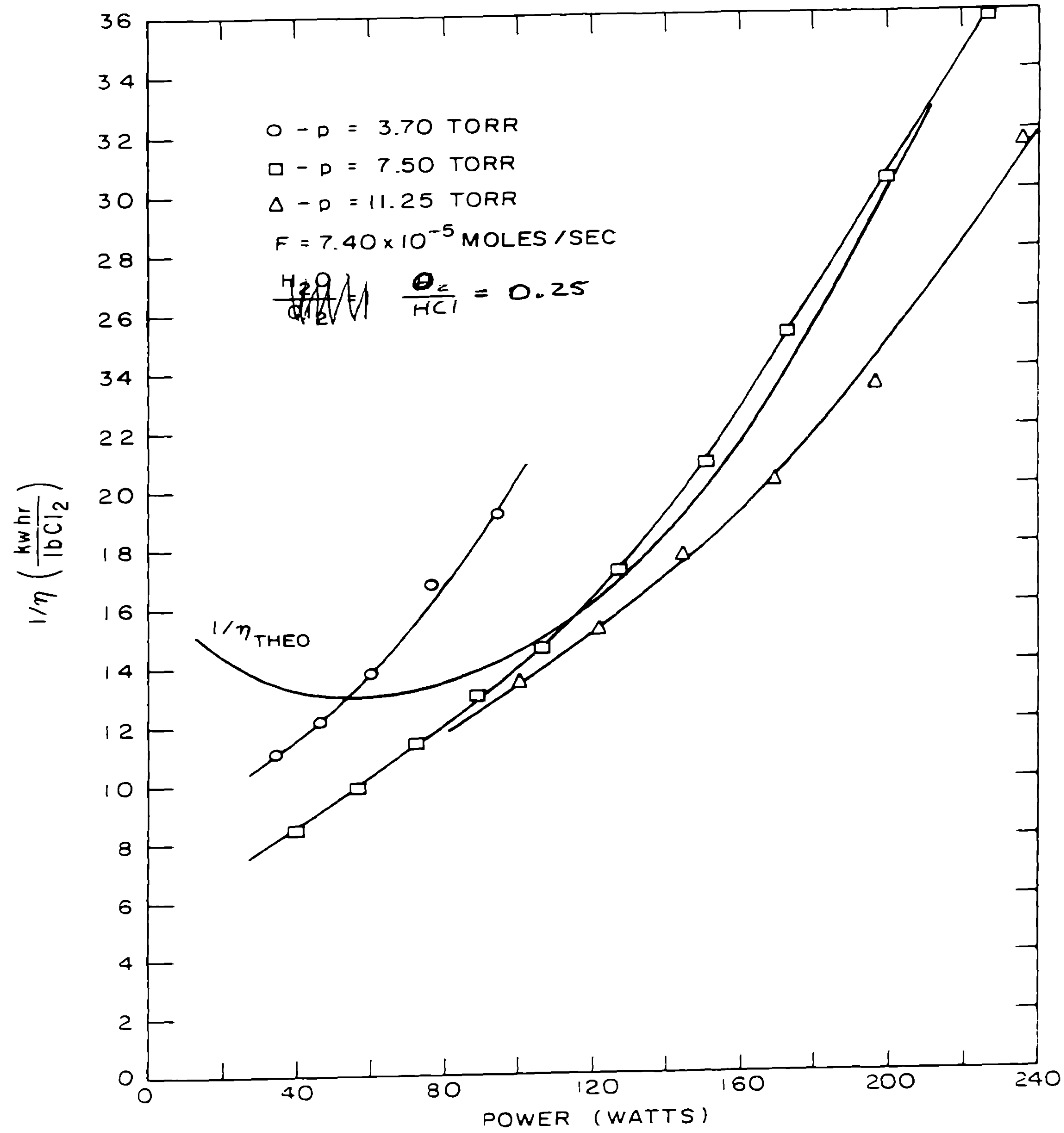

FIGURE 35 THE EFFECT OF PRESSURE ON THE POWER CONSUMED PER POUND OF CHLORINE PRODUCED

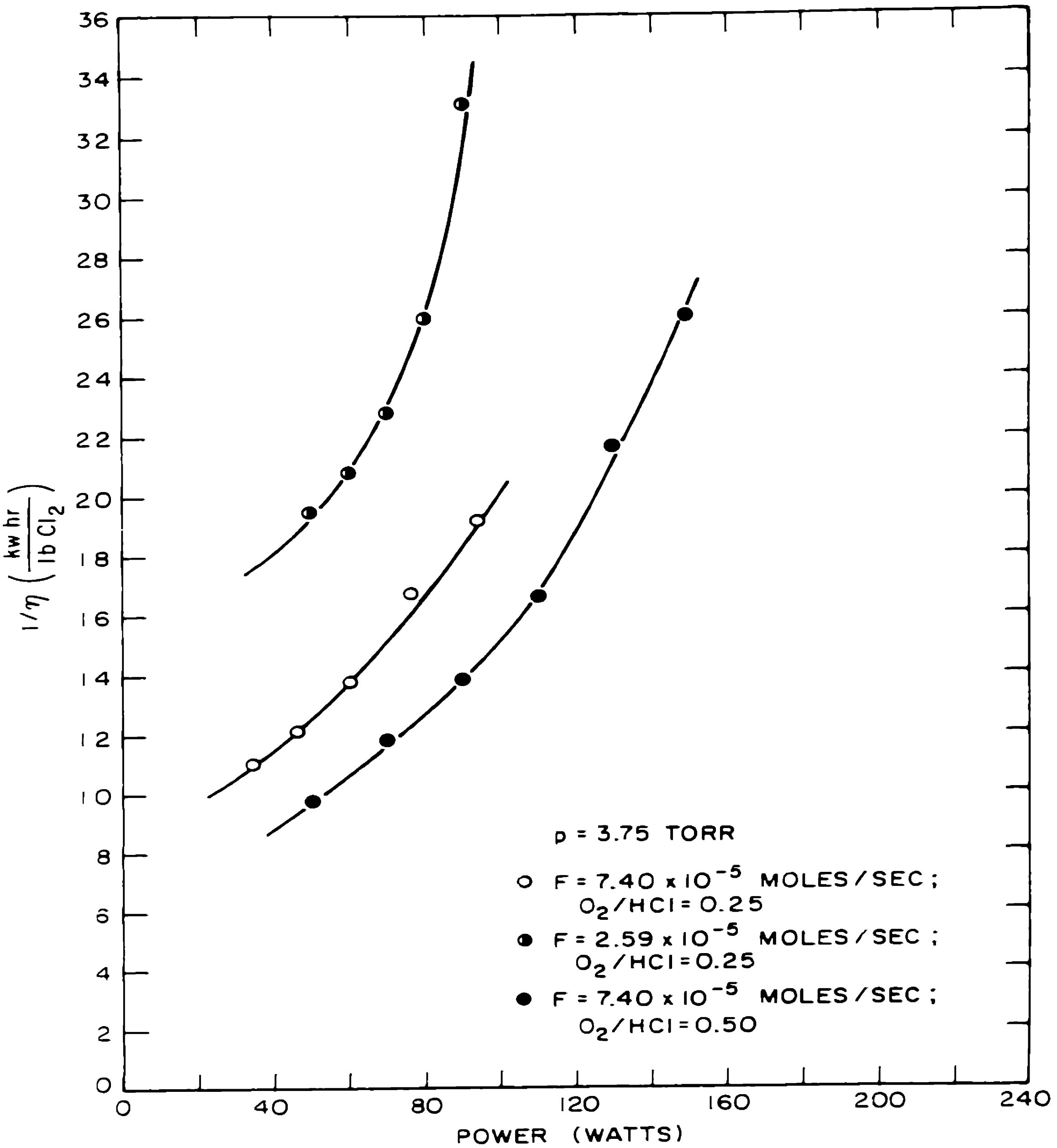

FIGURE 36 THE EFFECT OF FLOW RATE AND O_2/HCl RATIO ON THE POWER CONSUMED PER POUND OF CHLORINE PRODUCED

value is to be compared with $1/\eta = 2.38$ kwhr/lb Cl_2 obtained by Cooper (31) in a microwave discharge operating at 2450 MHz, P = 265 watts, p = 20 Torr, $F_{HCl} = 1.41 \times 10^{-4}$ moles/sec, and $O_2/HCl = 0.25$.

A theoretical curve of power consumption at 7.50 Torr has been drawn in Figure 35. This curve is determined by evaluating equation (33) from $1/\eta^*$ and the calculated values of x. The theoretical curve of $1/\eta$ is seen to diverge from the experimental one at low power and pass through a minimum of 13 kwhr/lb Cl_2. This value, thus, represents the minimum energy required as determined from the model for the reaction process. It is expected that the experimental data should also pass through a minimum for very low powers as a result of E/p' becoming so small that the reaction rate constant approaches zero. At present these powers cannot be reached since they lie below the power at which the discharge will extinguish. The discrepancy between the theoretical and experimental minimum values of $1/\eta$ is due to the form of $1/\eta^*$ and in turn k_1. Had the curve of k_1 versus E/p' risen more rapidly for low values of E/p', the theoretical minimum value of $1/\eta$ would have been less.

2. Reverse Reaction

a. Effect of Power on Conversion at Constant Pressure

Reactions 3,8,9,10, and 14 were chosen to describe the reverse reaction in which a stoichiometric mixture of water vapor and chlorine are passed through the discharge. The dissociative attachment involving chlorine has been neglected since it was shown from the separated feed results that the dissociation of chlorine does not lead to the conversion of chlorine to hydrogen chloride.

The five reaction steps considered given an expression for the rate of hydrogen chloride appearance of the following form:

$$\frac{d(HCl)}{dt} = Dk_3(H_2O)(e)$$

where D = 4/3. Taking a mass balance around a differential slice of the reactor, for the assumption of plug flow, and around the whole reactor, for the assumption of well-mixed flow, the following equations are obtained.

$$Dk_3(H_2O)(e) = 2\, F_{H_2O}\, \frac{dx}{dV} \qquad (36a)$$

$$Dk_3(H_2O)(e) = 2\, F_{H_2O}\, \frac{x}{V} \qquad (36b)$$

Rewriting equations (36a) and (36b) in terms of the fractional conversion of chlorine, we obtain

$$Dk_3 \ \frac{2(1-x)}{(4+x)} \ \frac{p}{RT_g} \ n_e \ = \ 2 \ F_{H_2O} \ \frac{dx}{dV} \qquad (37a)$$

$$Dk_3 \ \frac{2(1-x)}{(4+x)} \ \frac{p}{RT_g} \ n_e \ = \ 2 \ F_{H_2O} \ \frac{x}{V} \qquad (37b)$$

Equation (37c) can be integrated from zero to x, and this integral and equation (37b) can be expressed as

$$k_3 \ \frac{p}{RT_g} \ n_e \ V/F_{H_2O} \ = \ y_1/D_1 \qquad (38a)$$

$$k_3 \ \frac{p}{RT_g} \ n_e \ V/F_{H_2O} \ = \ y_2/D_2 \qquad (38b)$$

where y_1 and y_2 are given by

$$y_1 \ = \ -5\ln(1-x)-x$$

$$y_2 \ = \ x(4+x)/(1-x)$$

The constants on the right hand side of equations (38a) and (38b) can be computed in the same manner as were those in the case of the forward reaction. Since the feed for the reverse reaction is an equimolar mixture of chlorine and water vapor, it was decided to determine T_e and v_d for the mixture rather than using the values for only one of the reactants. The drift velocity for the mixture is approximated by choosing a value from a plot of v_d versus E/p' for chlorine and water vapor which lies intermediate between those for the pure components. The electrom temperature is approximated by taking advantage of the expression

$$T_e = \frac{G}{\delta^{1/2}\,\overline{Q}}\,\frac{E}{p'} \qquad (39)$$

where $\overline{Q}$ is the average elastic collision cross section, δ the fraction of energy lost by an electron per collision and G = const. Equation(39) was previously derived in Chapter III to illustrate the qualitative relationship between T_e and E/p'. For a mixture of gases we may write

$$(E/p')_m^2 = \frac{1}{G^2}\,T_e^2\,\delta_T\,\overline{Q}_m^{\,2} \qquad (40)$$

where

$$\delta_T = x_1\delta_1 + x_2\delta_2 \qquad (41)$$

and $\overline{Q}_m$ is the average elastic cross section for the mixture. If Q_m does not differ very greatly from Q_1 or Q_2, it is possible to express equation (40) as

$$(E/p')^2_m = \frac{1}{G^2} T^2_e \left[x_1\delta_1 + x_2\delta_2 \right] \overline{Q}_m^{\,2} \qquad (42)$$

$$= x_1(E/p')^2_1 + x_2(E/p')^2_2$$

Equation (41) can then be used to evaluate E/p' for each value of T_e, using the data for the pure components.

An evaluation of the ability of equations (38a) and (38b) to describe the conversion of chlorine was carried out for the case of p = 7.50 Torr, $F_{H_2O} = 3.7 \times 10^{-5}$ moles/sec. The value of ΔT^* which gave the best fit at 7.50 Torr for the forward reaction was again used in the calculations here. The results are shown in Figure 37. It is seen that, although the calculated points show the correct trend, the rate of increase with conversion is greater than that exhibited by the data. The values of D_1 and D_2 used to fit the data in this case are equal to 20.4 and 25.2 respectively. These values do not coincide very well with the value of 4/3 derived for the proposed mechanism. It should be noted, however, that the calculated conversions rise monatonicly and do not pass through a maximum. This behaviour is due to the fact that for the range of T_e considered the value of k_3 does not pass through a maximum.

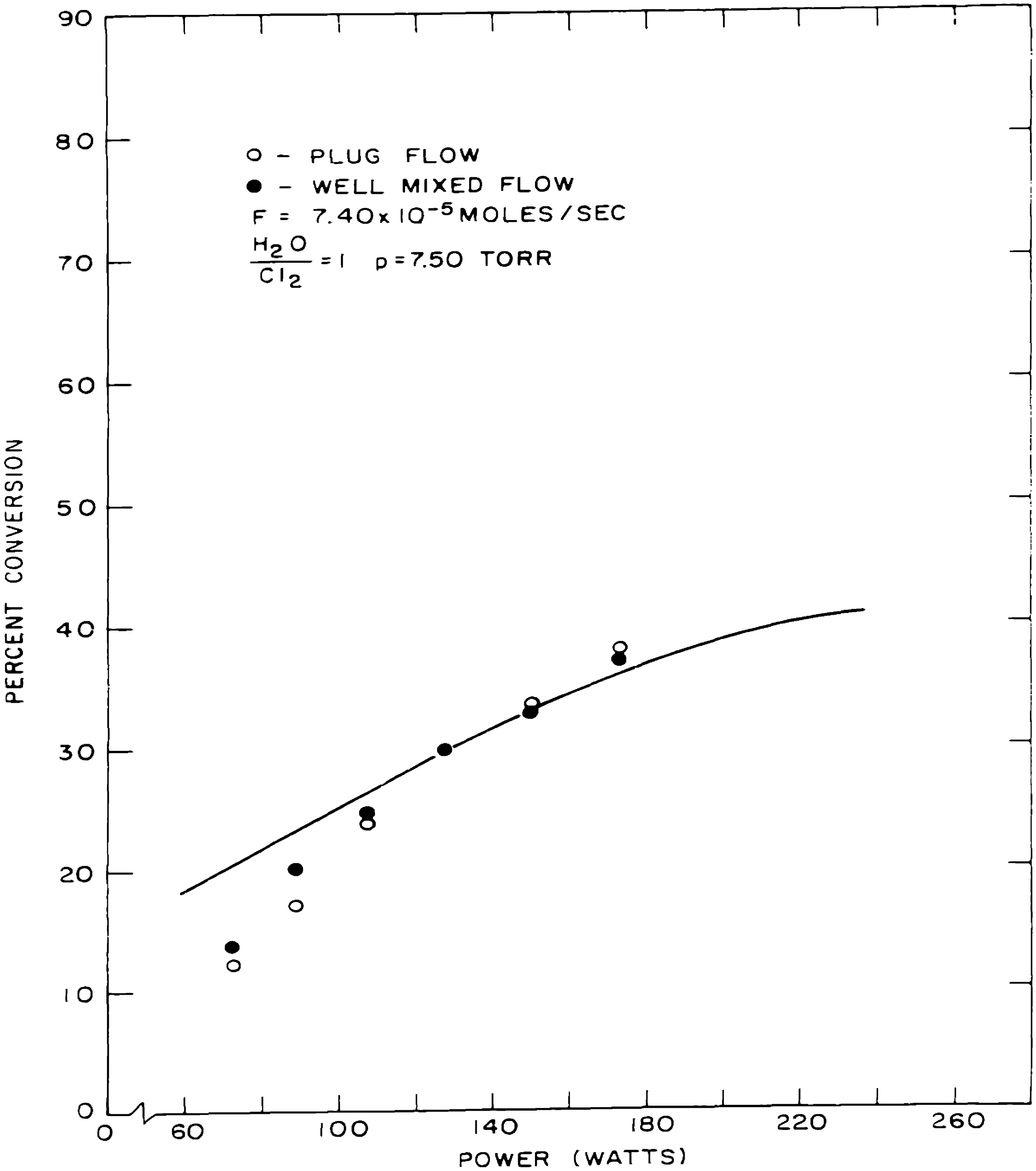

FIGURE 37 CALCULATED CONVERSION FOR THE REVERSE REACTION

B. Equilibrium

The relation of thermodynamic equilibrium to a chemical reaction occurring in a gas discharge is of great interest. At steady state in such a system two temperatures are needed to describe the average energies of the particles, and, consequently, the question arises as to whether the conventional concepts of chemical equilibrium can be used in order to predict the uppermost degree of conversion. Several investigators have examined this topic and have found that in some ways chemical reactions occurring in gas discharges do behave in a manner predicted by classical thermodynamics. On the other hand it has also been shown that the normal composition-temperature relations do not always hold. As a consequence, it will be useful to review these previous observations before examining the case for the present system.

Extensive investigations were made by Vasilev (50) on the formation of nitric oxide from nitrogen and oxygen in a 50 Hz arc operating at moderate powers over the pressure range of 20 to 760 Torr. Of specific interest are those studies which were made with a flow system in order to investigate the effects of the discharge on the forward and reverse reactions. These results are shown in Figure 38 as the percent of nitric oxide in the products as a function of the inverse volumetric flow rate. Looking at

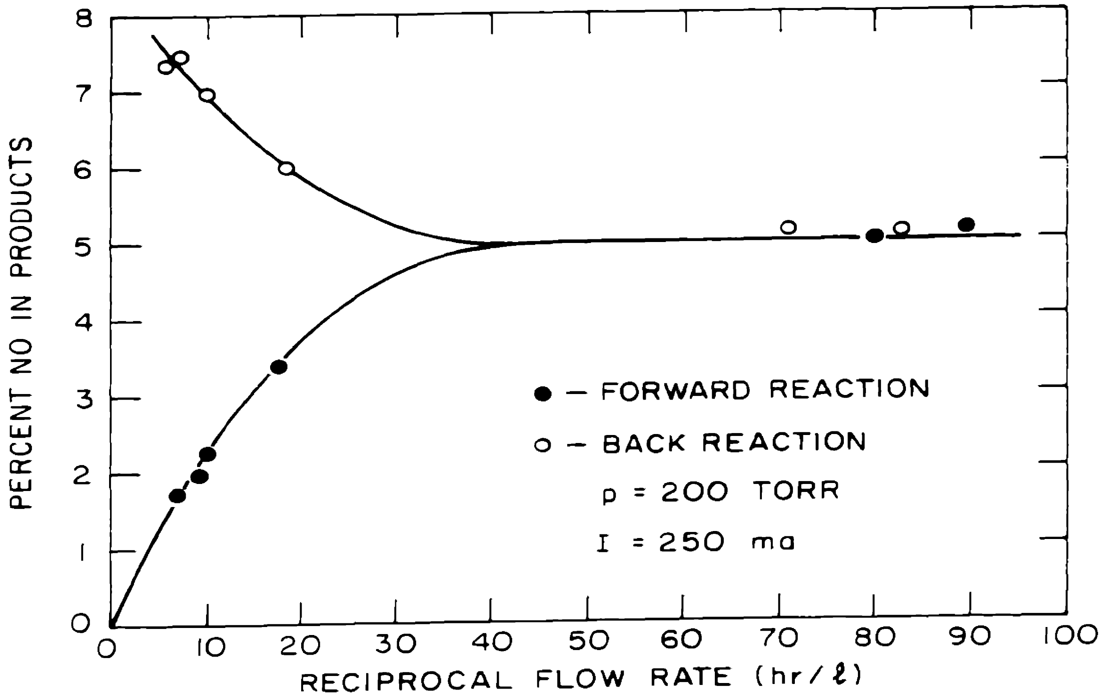

FIGURE 38 KINETIC CURVES FOR THE OXIDATION OF NITROGEN

this curve we see that a steady state concentration of nitric oxide is approached independent of whether air is used as the starting material or air to which ~9% nitric oxide has been added.

A later investigation by Vasil'ev (28) studied the effects of the discharge conditions on the steady state production of nitric oxide in a closed system. A summary of part of this data is given in Table 4. It is evident that the percent of nitric oxide found in the products is considerably higher than that predicted by chemical equilibrium for the measured temperature of the arc. Alternately, evaluating the equilibrium predicted gas temperatures to which the observed concentrations correspond, it was found that this value was higher than the measured value. To this is added the observation that even had the equilibrium temperature existed in the discharge, the decomposition rate of nitric oxide at this temperature would have been so high that it would have been impossible to quench the gas sufficiently rapidly to preserve the high temperature product composition. Further observations showed that, although equilibrium predicted a maximum yield of nitric oxide from an equimolar mixture of nitrogen and oxygen, this was not observed when the reaction was carried out in the discharge. There it was found that at a pressure of 130 Torr the maximum yield occurred for a nitrogen rich

Table 4

Summary of Vasil'ev's Data on Nitric Oxide Formation in an Arc

Pressure (Torr)	Current (ma)	Power (watts/cm)	Feed Composition	Observed % NO	Equilibrium % NO
760	100	25.5	air	4.0	0
150	200	46	air	8.12	0.9
150	800	92	air	8.32	1.8
150	860	86	45% N_2	11.75	1.8

% NO	Equilibrium Temperature (°K)	Measured Temperature (°K)
4	3000	1000
8	3900	1400
12	4100	1900

mixture and that at 560 Torr for an oxygen rich mixture.

Blaustein and Fu (20) found in their study on the formation of hydrocarbons from carbon monoxide and hydrogen in a static system using a mixrowave discharge to excite the gas that the amount of acetylene formed was greater than that predicted by equilibrium for the estimated gas temperature. However, the response of this system to composition changes was in keeping with Le Chatelier's principle applied to equilibrium systems.

A theoretical model of chemical reaction occurring in a nonequilibrium steady state discharge has been postulated by Manes (51). He proposes that a unique "temperature" might be associated with each degree of freedom of each molecular specie. A statistical mechanical treatment of this model shows that the composition dependence for any fixed set of "temperatures" is the same as for an equilibrium system, although, now, the equilibrium constant dependence on temperature becomes quite complex. A similar conclusion was arrived at by Potapov (52) who, in addition, proposes an expression which describes the temperature variation of the equilibrium constant. This relationship is given by

$$K_n = \pi_i \, n_i^{\nu_i} = e^{-\sum_i \frac{\nu_i \epsilon_{io}}{kT_g}} \; \pi_i \left[\left(\frac{m_i kT_g}{2\pi \hbar^2}\right)^{3/2} \pi_p \, (Z_{ip})^{\frac{T_{ip}}{T_g}} \right]^{\nu_i} \tag{43}$$

where

$$Z_{ip} = \sum_j \exp\left(- \frac{\epsilon^p_{ij} - \epsilon^p_{io}}{kT_{ip}}\right) \tag{44}$$

n_i is the concentration of the i-th specie, ν_i, the stoichiometric coefficient of the i-th specie, Z_{ip}, the partition function for the p-th degree of freedom of the i-th specie, ϵ_{io}, the lowest energy state for the i-th specie, ϵ^p_{ij}, the j-th energy level for the i-th specie and the p-th degree of freedom, T_{ip}, the temperature corresponding to the p-th degree of freedom of the i-th specie. For T_{ip} = T_g equation (43) reduces to the conventional expression for K_n in terms of the individual molecular partition functions. The effect of a difference between T_g and T_{ip} is felt through the fact that each partition function for each degree of freedom is evaluated at T_{ip} and, in addition, is raised to the power T_{ip}/T_g.

The above pieces of evidence indicate that, although a steady state product composition can be observed for chemical reactions occurring in an electric discharge, the magnitude of this composition is not necessarily predicted by the gas temperature alone. There are indications, however, that the composition will respond to the Law of Mass Action in a manner identical to that for an equilibrium system. These conclusions are found to hold for the chemical system studied in this work.

The data presented in Figure 21 show that as the total molar flow rate is reduced and the pressure is increased, an asymptotic concentration of chlorine is approached for both forward and reverse reactions. This approach to a steady state value is identical to one in which the space time is decreased, since for the present situation an increase in pressure or a decrease in total molar flow rate leads to an increase in the reaction rate. As the pressure is raised beyond the point of convergence, it is found that the asymptotic concentration decreases slightly.

A calculation of the effects of temperature on the equilibrium conversion of hydrogen chloride is illustrated in Figure 39. An increase in temperature produces a decrease in conversion, while increases in either the total pressure or the ratio of oxygen to hydrogen chloride produce an increase. It should also be noted that if a simultaneous change in pressure and temperature is made, the conversion will decrease if the temperature increase is greater than that between two isobars at constant conversion and correspondingly will increase if the temperature increase is less than this value. The question that now arises is

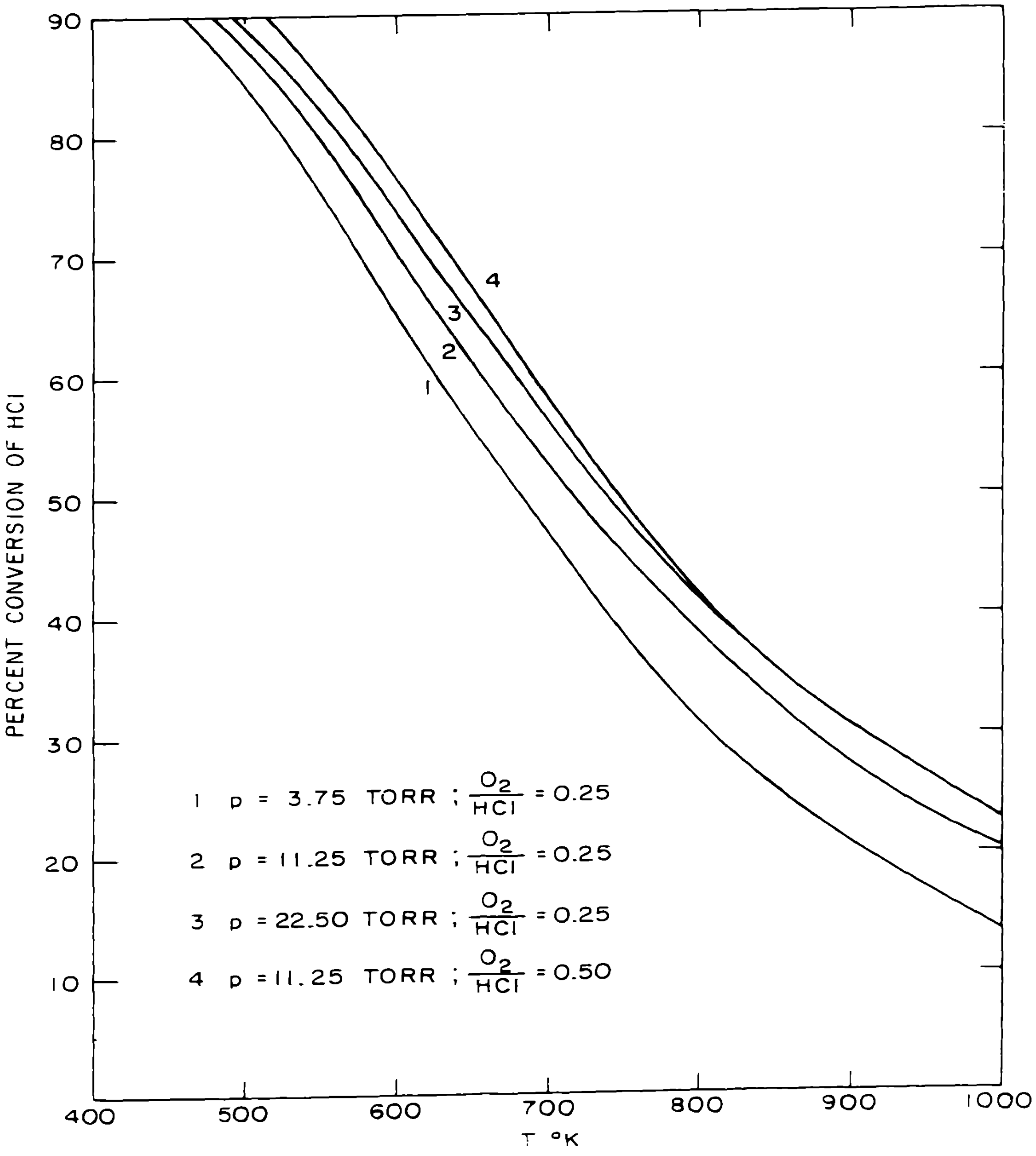

FIGURE 39 EQUILIBRIUM CONVERSION VERSUS TEMPERATURE

whether the observed behaviour of the asymptotic chlorine concentration is consistent with the trends predicted by equilibrium for the over-all reaction.

Figure 21 shows that at 11.25 Torr $a_\infty = 0.4$ or $x_\infty = 57\%$. This conversion corresponds to an equilibrium temperature of 402°C which can be compared with the value of 320°C used in the discussion of the kinetics of the reaction. At 22.50 Torr $a_\infty = 0.375$ or $x_\infty = 54.5\%$, and the equilibrium temperature is equal to 445 °C. On the other hand, if the same rate of gas temperature increase with pressure is assumed as was used for the kinetic discussion, a gas temperature of 600 °C would be estimated for this pressure. Thus, although the values of a_∞ decrease in a manner predicted by equilibrium for a simultaneous increase in temperature and pressure, the values of the equilibrium and gas temperatures for a particular conversion do not agree.

For a series of runs made at 11.25 Torr, $O_2/HCl = 0.5$, and $F = 2.59 \times 10^{-5}$ moles/sec, i.e., at sufficiently high pressure and low molar flow rates as to assure steady state conditions, the conversion was 68% or $a_\infty = 0.51$. The equilibrium diagram shows that had the change in feed composition not affected the gas temperature the conversion at this pressure should have risen to 63%. Again the observed behaviour follows the direction established by conventional thermodynamics, but the numerical values do not quite agree.

The variation of the conversion with respect to changes in pressure, gas temperature, and the ratio of oxygen to hydrogen chloride in the feed indicates that the system behaves as though it were at a steady state describable by an equilibrium constant. However, it does not appear that the numerical values of the conversion can be derived solely from a knowledge of the gas temperature, pressure, and the ratio of oxygen to hydrogen chloride in the feed.

C. Separated Feed

Investigation of the separate introduction of either hydrogen chloride or oxygen into the discharge with the subsequent addition of the second reactant immediately below the discharge showed that dissociation of either reactant will lead to a conversion of hydrogen chloride. The data in Figure 22 show that the dissociation of oxygen leads to a slightly higher conversion at low power, but that for powers above 160 watts the dissociation of hydrogen chloride becomes much more effective.

A possible reaction mechanism for the case in which hydrogen chloride is discharged might consist of the steps

6. $H + O_2 \longrightarrow OH + O$

or 6a. $H + O_2 + M \longrightarrow HO_2 + M$

6b. $H + HO_2 \longrightarrow 2\ OH$

5. $O + HCl \longrightarrow OH + Cl$
7. $OH + HCl \longrightarrow H_2O + Cl$
14. $2\,Cl + M \longrightarrow Cl_2 + M$
11. $H + Cl + M \longrightarrow HCl + M$

This set of reactions would give a ratio of chlorine produced to hydrogen chloride dissociated which is less than or equal to two if step 6 is considered and less than or equal to one if steps 6a and 6b are considered. For the case in which oxygen is discharged, the reaction mechanism might take the form

5. $O + HCl \longrightarrow OH + Cl$
7. $OH + HCl \longrightarrow H_2O + Cl$
14. $2\,Cl + M \longrightarrow Cl_2 + M$
12. $2\,O + M \longrightarrow O_2 + M$

Here the ratio of chlorine produced to oxygen dissociated would be less than or equal to two. Hence, the mechanisms for the conversion of hydrogen chloride to chlorine predict that for equal degrees of dissociation of the discharged gas either activation process should give approximately the same amount of chlorine. If the postulated reaction mechanisms are correct, then in order that the observed conversions be obtained it is necessary that the rates of dissociation in a pure hydrogen chloride and a pure oxygen discharge be comprable.

In order to compare the rates of dissociation in a hydrogen chloride and an oxygen discharge, it is assumed that for a given power E/p' is the same for both kinds of discharge. The dissociation rate is given by $k_1 n_e N$ which is proportional to $k_1 n_e p'$. We see from equation(7) that if the power density in both kinds of discharge is identical

$$\left(\frac{n_e\ E^2}{\nu_m}\right)_{HCl} = \left(\frac{n_e\ E^2}{\nu_m}\right)_{O_2} \qquad (45)$$

Noting that $\nu_m = \nu_m\ (p' = 1\ \text{Torr})p' = \nu_{m_1} p'$ and dividing both sides of the equation by p', we find

$$\left(\frac{n_e\ E^2}{\nu_{m_1} p'^2}\right)_{HCl} = \left(\frac{n_e\ E^2}{\nu_{m_1} p'^2}\right)_{O_2} \qquad (46)$$

or, consequently, $(n_e/\nu_{m_1})_{HCl} = (n_e/\nu_{m_1})_{O_2}$. The elastic collision frequencies for the two gases should not differ very widely and, as a result, the electron densities will be roughly equal. Hence, for identical power densities the relative rate of dissociation will be given by k_1/k_2. The values of this ratio are shown in Table 5 along with the resulting relative yields of chlorine. The results show

Table 5

Relative Yields of Chlorine Using a Hydrogen Chloride and an Oxygen Discharge

		Relative Yields of Chlorine Assuming	
		Step 6	Steps 6a,6b
E/p'	k_1/k_2	$(Cl_2)_{HCl}/(Cl_2)_{O_2}$	$(Cl_2)_{HCl}/(Cl_2)_{O_2}$
10	1.3	0.7	1.3
15	3.0	1.5	3.0
20	3.8	1.9	3.8
30	4.8	2.4	4.8

that for low values of E/p' an equivalent amount of chlorine will be found as a result of discharging either hydrogen chloride or oxygen, but that as E/p' is raised the former process will give higher conversions. Within the limits of the assumptions on which Table 5 is prepared, it would appear that the assumption of step 6 leads to a more nearly correct prediction of the relative yields of chlorine (see Figure 22).

The use of excess oxygen in conjunction with a hydrogen chloride discharge leads to an increased yield of chlorine (see Figure 23). The increase appears to level off as a greater excess of oxygen is used. This behaviour can be explained by regarding the oxygen as a getter of hydrogen atoms, preventing their recombination with chlorine atoms. Consequently, an upper limit to the yield of chlorine is set by the condition that all the hydrogen atoms produced as a result of hydrogen chloride dissociation are reacted to form water.

The addition of chlorine together with a stoichiometric amount of oxygen leads to a decrease in conversion. The possibility that this might be due to a dilution of the oxygen was tested by replacing the chlorine with an equivalent amount of helium. This substitution gave results identical to those in which only stoichiometric oxygen had been used. The action of the chlorine is consequently a chemical one involving, most likely, a competition with oxygen for hydrogen atoms via the reaction

8. $H + Cl_2 \longrightarrow HCl + Cl$

The effect of the addition of excess oxygen or the addition of chlorine on the conversion reveals that hydrogen atoms are an important reaction specie. The presence of atomic hydrogen in an electric discharge in a gas mixture identical to the one described here has already been reported by Cooper (31). His work showed that the hydrogen Balmer lines were present in the spectrum of the visible radiation from a microwave discharge.

An examination was also made of the relative effects of discharging water vapor and chlorine on the conversion of chlorine to hydrogen chloride by the reverse reaction. These data are shown in Figure 24. In this case the passage of chlorine through a discharge leads to only a negligible conversion (< 4%), whereas the passage of water vapor through the discharge gives up to 29% conversion. The mechanism for the latter case might be envisaged as

8. $H + Cl_2 \longrightarrow HCl + Cl$

14. $2\ Cl + M \longrightarrow Cl_2 + M$

9. $2\ OH \longrightarrow H_2O + O$

10. $O + OH \longrightarrow O_2 + H$

Reactions 9 and 10 have been shown to be very fast and are given by Kaufman (53) as an explanation for the absence of hydroxyl radicals in the products of a water vapor discharge. For the case in which chlorine is discharged, the initial step would have to be

$$\mathrm{Cl} + \mathrm{H_2O} \longrightarrow \mathrm{OH} + \mathrm{HCl} \qquad \Delta F_{298} = 14.94 \text{ kcal}$$

$$\Delta H_{298} = 16.2\text{[illegible]} \text{ kcal}$$

Since this reaction has a positive free energy change associated with it, it is not expected to proceed to any significant extent. This would account for the observation of very limited conversion of chlorine to hydrogen chloride in this case.

D. Evaluation of Relative Power Losses

The energy absorbed from the electric field by the free electrons in the discharge is dissipated in a number of ways. It is of great interest to attempt to numerically evaluate the fraction of energy which is carried away by some of these processes. In particular, the processes of diffusion, ionization, dissociative attachment, detachment, and infrared radiation will be examined for a hydrogen chloride discharge assumed to be operating at $E/p' = 30$. A summary of the relevant physical parameters is given in Table 6.

Table 6

Discharge Parameters

$E/p' = 30$ V/cm Torr

$p = 7.50$ Torr

$p' = 5.38$ Torr*

$E = 162$ V

$3/2kT_e = 0.456$ eV

$v_{d_e} = 5.2 \times 10^6$ cm/sec

$v_{r_e} = 4 \times 10^7$ cm/sec

$N = 1.77 \times 10^{17}$ molecules/cm^3 *

$v_{r_+} = 5.3 \times 10^4$ cm/sec*

$\lambda_+ = 2 \times 10^{-3}$ cm*

* Based on $T_g = 407$ °K

Diffusion of electrons to the walls of the discharge tube results in an energy loss since each electron carries away, on the average, an amount equal to 3/2 kT_e. The fraction of the total energy lost in this manner can be expressed as

$$F_{diff} = \frac{j_{diff}\ \frac{3}{2}\ kT_e\ A}{\bar{n}_e\ e\ v_d\ E\ V} \qquad (47)$$

where j_{diff} $(r = a)$ is the electron flux evaluated at the wall, and A/V is the ratio of surface area to volume of the discharge zone. The electron flux is given by

$$j_{diff} = -\ D_a\ \left.\frac{\partial\ n_e}{\partial r}\right)_{r=a} \qquad (48)$$

where D_a is the ambipolar diffusion coefficient. For the present situation it is assumed that the radial distribution of electrons is given by $n_e = n_{e_o}\ J_o(r/\Lambda)$ where $\Lambda = a/2.405$ and n_{e_o} is the electron density at $r = 0$. This distribution is appropriate for the assumption that electrons are lost from the discharge volume only by diffusion. Substitution of this distribution into equation (48) gives

$$j_{diff} = 0.52\ \frac{n_{e_o}\ D_a}{\Lambda} \qquad (49)$$

$$= 1.20\ \frac{\bar{n}_e\ D_a}{\Lambda}$$

where $\bar{n}_e$ is the volume averaged electron density. The diffusion coefficient D_a can be evaluated from the equation for its definition

$$D_a = \frac{D_+ \mu_e + D_e \mu_+}{\mu_+ + \mu_e} \tag{50}$$

where D_+ and D_e are the diffusion coefficients for positive ions and electrons, and μ and μ_e are the mobilities for these species. In the limit that $T_e >> T_+ = T_g$ and since $\mu_e >> \mu_+$, equation (50) can be approximated as (54):

$$D_a \simeq D_e \frac{\mu_+}{\mu_e} = \frac{kT_e}{e} \mu_+ \tag{51}$$

The value of μ_+ can in turn be approximated from the classical expression for the ion mobility

$$\mu_+ = \frac{e \lambda_+}{M_+ v_{r_+}} \tag{52}$$

where λ_+ is the ionic mean free path, M_+ is the ionic mass, and v_{r_+} is the ionic thermal velocity. Substitution of equation (52) into equation (51) and numerical evaluation using the values given in Table 5 yields $D_a = 3.4 \times 10^2$ cm^2/sec. This value of D_a is then substituted in equation (49) to give

$$j_{diff} = 2.04 \times 10^3 \, \bar{n}_e \text{ electrons/cm}^2 \text{ sec} \qquad (53)$$

Equation (47) now gives $F_{diff} = 9.1 \times 10^{-5}$. Consequently only a very small fraction of the total energy is lost due to diffusion of electrons to the walls of the discharge tube.

The fractional loss due to ionization can be evaluated very readily. Since it was assumed that volumetric attachment and recombination of electrons could be neglected all the electrons lost by diffusion must be replaced by ionization. Consequently, the fraction of the total energy consumed by ionization can be evaluated by multiplying F_{diff} by the ratio $\epsilon_i/(3/2\ kT_e)$ where $\epsilon_i = 13.8$ eV is the ionization energy for hydrogen chloride. This leads to $F_{ion} = 2.7 \times 10^{-4}$ which again does not represent an appreciable loss. As is shown in part F of this chapter, the presence of negative ions in the discharge can lead to an appreciable increase in the value of the electron ambipolar diffusion coefficient. Since negative ions do, in fact, occur in hydrogen chloride, the values of F_{diff} and F_{ion} calculated above may both be low by one or two orders of magnitude.

The consumption of energy for dissociative attachment can be calculated from the reaction rate constant for this process. Thus

$$F_{diss} = \frac{k_1 N \epsilon_d}{e\, v_d\, E} \qquad (54)$$

where $\epsilon_d = 0.66$ eV. Evaluation of F_{diss} from equation (54) leads to a value of 7×10^{-3}. Thus slightly less than one percent of the total energy is consumed via this process. It should be noted, however, that since all attached electrons are eventually detached, this will result in a further expenditure of energy. The detachment energy for chlorine atoms is 3.7 eV. This represents an additional fractional loss of $F_{det} = 3.9 \times 10^{-2}$.

An examination of the fractional loss of energy for the three processes considered shows that the major portion of the energy remains unaccounted for. Because the electron temperature in hydrogen chloride for the given value of E/p' is relatively low by comparison with many other gases (see Figure 6), the possibility of exciting states which require several electron volts or more is very small. This conclusion would hold even if the cross sections for excitation to these states were large. As a result, the search for an excited state which could account for an appreciable dissipation of the total energy must be limited to those below one electron volt.

A look at the curves of δ, the fraction of energy lost by an electron, as a function of electron energy (see Figure 7) shows that the curve for hydrogen chloride passes through a maximum for very low energies. Classical mechanics predicts that, in the absence of any excitation in this range, all collisions should be elastic and δ should be $\sim 10^{-5}$.

Figure 7 shows that in this region $\delta = 5 \times 10^{-2}$. As a result one must look for an excitation in the range of 0.13 to 0.50 eV. This range of energies lies within the infrared portion of the spectrum. Herzberg (55) shows that the fundamental absorption band for hydrogen chloride in the infrared lies at 3.46 μ or 0.358 eV. A line has been marked in Figure 7 at this position and shows that the absorbtion band lies within the hump on the curve. The possibility therefore arises that infrared emission due to electron collision excitation might occur at this same energy and be responsible for the maximum in the curve of δ.

Data on the emission of infrared radiation from a hydrogen chloride discharge have not been reported in the literature, but evidence can be found for the occurrence of this process in carbon monoxide and carbon dioxide. Figure 40 illustrates the curves of δ for these gases and the energy at which each gas absorbs infrared. Terenin and Neuimin (56) report that carbon monoxide in an electric discharge gives rise to an emission band at 4.7 μ and carbon dioxide to one at 4.6 μ. Since thse wavelengths agree very closely with those for absorbtion, it can be concluded that both carbon monoxide and carbon dioxide will radiate in an electric discharge at the same wavelengths at which they absorb.

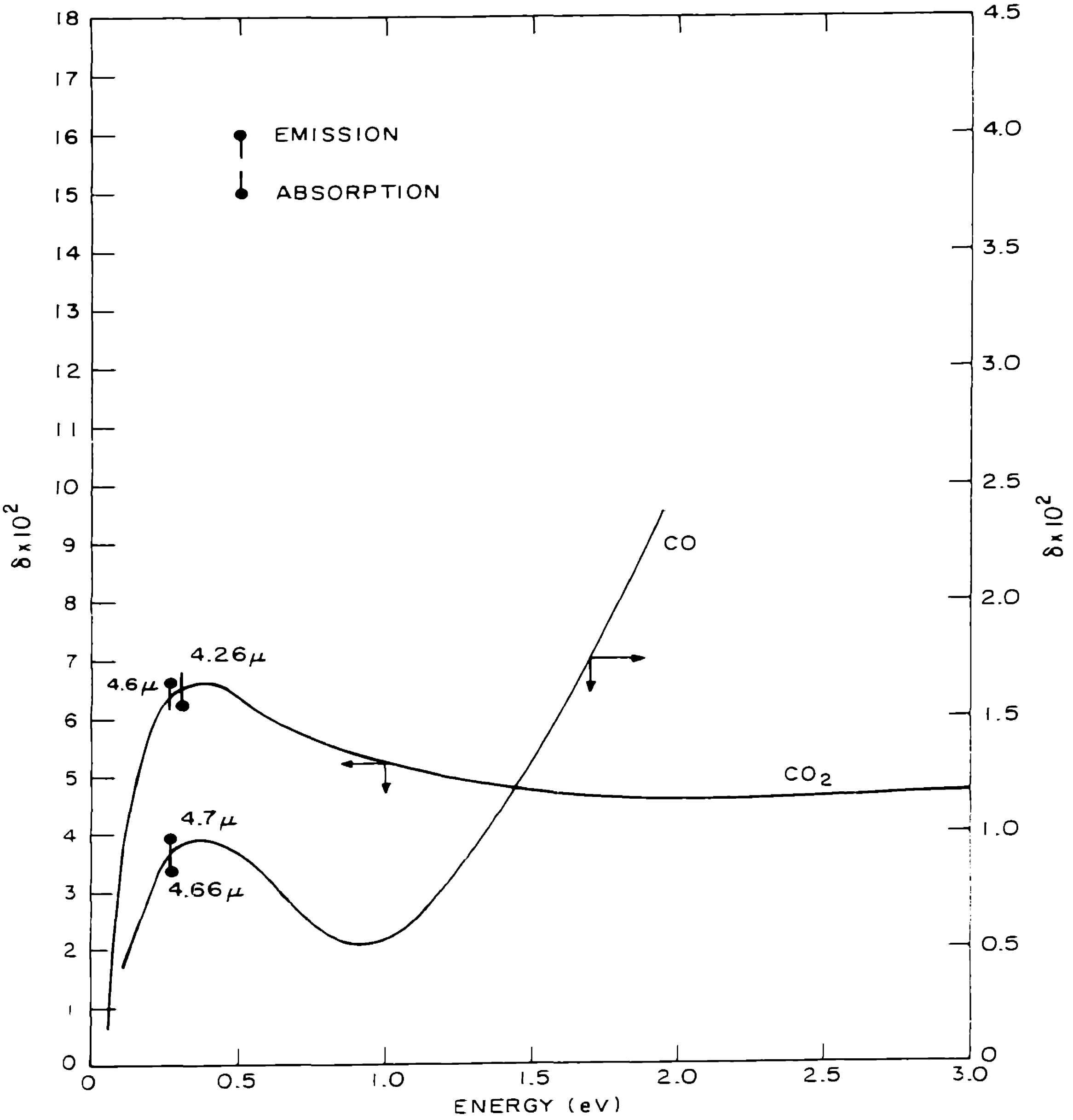

FIGURE 40 FRACTIONAL ENERGY LOSS BY AN ELECTRON UPON COLLISION WITH CARBON MONOXIDE AND CARBON DIOXIDE

Terenin and Neuimin further conclude that the observed emission is not of a thermal nature. An estimate of the excitation temperature for carbon dioxide was made on the basis of the shift of its emission band from its location at 4.26 μ at room temperature. This resulted in a value of 4000 °C, while estimates of the actual gas temperature showed that it could not be above 600 °C. Consequently, it was postulated that the emission was due to low energy inelastic collisions between electrons and molecules.

Kaufman (53) notes that the cross sections for the vibrational excitation of nitrogen, carbon monoxide, and carbon dioxide by electron collisions lies in the range from 1 to 5 x 10^{-16} cm^2/molecule. If it is assumed that a similar range of values might apply for the vibrational excitation of hydrogen chloride, a rough calculation can be made of the rate constant for the process. For a Maxwellian distribution of electron energies, the excitation rate constant is given by

$$k_{1r} = 2\sqrt{\frac{2}{\pi m}}\,(kT_e)^{-\frac{3}{2}} \int_{\epsilon_{1r}}^{\infty} \epsilon\, Q_{1r}\, e^{-\epsilon/kT_e}\, d\epsilon \tag{55}$$

where ϵ_{1r} is the excitation energy and Q_{1r}, the cross section. For hydrogen chloride ϵ_{1r} = 0.358 eV and taking $Q_{1r} = 10^{-16}$ cm^2 a value of k_{1r} = 2.5 x 10^{-9} cm^3/molecule sec results. The fractional energy loss by this process is evaluated from

$$F_{ir} = \frac{k_{ir} \, N \, \epsilon_{ir}}{e \, v_d \, E} \qquad (56)$$

Using the computed value of k_{ir} and the numerical values of Table 5, a value of F_{ir} is obtained. This value is larger than that for any of the other processes considered. Thus, bearing in mind the assumptions on which the calculation of F_{ir} is made, there appears to be strong evidence for the occurrence of infrared emission in a hydrogen chloride discharge. The presence of such a process would serve to explain both the nature of the curve of δ and the reason why for a given E/p' the electron temperature is considerably lower in hydrogen chloride than in most gases.

E. Estimation of Gas Temperature

In the discussion of the reaction kinetics, it was necessary to assume a value for the gas temperature at each pressure. It is of interest now to determine whether these values are consistent with other observations of the discharge and to explore the possibility of predicting the gas temperature from a knowledge of the gas pressure and the amount of power consumed.

At a power of 200 watts it was observed that small vapor bubbles were formed in the heat transfer oil at the edges of the electrodes. These bubbles are taken to be an indication of incipient boiling. A sample of Bayol 35 was heated, and it was found that the first bubbles of vapor appeared at 180 °C and that vigorous boiling occurred at 217 °C. These values can then be taken as an indication of the upper limit of the temperature at the outer wall of the discharge tube.

Careful visual observation of the thermal eddies formed in the oil showed that they rose with a velocity which was greater than that of the bulk oil flow. This led to the postulation that the major heat transfer process was natural convection. If it is assumed that all the power dissipated in the discharge is transferred to the oil by natural convection, it is possible to compute a value for the temperature drop across the oil film. This calculation begins with the choice of a value for the temperature drop. The oil properties (most notably the viscosity) are evaluated at the film temperature for the chosen ΔT, and a heat transfer coefficient is calculated from the product of the Grashof and Prandtl Numbers (57). The heat transfer coefficient is in turn used to calculate the temperature drop necessary to drive an assumed 200 watts through the oil film. The new value of ΔT is compared with that originally assumed. If the two values do not agree, the calculation is repeated for a different value of ΔT. The iteration process, which is described in Appendix A, is continued until the initially chosen and the drived values of ΔT agree. This procedure gives a heat transfer coefficient equal to 1.08×10^{-2} cal cm/cm^2 sec $^\circ$C and an oil film temperature drop of 210 $^\circ$C. Thus, under the assumption that the only heat transfer mechanism is natural convection, the outer wall temperature would be at 220 $^\circ$C. This value is somewhat high since only incipient boiling is observed for a power of 200 watts. A calculation of the forced convection heat transfer coefficient gives a value of 5.84×10^{-4} cal cm/cm^2 sec $^\circ$C for the same wall temperature. Consequently, the amount of forced convection present is insufficient to reduce the outer wall temperature below 220 $^\circ$C.

Turning now to the transfer of heat from the gas, it is of interest to first assume that all 200 watts of power are dissipated through gaseous conduction. This assumption leads to an expected temperature drop of 9.1×10^3 $^\circ$C, a value which is obviously much too high. A more realistic estimate of the temperature drop across the gas might be made by first determining the amount of power which goes into homogeneous heating processes. This quantity should then be used to calculate a temperature drop.

Two major processes contribute to homogeneous heating of the gas--elastic collision transfer of translational energy and heating as a result of the release of the heat of reaction. For the first process the energy density is given by

$$\bar{P}_e = \frac{2m}{M} \frac{3}{2} kT_e \; n_e \nu_m \tag{57}$$

where $\nu_m \approx 5 \times 10^9$ p. Numerical evaluation of this term using the data of Table 6 and $n_e = 1.5 \times 10^{11}$ electrons/cm^3 gives $\bar{P}_e = 0.09$ watts/cm^3. The contribution of the second process is given by

$$\bar{P}_{chem} = \frac{x \, F_{HCl} \; \Delta H/4}{V} \tag{58}$$

where $\Delta H = 27.3$ kcal is the heat of reaction and V is the discharge volume. For a molar flow rate of $F_{HCl} = 5.91 \times 10^{-5}$ moles/sec and x = 44%, $\bar{P}_{chem} = 0.12$ watts/cm^3. The sum of these two sources amounts to 0.21 watts/cm^3 which results in a 52 °C increase in the gas temperature from the inner wall to the center of the discharge.

From the preceding discussions of the natural convection losses from the outer wall of the discharge tube and the temperature drop through the gas, it becomes evident that the total power cannot be escaping by purely thermal means. Since it was shown in the previous section that a fair portion of the total power may be dissipated as infrared radiation, it will be useful to further pursue the consequences of such a possibility.

The transmission properties of commercially made quartz (58) show that at a wavelength of 3.46 μ, 80% of the incident radiation will be transmitted. This wavelength represents that at which vibrationally excited hydrogen chloride will emit. As a result, only a small portion of the emitted radiation will be absorbed in the wall of the quartz discharge tube. On the other hand, an experimental measurement of the transmission properties of Bayol 35 (see Figure 41) shows that a 0.5 mm film will absorb essentially all the radiation at 3.46 μ. Consequently, the infrared radiation should be absorbed in a thin layer of oil near the wall of the discharge tube. This film can, in turn, heat the outer wall of the discharge tube which receives very little heat via conduction from the discharged gas. Depending on the thickness of the oil film, the temperature in the film may never rise to the point where boiling of the oil might occur. In the vicinity of the electrodes a different situation would arise. Here the metal electrodes will absorb all the radiation and become sufficiently hot to boil the oil. Since the edges of the copper sleeves are rough, preferential nucleation of boiling should be expected at these points.

F. Contraction of the Discharge Column

A theoretical explanation of the contraction of a discharge column with increasing pressure in the presence of electronegative gases has been offered by Albrecht, Ecker,

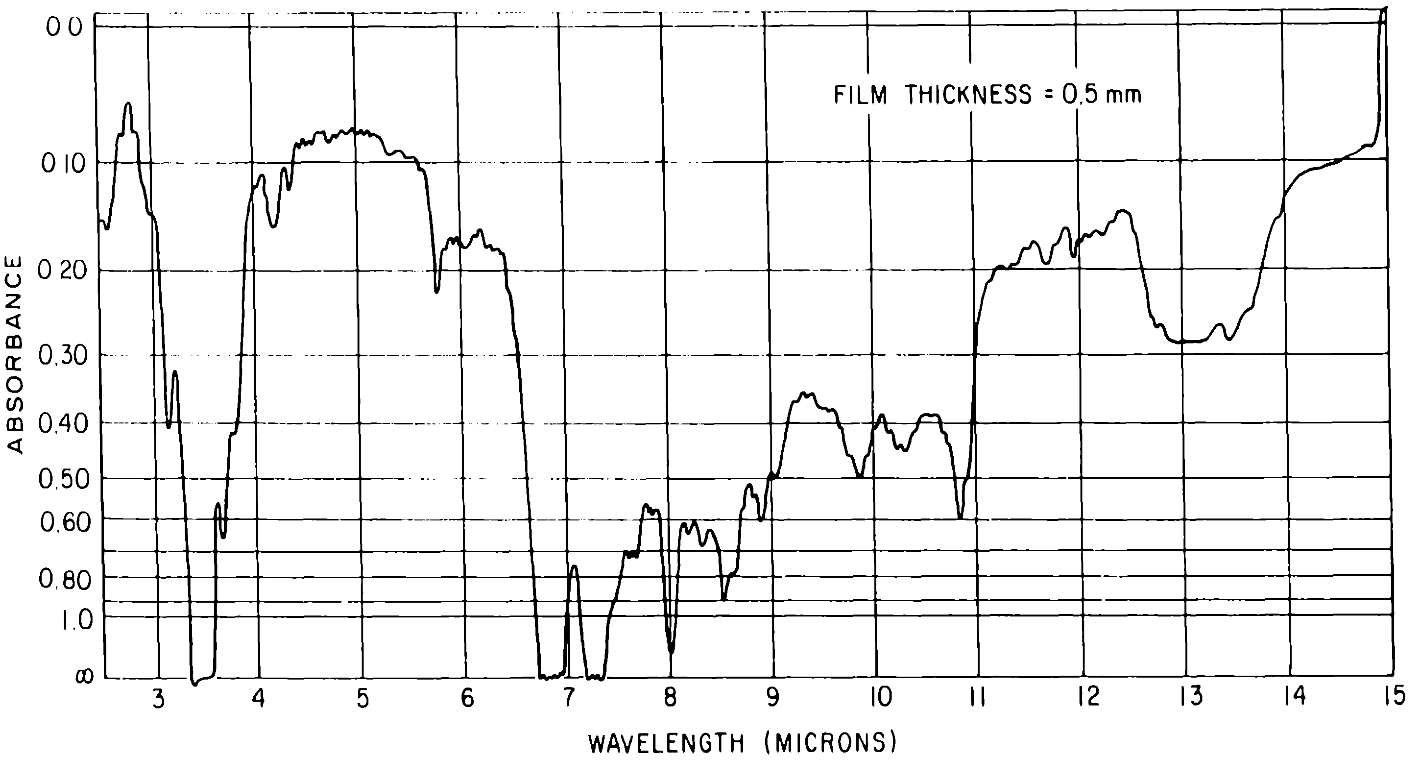

FIGURE 41 INFRARED SPECTRUM OF BAYOL 35

and Muller (59). The effect is found to be due to the ability of electronegative gases to form negative ions which cause an increase in the ambipolar diffusion coefficient of the electrons.

For a system containing electrons, positive ions, and negative ions the particle flux equations can be written as

$$\begin{aligned} j_+ &= -D_+ \nabla n_+ + \mu_+ n_+ E_{sc} \\ j_- &= -D_- \nabla n_- - \mu_- n_- E_{sc} \qquad (59) \\ j_e &= -D_e \nabla n_e - \mu_e n_e E_{sc} \end{aligned}$$

The space charge field E_{sc} arises as a consequence of the ability of the electrons to drift more rapidly than the positive ions. This causes a slight amount of charge separation which in turn results in the establishment of a field which opposes the separation. In the case where the charged particle density is sufficiently great ($n > 10^9$ cm^{-3}), the approximations $n_+ = n_e + n_-$ and $j_+ = j_e + j_-$ can be made, leading to the following simplification:

$$\begin{aligned} j_+ &= -D_{a_+} \nabla n_+ \\ j_- &= -D_a \nabla n_- \qquad (60) \\ j_e &= -D_{a_e} \nabla n_e \end{aligned}$$

$$D_{a_+} = D_+ \left[\frac{(1 + \gamma + 2\alpha\gamma)(1 + \alpha\mu_-/\mu_e)}{(1 + \alpha\gamma)\left\{1 + \mu_+(1 + \alpha)/\mu_e + \alpha\mu_-/\mu_e\right\}} \right]$$

$$D_{a_-} = D_+ \left[\frac{1}{\gamma} \frac{\mu_-}{\mu_e} \frac{1 + \gamma + 2\alpha\gamma}{1 + \mu_+(1 + \alpha)/\mu_e + \alpha\mu_-/\mu_e} \right] \qquad (61)$$

$$D_{a_e} = D_+ \left[\frac{1 + \gamma + 2\alpha\gamma}{1 + \mu_+(1 + \alpha)/\mu_e + \alpha\mu_-/\mu_e} \right]$$

and $\alpha = n_-/n_e$ and $\gamma = T_e/T_+ = T_e/T_-$. A plot of D_a/D_+ as a function of α given by Thompson (60) is shown in Figure 42. For the case where $\alpha = 0$, $D_{a_+} = D_{a_-} = \dfrac{D_+ \mu_e + D_e \mu_+}{\mu_e + \mu_+}$ which represents the ambipolar diffusion coefficient in the absence of negative ions. It can be seen that an increasing presence of negative ions very rapidly leads to an increase in D_{a_e} .

The continuity equations for electrons and negative ions can be written as

$$\frac{1}{r} \frac{d}{d} (r D_{a_e} \frac{dn_e}{dr}) = n_e \left[(\frac{\alpha}{p} - \frac{\beta}{p}) v_{d_e} p + q v_{r_e} n_- \right] \qquad (62a)$$

$$\frac{1}{r} \frac{d}{dr} (r D_{a_-} \frac{dn_-}{dr}) = n_e \left[\frac{\beta}{p} p v_{d_e} - (q v_{r_e} + \sigma \sqrt{2}\, v_{r_-}) n_- \right]$$

$$- \sigma \sqrt{2}\, v_{r_-} n_-^2 \qquad (62b)$$

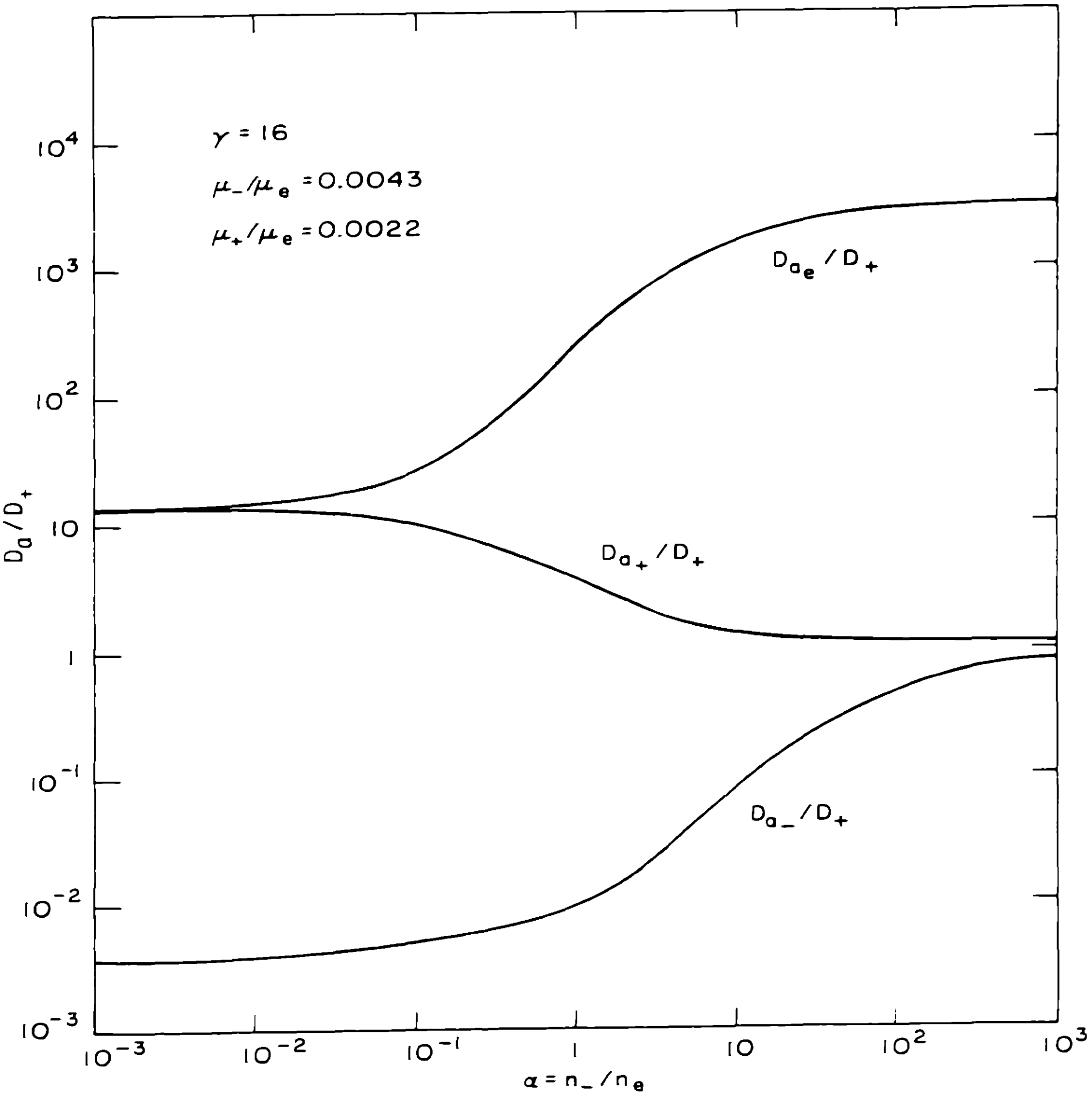

FIGURE 42 AMBIPOLAR DIFFUSION COEFFICIENTS AS A FUNCTION OF $\alpha = n_-/n_e$

where α is the number of ionizations by an electron per centimeter of its drift path, β, the number of attachments per centimeter of drift path, q, the collision cross section for the detachment of electrons from negative ions, σ, the cross section for positive-negative ion recombination, v_{d_e} and v_{r_e}, the drift and random electron velocities, and v_{r_-} the random velocity of negative ions. It should be noted that the terms inside the square bracket of equation (62a) give rise to an effective electron production rate which will decrease with radial position, while equation (61) shows that D_{a_e} will increase radially provided n_-/n_e increases. A solution to equation (62a) and (62b) has been given by Albrecht et al. (59), using the constants appropriate for oxygen. Several of the resulting solutions for the radial electron distribution are shown in Figure 43. The parameter h/a is the ratio of the radius at which the normalized distribution equals 0.5 to the radius of the container. The value of h/a is found to decrease as either the pressure or the discharge current is increased. Thus for a = 0.5 cm, h/a = 0.26 at I = 0.2 amp, p = 25 Torr; h/a = 0.43 at I = 0.1 amp, p = 35 Torr; h/a = 0.54 at I = 0.1 amp, p = 10 Torr. These values are seen to fall within the range of current and pressure investigated in the present work. Consequently, the proposed description of the contraction phenomenon is felt to be correct.

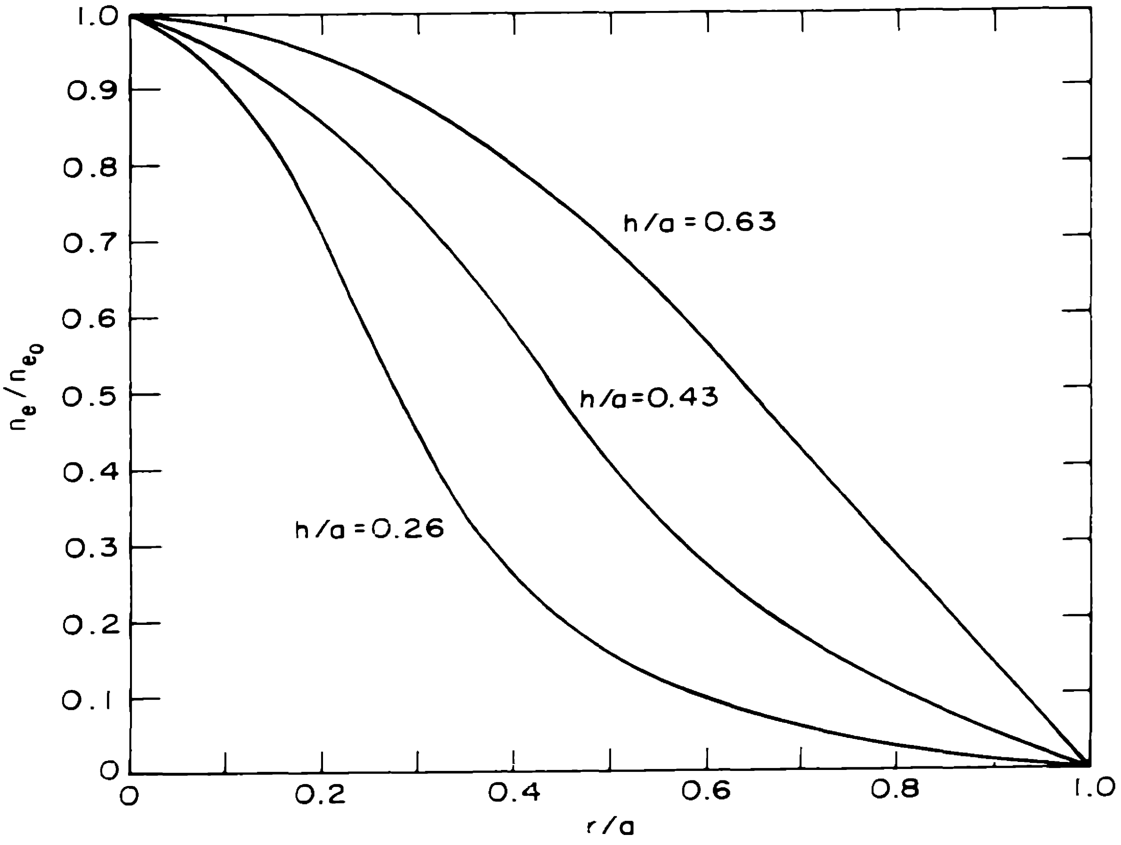

FIGURE 43 NORMALIZED RADIAL ELECTRON DISTRIBUTION

G. Distribution of Electric Field Strength and Emitted Light

Observations of the light emitted by the discharge showed that two distinct regions could be identified. The first of these regions occupied the volume beneath the electrodes while the second filled the remaining discharge volume. Since the light from the electrode regions is of shorter wavelength, this implies that T_e and consequently E are higher there than in the remaining volume. Similar characteristics were noted by Banerji and Ganguli (61) in their investigation of a 1 MHz capacitively coupled discharge in oxygen. Their observations showed that the two electrodes behaved as if they were cathodes in a corresponding d.c. discharge. The negative glow, the Faraday space, and the positive column appeared in succession on moving away from either of the electrodes. As is well known the field strength in the negative flow of a d.c. glow discharge is higher than that in the positive column.

An explanation of the observed phenomena can be found in terms of the development given by Perel' and Pinskii (62) for the effect of an inhomogeneous a.c. field on a high frequency discharge. The presence of gradients in a high frequency field leads to an additional force which the field can exert on free electrons. This force is given by

$$F_k = \frac{-e_k^2}{4m_k(\omega^2 + \nu_k^2)} \frac{dE^2}{dx} \qquad (63)$$

and will result in the appearance of an additional term in the charged particle flux equations. For a parallel plate geometry (each plate representing an electrode), the flux equations will be given by

$$J_+ = -D_+ \frac{dn_+}{dx} + \mu_+ n_+ E_{sc} - \mu_+ n_+ \frac{F_+}{e} \qquad (64)$$

$$J_e = -D_e \frac{dn_e}{dx} - \mu_e n_e E_{sc} + \mu_e n_e \frac{F_e}{e}$$

Assuming $J_+ = J_e$ and $n_+ = n_e$, equation (64) can be rewritten as

$$J = -D_a \frac{dn}{dx} + \frac{\mu_+ \mu_e}{\mu_+ + \mu_e} \frac{n}{e} (F_e - F_+) \qquad (65)$$

The effect of F_+ can be neglected since $\frac{m_e(\nu_e^2 + \omega^2)}{m_+(\nu_+^2 + \omega^2)} >> 1$.

By writing the expression for the sum of the conduction and displacement currents, a relation may be obtained between the field strength at any position and the electron density at that position and the magnitude of the total current density. The force F_e can then be expressed in terms of n_e and the magnitude of the total current density J_o. Introduction of this form of F_e into equation (65) leads to

$$J = - D^* \frac{dn}{dx}$$

$$D^* = D_a \left[1 + g \frac{h(1+\alpha^2-h)}{\{(h-1)^2 + \alpha^2\}^2} \right] \quad (66)$$

where

$$g = \frac{e^2 J_o^2}{2m\omega^4 \epsilon_o^2 k(T_e + T_+)} \quad (67)$$

and $\alpha = \nu/\omega$, $h = ne^2/\epsilon_o m\omega^2$.

The quantity D^* has the meaning of an effective diffusion coefficient which depends on the electron density and can differ appreciably from the ambipolar diffusion coefficient D_a. It is interesting to note that D^* can go to zero or even negative for certain values of the discharge parameters. Setting the terms in the curved brackets of equation (66) equal to zero, it is possible to determine a curve of $1/g$ as a function of h, for each value of α, along which $D^* = 0$. For points above this curve $D^* > 0$ and for points below the curve $D^* < 0$. The curve itself passes through a maximum and crosses $1/g = 0$ for some low value of h (see Figure 44).

The parameter g can be approximated as $g = \delta h_o^2$ where δ is the fraction of the energy lost by an electron per

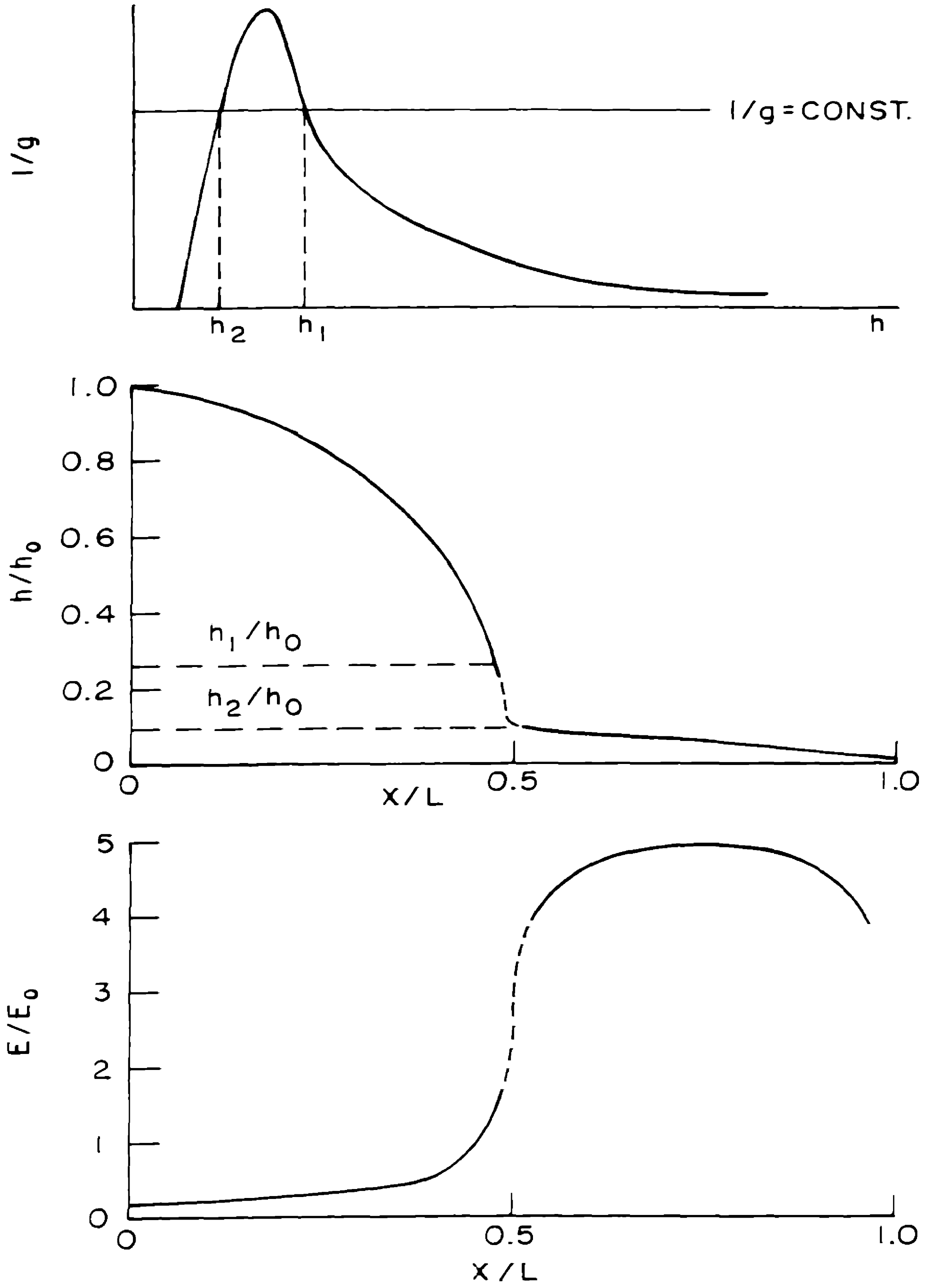

FIGURE 44 DISCHARGE CHARACTERISTICS IN THE PRESENCE OF AN INHOMOGENEOUS ELECTRIC FIELD

collision and h_o corresponds to the density at the center of the discharge. A line of constant 1/g can then be drawn on the plot of 1/g versus h. Providing that $g > g_c \approx 6.75\ \alpha^4$, this line will cut across the maximum of the described curve. If a point to the right of the maximum is picked (corresponding to high densities in the center of the discharge) and followed towards decreasing values of h, it will eventually reach a value h_1 at which $D^* = 0$. Since the flux of electrons must continue to the walls of the container, this necessitates that $dn/dx \longrightarrow \infty$ as $h \longrightarrow h_1$. Physically this means that at some position in the discharge as we move away from the center, the gradient of electron density becomes very large. In the region between h_1 and h_2, $D^* < 0$ and it is shown by Perel' and Pinskii that the assumptions under which equation (63) was derived will no longer be valid. For values of $h < h_2$, D^* is again greater than zero. The picture of the electron density distribution which thus evolves consists of two regions. From the center of the discharge the density will decrease until at some position x_1 the value of h_1 is approached. Within a very short distance the density will drop to a lower value corresponding to h_2 and will further decrease as the wall is approached. Thus the central region of the discharge is separated from the electrodes by a sharply defined region of lower density. Figure 44 illustrates the form of the density distribution.

The electric field strength at each position can be determined from the relationship between the field strength and the electron density at that position. This relationship is given by

$$E^2(x) = \frac{J_o^2}{\omega^2 \epsilon_o^2} \left[\frac{(1 + \alpha^2)}{(h-1)^2 + \alpha^2} \right] \qquad (68)$$

The variation of field strength with position in the discharge is shown in Figure 44. It is seen that the field strength in the central region is low but rises quite rapidly in the region near the electrodes. Integrating this field with position shows that the voltage drop across a half-width of the discharge consists of two portions:

$$V_1(t) = \frac{E_o}{\Lambda_{eff}} \sqrt{2\delta} \, \ln\left(\frac{2}{\delta^{1/2}}\right) \left[\alpha \cos \omega t - \sin \omega t \right]$$

$$(69)$$

$$V_2(t) = \frac{E_o}{\Lambda_{eff}} \sqrt{2\delta} \, \delta h_o^2 \left(\frac{1-\alpha^2}{4\alpha^3}\right) \left[\left(1 + \frac{\alpha\pi}{4}\right) \cos \omega t + \left(\alpha + \frac{\pi}{4}\right) \sin \omega t \right]$$

where $E_o = J_o/\omega \epsilon_o$ and $V_1(t)$ corresponds to the potential drop in the central region and $V_2(t)$ to the potential drop in the electrode region. The effective diffusion length Λ_{eff} is given by

$$\Lambda_{eff} = \frac{L}{\left[\pi/2 + \frac{\delta h_o}{2} \left(\frac{1 + \alpha^2}{\alpha^2} \right) \right]} \tag{70}$$

where L is the half-width of the discharge. From equation (69) it is seen that the major potential drop occurs in the electrode region. It should also be noted that an increase in the magnitude of the current density J_o will lead to a voltage increase and therefore will give rise to a positive voltage-current characteristic.

The effect of field gradients on the distribution of the electric field in a discharge were discussed by Perel' and Pinskii in terms of a parallel plate geometry. A similar development can be given in terms of a cylindrical geometry and should lead to the observation of a contracted discharge column. Such an observation has, in fact, been made by Golovanivski and Kuzovnikov (63). Two closely spaced ring electrodes were placed on the outside of a tube in which a d.c. glow discharge was maintained. When a 1 MHz r.f. signal was applied to the rings, it was noted that the column in the immediate vicinity of the rings contracted radially.

Another experimental verification of the theories of Perel' and Pinskii can be found in the work of Dzherpetov *et al.* (64). These investigators made measurements of the electron density and temperature in a helium discharge sustained by ring electrodes and operating at 1.2 MHz. Their measurements in the vicinity of the electrode are shown in Figure 45. It is seen that as the electrode is approached the electron temperature rises rapidly, and the electron density begins to fall with increasing rapidity. A similar variation in T_e is observed by Polman (65) in a hydrogen discharge operating at 30 MHz and 0.04 Torr.

In the light of the theoretical explanation of Perel' and Pinskii and the experimental observations of Dzherpetov *et al.* and Polman, it can be concluded that gradients in the electric field can give rise to regions of high field strength in the vicinity of the electrodes sustaining a high frequency discharge. These regions will be characterized by a higher electron temperature by comparison with the balance of the discharge and as a result will emit light of a shorter wavelength.

By suitable design of a discharge tube, it should be possible to pass the reactant through only one of these two regions. This would allow a determination to be made of the relative effects of high and low field strength on the chemical reaction.

H. Discussion of Errors and Reproducibility

1. Power Measurement

The rate at which energy is absorbed in the oil surrounding the discharge tube is used as a measure of the power dissipated in the discharge. The assumption underlying this

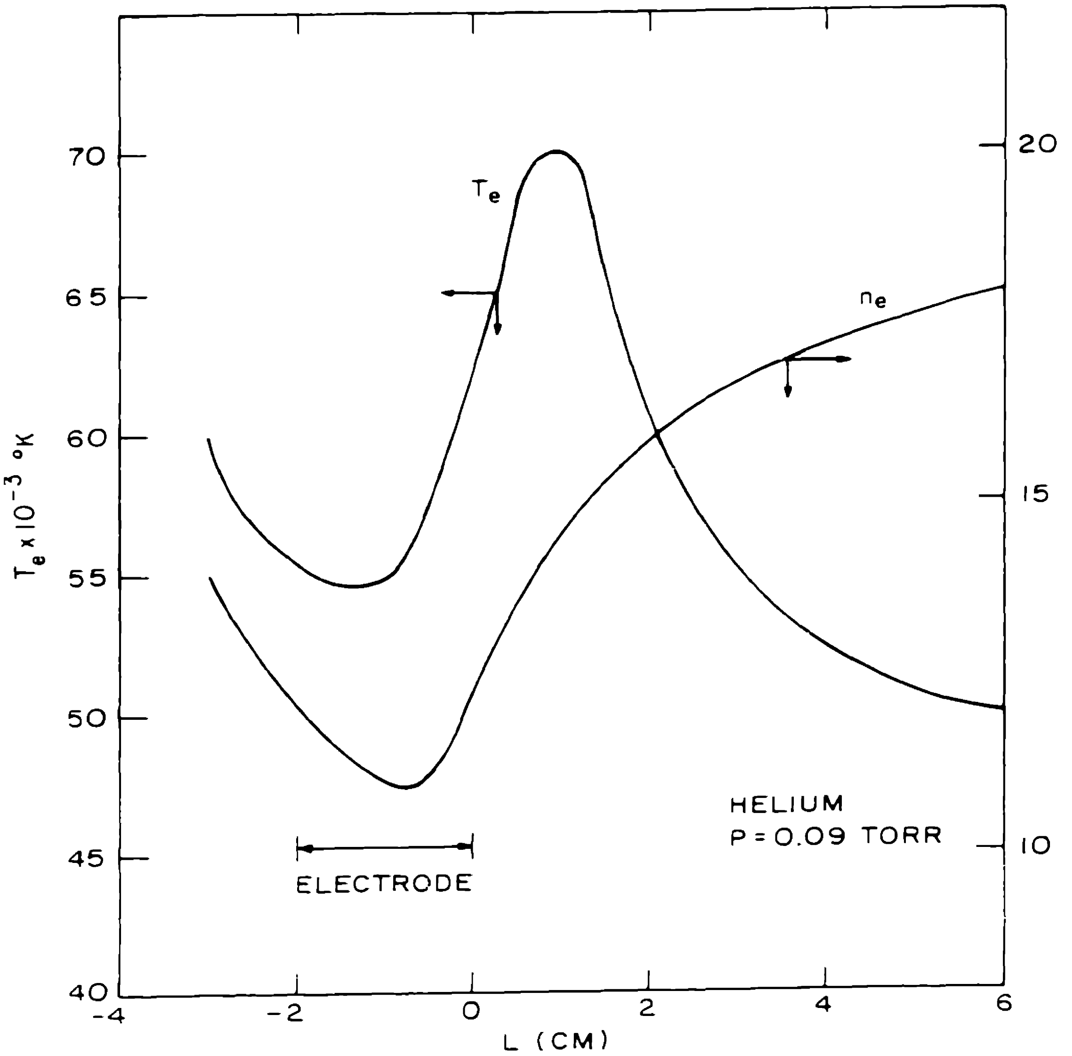

FIGURE 45 AXIAL DISTRIBUTION OF ELECTRON TEMPERATURE AND DENSITY NEAR AN EXTERNAL ELECTRODE OF A HIGH FREQUENCY DISCHARGE

type of measurement is that none of the energy leaving the discharge escapes the oil. Two possible routes by which part of the energy might bypass the oil are: a) failure of the oil to absorb the emitted radiation; b) failure of the oil to reduce the exit gas temperature to room temperature.

It has been shown in part E of this chapter that Bayol 35 will absorb essentially all of the infrared radiation emitted by hydrogen chloride. The only part of the radiated energy which might escape is in the visible range, but no estimate has been made of its magnitude. However, in view of the low electron temperature in the discharge, significant excitation of the energy levels which could radiate in the visible range is probably not very large.

In the course of the present work no direct measurements have been made of the entering and exiting gas temperatures to determine the possibility of insufficient cooling. A set of experiments were done to determine whether the measured power would differ when a particular voltage was applied across the electrodes and the gas flow rate was varied. The results of these experiments showed that no variation in the measured power could be discerned. Temperature measurements made on an identical system in which microwaves were used to excite the discharge (31) showed that the gas left the heat exchanger at ambient temperature. This evidence indicates that the heat exchanger is, in fact, capable of reducing the gas temperature back to ambient and that as a result no errors in the measurement of power should arise due to the escape of sensible heat with the gas.

The temperature difference across the heat exchanger was found to fluctuate around a mean value due to incomplete mixing of the thermal eddies by the sections of polyethylene tubing placed in the upper quarter of the heat exchanger. As a result, the error in temperature difference measurements is about 0.05 °C for powers below 50 watts and about 0.10 °C for powers above 100 watts. This corresponds to an error of ± 2.5 watts at the low end of the power scale and ± 5 watts at the high end.

2. Product Composition

In the determination of the product composition the possibility arises that some of the unreacted hydrogen chloride may dissolve in the droplets of water present in the trap. To test for this possibility a trap containing the reaction products was allowed to sit in an ice bath for several hours. During the course of this time samples were withdrawn with a syringe and analyzed by gas chromatography. No difference in the product composition was noted over this period of time nor did the pressure in the trap change noticeably. As a result it was assumed that the process of hydrogen chloride absorbtion was a sufficiently slow one so that over the period of time in which the reaction products were at ice temperature the gas composition in the trap corresponded to the actual product composition.

The error in the determination of product composition from the measured areas on the chromatogram can be interpreted in the following manner. If it is assumed that the absolute error in measuring the peak areas is Δ, then the fractional conversion of hydrogen chloride from a stoichiometric feed of oxygen and hydrogen chloride is given by

$$x = \frac{A_2 \pm \Delta}{(A_2 + 1.3A_1) \pm \Delta} \tag{71}$$

where A_1 and A_2 are the areas of the chlorine and hydrogen chloride peaks. Equation (66) can be rewritten as

$$\begin{aligned} x &= \frac{A_2}{A_2 + 1.3A_1} \pm \Delta^* \\ &= \bar{x} \pm \Delta^* \end{aligned} \tag{72}$$

where

$$\begin{aligned} \Delta^* &= \left(\frac{A_2}{A_2 + 1.3A_1}\right)\left[\frac{\Delta}{A_2} + \frac{2.3\Delta}{A_2 + 1.3A_1}\right] \\ &= \frac{\Delta}{A_2 + 1.3A_1}\left[1 + 2.3\,\bar{x}\right] \end{aligned} \tag{73}$$

The quantity in the denominator of equation (68) is roughly constant over a large number of runs and equal to $\sim$ 23. The absolute error Δ is equal to 0.14. Thus the error in measuring the conversion is

$$\Delta^* = (.006)\ 1 + 2.3\,\bar{x} \tag{74}$$

and is seen to increase linearly with $\bar{x}$. This explains the larger scatter in experimental values which occurs at higher conversions. For $x = 0.50$, the absolute error will be ± 1.3%.

3. Reproducibility

As a test of the reproducibility of the experimentally measured conversions, some of the runs at 7.50 Torr were repeated. The second set of runs was made a month after the first and with a new discharge tube. The results of the first set of runs at this pressure are shown as the open squares in Figure 13 and the results of the second set by the shaded squares. As can be seen the reproducibility is satisfactory.

CHAPTER VIII

CONCLUSIONS

1. Over 50% conversion of hydrogen chloride to chlorine and water can be obtained in the oxidation of hydrogen chloride to chlorine in a radiofrequency discharge operating at 20 MHz.

2. An increase in gas pressure produces an increase in the conversion for both the forward and reverse reactions. For pressures above 15 Torr the conversion for the forward reaction reaches a maximum and begins to decrease gradually.

3. An increase in the ratio of oxygen to hydrogen chloride in the feed causes an increase in the conversion for the forward reaction.

4. A decrease in the total molar flow rate causes an increase in the conversion for both the forward and the reverse reactions.

5. An asymptotic concentration of chlorine in the hydrogen chloride-chlorine product mixture is approached from both the forward and reverse reaction as the pressure is increased and the total molar flow rate is decreased.

6. The passage of only one reactant through the discharge with subsequent addition of the second downstream shows that for the forward reaction either hydrogen chloride or oxygen can provide the necessary reactive species, hydrogen

chloride being the more effective of the two. A similar study on the reverse reaction shows that only the dissociation of water results in a significant conversion of chlorine.

7. The over-all rate of the forward reaction is governed by the reaction step

$$1. \quad HCl + e \longrightarrow H + Cl^{-} \qquad \epsilon_1 = 0.66 \text{ eV}$$

and the rate of hydrogen chloride consumption can be expressed as

$$\frac{d(HCl)}{dt} = - Ak_1(HCl)(e)$$

where k_1 is a function of the electron temperature T_e. The following simplifying assumptions are used together with the above rate expression in order to calculate values for the conversion:

a) The electric field strength throughout the discharge is constant and is given by dividing the voltage across the electrodes by the length of the discharge zone.

b) The resistance of the discharge is constant.

c) The gas temperature in the discharge is proportional to the power dissipated and is given by

$$T_g = 293 + \Delta T^{*} P/200$$

where ΔT^* is left as an adjustable constant, which is chosen so that the calculated conversions match the experimental ones.

d) The reactor volume is taken as the volume of the discharge zone.

e) The value of T_e can be chosen from a plot of T_e versus E/p' given by Bailey (48) for pure hydrogen chloride.

f) The electron density in the discharge is uniform and given by

$$n_e = \frac{I}{\pi a^2 e v_d}$$

where v_d can be determined from a plot of v_d versus E/p' given by Bailey (48) for pure hydrogen chloride.

g) The rate constant k_1 can be calculated from the experimentally determined value of the collision cross section for reaction 1 and the assumption of a Maxwellian distribution of electron energies.

h) The flow pattern through the discharge is either plug flow or well-mixed flow.

i) The constant A appearing in the rate expression is left as an adjustable constant.

The theoretical value of conversion can then be determined from

$$12.8\ k_1\ (\frac{p}{RT_g})\ n_e\ \frac{V}{F_{HCl}} = -\ 4\ln(1-x) + x$$

for the assumption of plug flow and from

$$16.8\ k_1\ (\frac{p}{RT_g})\ n_e\ \frac{V}{F_{HCl}} = \frac{x(5+x)}{(1-x)}$$

for the assumption of well-mixed flow. The conversions calculated from these equations agree very closely with the experimental ones. The model of the reaction system, also, correctly predicts a maximum in the plot of percent conversion versus power at constant pressure and the shift of this maximum to higher power as the pressure is increased. Multiplication of the above two equations by $\frac{\alpha}{0.25}\ \frac{1+\alpha}{1.25}$, where $\alpha = (O_2)/(HCl)$, allows the effects of an increase in the ratio of oxygen to hydrogen chloride to be taken into account.

8. Assumption of well-mixed flow gives a better fit between the calculated and experimental values of the conversion. This is due to axial dispersion as a result of molecular diffusion.

9. The lowest power required per pound of chlorine produced in these experiments is 8.4 kwhr/lb of Cl_2, obtained at P = 40 watts, p = 7.50 Torr, F = 7.40×10^{-5} moles/sec, $O_2/HCl = 0.25$.

10. A calculation of the manner in which the power supplied to the discharge is consumed shows that the largest fraction is used to excite hydrogen chloride to emit infrared radiation.

11. The discharge column contracts with increasing pressure, which can be attributed to the presence of negative ions.

12. Light of a shorter wavelength is emitted from the electrode regions than from the center of the discharge. This phenomenon can be explained in terms of gradients in the electric field.

CHAPTER IX

RECOMMENDATIONS

1. A study should be made of the oxidation of hydrogen chloride in a closed system to determine the behavior of the steady state conversion with respect to T_g, T_e, p, and O_2/HCl. With such a system the gas temperature might be measured by using the discharge as a gas thermometer.
2. Calculations of the equilibrium conversion of hydrogen chloride should be made using the form of the equilibrium constant proposed by Potapov.
3. The role of electrode geometry and total molar flow rate should be investigated for a discharge operated near extinction. Such a study would provide information on the means for improving the maximum yield of product per unit of electric power.
4. A discharge tube should be designed in which the reactants are preferentially passed through the electrode and central regions of the discharge in order to determine the relative effects of each of these regions.
5. The mixed feed experiments described in this work should be repeated for a larger and a smaller discharge tube diameter to determine the validity of neglecting surface reactions.

6. Measurements of the spectral distribution and total emitted power of the infrared radiation should be made to determine its importance as a loss mechanism.

APPENDIX A

SAMPLE CALCULATIONS

A. Calculation of Absorbed Power

The amount of power absorbed in the oil passing through the reactor heat exchanger is calculated from the expression

$$P = Q_{oil} \, (\rho \, C_p)_{T_i} \, \Delta \, T_{oil} \qquad \text{(A-1)}$$

where the oil properties are evaluated at the inlet temperature. Figure A-1 shows the product of the specific heat and density for Bayol 35 as a function of temperature. For Run 78 the following data were taken.

$T_i = 14\ ^\circ C$

$T_{oil} = 1.84\ ^\circ C$

$(\rho \, C_p)_{T_i} = 0.359 \text{ cal/ml } ^\circ C$

$F_{HCl} = 5.91 \times 10^{-5}$ moles/sec

$x = 0.398$

$Q_{oil} = 68.3$ ml/sec

The power absorbed is

$$P = (4.18)(68.3)(0.359)(1.84) \qquad \text{(A-2)}$$

$$= 188 \text{ watts}$$

Table A-1

Data for the Calculation of a Theoretical Conversion

V_{rms} (v)	P (watts)	T_g/T_s	p' (Torr)	E/p' (V/cm Torr)	$k_1 \times 10^{11}$ (cm^3/molecule sec)	$N \times 10^7$ (moles/cm^3)	I_{rms} (amp)	$v_d \times 10^{-6}$ (cm/sec)	$n_e \times 10^{-11}$ (elec/cm^3)	y_1	x_1 (%)	y_2	x_2 (%)
800	56	1.19	6.30	18.0	2.3	3.44	0.071	4.50	1.25	1.18	24	1.54	25
900	72	1.25	6.00	21.5	3.3	3.27	0.080	4.75	1.34	1.72	31	2.25	33
1000	89	1.31	5.72	25.0	4.3	3.12	0.089	5.00	1.41	2.26	37	2.96	39
1100	107	1.37	5.47	28.0	5.0	3.00	0.097	5.20	1.48	2.56	42	3.36	42
1200	127	1.45	5.17	33.0	5.6	2.82	0.106	5.45	1.54	2.90	45	3.80	45
1300	150	1.52	4.94	37.5	5.6	2.70	0.115	5.65	1.62	2.92	45	3.82	45
1400	173	1.60	4.69	42.5	5.2	2.56	0.124	5.90	1.67	2.64	43	3.47	43
1500	199	1.69	4.44	48.0	4.5	2.42	0.133	6.15	1.72	2.23	37	2.93	40
1600	226	1.79	4.19	54.5	3.8	2.29	0.142	6.45	1.75	1.72	31	2.25	33

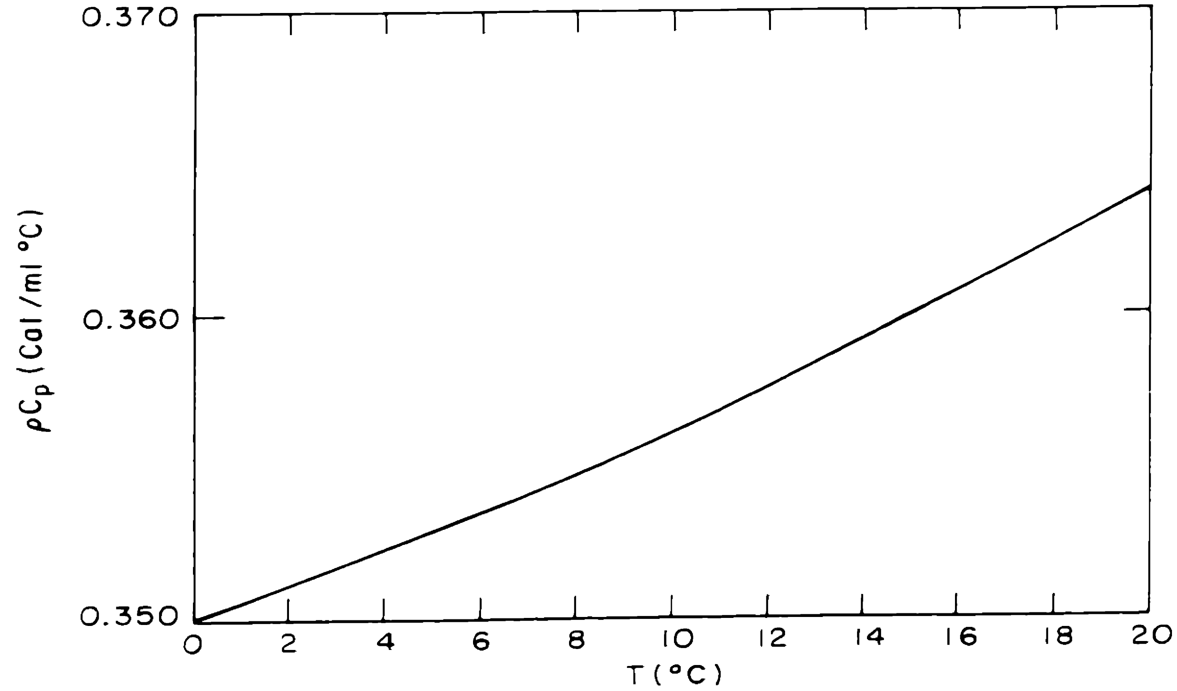

FIGURE A-1 THERMAL CHARACTERISTICS OF BAYOL 35

Since the over-all chemical reaction is exothermic, the heat released by the reaction must be subtracted from the absorbed energy. For a molar flow rate of hydrogen chloride equal to 5.91×10^{-5} moles/sec and a 39.8% conversion,

$$P_{chem} = (4.18)(0.398)(5.9\text{x}10^{-5})(2.733\text{x}10^{4}) \qquad \text{(A-3)}$$

$$= 2.7 \text{ watts}$$

Subtracting this from the absorbed power of 188 watts gives 185.3 watts.

B. Calculation of the Percent Conversion from the Chromatographic Data

The percent conversion for the forward reaction is calculated from the equation

$$x = \frac{2a}{1 + a} \times 10^{2} \qquad \text{(A-4)}$$

where

$$a = \frac{A_{Cl_2}}{A_{Cl_2} + 2.6\, A_{HCl}} \qquad \text{(A-5)}$$

and A_{Cl_2} and A_{HCl} are the areas of the chlorine and hydrogen chloride peaks on the chromatogram. The factor of 2.6 appearing in equation (A-5) accounts for the relative sensitivites of hydrogen chloride and chlorine. In a similar fashion the equation for the reverse reaction is

$$x = \frac{1 - a}{1 + a} \times 10^2 \qquad \text{(A-7)}$$

For Run 78 the measured areas are $A_{Cl_2} = 9.7$ and $A_{HCl} = 11.3$ so that the conversion for the forward reaction is

$$x = \frac{A_{Cl_2}}{A_{Cl_2} + 1.3\ A_{HCl}} \times 10^2 \qquad \text{(A-8)}$$

$$= \frac{9.7}{9.7 + 1.3\ (11.3)} \times 10^2$$

$$= 39.8\%$$

C. Calculation of the Dissociative Attachment Reaction Rate Constants

The rate constants for the dissociative attachment reactions are given by

$$k_1 = 2 \sqrt{\frac{2}{\pi m}}\ (kT_e)^{-3/2} \int_0^\infty \epsilon\ \ Q_1(\epsilon) e^{-\epsilon/kT_e}\ d\epsilon \qquad \text{(A-9)}$$

For each value of T_e, the integral in equation (A-9) is evaluated numerically using Simpson's Rule. The cross section data for hydrogen chloride and water vapor are taken from Buchel'nikova (46) and that for oxygen from Schulz (47). A sample of the Fortran program used to carry out the integration is shown below.

Calculation of the Rate Constant for HCl

```
22        FORMAT (13H GIVE ME DATA)
          DIMENSION A(25), Q(25)
          PRINT 22
          READ 10, (Q(L), L = 1, 16)
10        FORMAT (6E12.3)
          TE = 5000.
          TEMAX = 10000.
20        E = 0.33
          STEP = .05
          DELTAT = 100.
          EM = (8.64E-5)*TE
          DO 30 L = 1,16
          A(L) = 2.**1.5/(((3.1416*9.1E-28)*EM**3.)**.5*
       X  E/EXP(E/EM)*Q(L)*(1.6E-12)**.5
30        E = E + STEP
          SUM = 0
          DO 40 L = 2, 15
40        SUM = SUM + A(L)
          SIGMA = STEP/2.*(A(L) + 2.*SUM + A(16))
          PRINT 50, SIGMA, TE
50        FORMAT (E16.4, E16.4)
          TE = TE + DELTAT
          IF (TE-TEMAX) 20, 20, 60
60        CALLEXIT
          END
```

The resulting values of k_1 are shown in Figures 27 and 28.

D. Calculation of the Conversion for the Postulated Reaction Mechanism

The percent conversion for the postulated forward reaction mechanism can be determined from equations (23a) and (23b). A sample calculation will be given here for the conditions p = 7.50 Torr, $F_{HCl} = 5.91 \times 10^{-5}$ moles/sec, $R = 1.13 \times 10^4$ ohms, $\Delta T^* = 200$ °C. For an rms voltage of 800 V across the discharge, the power dissipated in the discharge is

$$\begin{aligned} P &= V_{rms}^2/R \\ &= (8\text{x}10^2)^2/1.13\text{x}10^4 \\ &= 56 \text{ watts} \end{aligned} \tag{A-10}$$

and the current passed through the discharge is

$$\begin{aligned} I_{rms} &= V_{rms}/R \\ &= 8\text{x}10^2/1.13 \times 10^4 \\ &= 0.071 \text{ amp} \end{aligned} \tag{A-11}$$

The ratio of the gas temperature to the standard temperature is calculated from the expression

$$
\begin{aligned}
T_g/T_s &= 1 + \frac{\Delta T^*}{293} \; \frac{P}{200} && \text{(A-12)} \\
&= 1 + \frac{200}{293} \; \frac{56}{200} \\
&= 1.19
\end{aligned}
$$

The pressure p' can then be determined from

$$
\begin{aligned}
p' &= p \, \frac{T_s}{T_g} && \text{(A-13)} \\
&= \frac{7.50}{1.19} \\
&= 6.30 \text{ Torr}
\end{aligned}
$$

and the gas density from

$$
\begin{aligned}
N &= \frac{p}{RT_s} \left(\frac{T_s}{T_g}\right) && \text{(A-14)} \\
&= \frac{7.50}{(7.6 \text{ x } 10^2)(8.2 \text{ x } 10 \;)(2.93 \text{ x } 10^2)(1.19)} \\
&= 3.44 \text{ x } 10^{-7} \text{ moles/cm}^3
\end{aligned}
$$

With the values of p' and V_{rms} known, E/p' is given by

$$E/p' = V_{rms}/Lp' \tag{A-15}$$

$$= \frac{8 \times 10^2}{7 \times 6.30}$$

$$= 18.0 \text{ V/cm Torr}$$

This value of E/p' is used to find T_e from Figure 6 and v_d from Figure 29. The reaction rate constant k_1 is then found from Figure 27. Finally, the electron density n_e is determined from

$$n_e = \frac{I_{rms}}{(\pi a^2) e \, v_d} \tag{A-16}$$

$$= \frac{0.071}{(0.79)(1.6 \times 10^{-19})(4.8 \times 10^6)}$$

$$= 1.25 \times 10^{11} \text{ electrons/cm}^3$$

The values of y_1 and y_2, corresponding to the assumptions of plug flow and well-mixed flow, are determined from

$$4A_i k_1 \; N \, n_e \, \frac{V}{F_{HCl}} = y_i \quad (i = 1,2) \tag{A-17}$$

Using $A_1 = 3.2$ and $A_2 = 4.2$, we obtain

$$y_1 = 4(3.2)(2.3 \times 10^{-11})(3.44 \times 10^{-7}) \qquad \text{(A-18)}$$

$$(1.25 \times 10^{-11})(5.5)/5.91 \times 10^{-5}$$

$$= 1.18$$

$$y_2 = 4(4.2)(2.3 \times 10^{-11})(3.44 \times 10^{-7})$$

$$(1.25 \times 10^{-11})(5.5)/5.91 \times 10^{-5}$$

$$= 1.54$$

The values of y_1 and y_2 as functions of x, determined from equations (24a) and (24b), are given in Figure A-2. We see that for the calculated values of y, $x_1 = 24\%$ and $x_2 = 32\%$. The balance of the calculated conversions and the intermediate parameters are shown in Table A-1

E. Calculation of Heat Transfer Coefficients

The Nusselt Number for natural convection heat transfer can be determined in terms of the product of the Grashof and Prandtl Numbers. This product is defined as X,

$$X = \left(\frac{L^3 \rho_f \, g\beta \, \Delta T}{\mu_f^2}\right)\left(\frac{C_p \, \mu}{k}\right)_f \qquad \text{(A-19)}$$

where L is the discharge length, ρ, the oil density, C_p, the specific heat of the oil, μ, the oil viscosity, k, the

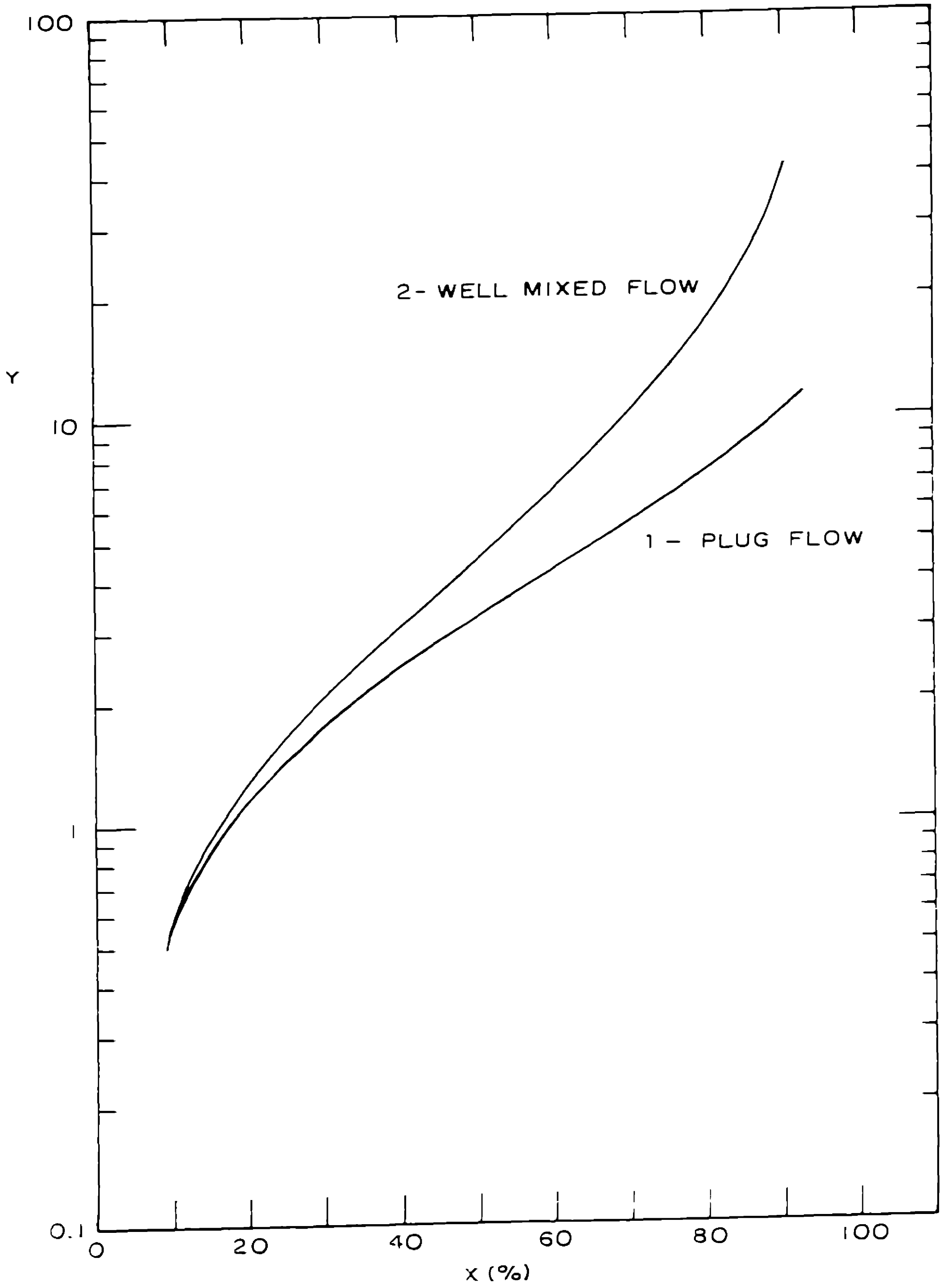

FIGURE A - 2 Y VERSUS PERCENT CONVERSION thermal conductivity of the oil, g, the acceleration of gravity, β, the coefficient of expansion for the oil, and ΔT, the temperature drop across the oil film. The subscript f appearing in equation (A-19) signifies that the oil properties are evaluated at the film temperature. The following values were used for the calculation:

$L = 7 \text{ cm}$ $\qquad k = 3.3 \times 10^{-4} \dfrac{\text{cal cm}}{\text{cm}^2\ {}^\circ\text{C sec}}$

$\rho = 0.70 \text{ gm/ml}$

$\beta = 1.02 \times 10^{-3}\ {}^\circ\text{C}^{-1}$ $\qquad g = 9.8 \times 10^{2} \text{ cm/sec}^2$

$C_p = 0.50 \text{ cal/gm }{}^\circ\text{C}$

The viscosity was evaluated as a function of temperature from an alignment chart given in McAdams (66) using the coordinates for kerosene since its properties most closely approximate those of Bayol 35.

The calculation of the heat transfer coefficient begins with the assumption of a value for ΔT and evaluation of the viscosity at the corresponding film temperature, given by

$$T_f = T_b + \frac{\Delta T}{2} \qquad \text{(A-20)}$$

where $T_b = 10\ {}^\circ\text{C}$ is the bulk oil temperature. The quantity X is then determined from equation (A-19) and used to find

Nu from a plot of Nu versus X given by McAdams (57). The heat transfer coefficient is determined from

$$h = Nu \frac{k_f}{L} \qquad \text{(A-21)}$$

To check for the correctness of the assumed ΔT, a value of $\Delta T'$ is calculated from equation (A-22) using the derived value of h.

$$\Delta T' = \frac{P}{2\pi a \ L \ h} \qquad \text{(A-22)}$$

$$= \frac{2 \times 10^2}{2\pi(0.5)(7)h}$$

$$= 2.18/h$$

If the values of ΔT and $\Delta T'$ do not agree, a new value is chosen for ΔT and the calculation is repeated. Table A-2 shows the results of these calculations. The best agreement between ΔT and $\Delta T'$ occurs at $\Delta T = 210$ °C.

For the sake of comparison, a value of the forced convection heat transfer coefficient is also calculated. For this purpose a correction developed for heat transfer due to laminar flow inside tubes was used. Thus,

$$\frac{hD}{k} = 1.75 \left(\frac{\omega \ C_p}{k \ L}\right)^{1/3} \qquad \text{(A-23)}$$

Table A-2

Calculated Values of the Natural Convection Heat Transfer Data

ΔT ($^\circ C$)	T_f ($^\circ C$)	$\log_{10} X$	$\log_{10} Nu$	$h \times 10^2$ (cal/cm^2 $^\circ C$)	$\Delta T'$ ($^\circ C$)
100	60	9.32	2.10	0.57	376
200	110	9.96	2.35	1.02	214
210	115	10.06	2.40	1.08	202
300	160	10.46	2.50	1.48	147

where w is the mass flow rate of oil and D is taken as the inner diameter of the reactor heat exchanger. Then the value of h is given by

$$h = \frac{k}{D}\ 1.75 \left(\frac{w\ C_p}{k\ L}\right)^{1/3} \qquad \text{(A-24)}$$

$$= \frac{3.3 \times 10^{-3}}{10} \times 1.75 \times \left[\frac{(4.78 \times 10^{2})(0.5)}{(3.3 \times 10^{-3})(7)}\right]^{1/3}$$

$$= 5.84 \times 10^{-4}\ \text{cal/cm}^2\ {}^{\circ}\text{C sec}$$

The forced convection heat transfer coefficient is, consequently, much smaller than that due to natural convection.

F. Evaluation of the Effect of Axial Dispersion

For the low flow rates used in this study, axial dispersion is due to molecular diffusion. In order to evaluate the variance in the output of a reactor to which has been applied a delta function input, it is necessary to know a characteristic diffusion coefficient. It is assumed that for the present case the appropriate diffusion coefficient is that for the diffusion of hydrogen atoms through a hydrogen chloride-oxygen mixture. The Gilliland correlation (67) gives

$$Dp = 1.78\text{x}10^{-3}\ \frac{T_g^{3/2}}{\left(V_H^{1/3} + V_{HCl,O_2}^{1/3}\right)^2}\left(\frac{1}{M_H} + \frac{1}{M_{HCl,O_2}}\right)^{1/2} \qquad \text{(A-25)}$$

where D is the diffusion coefficient, T_g, the gas temperature, V, a tabulated volumetric parameter, and M, the molecular weight. The following values are used:

$$T_g = 473\ ^{\circ}K$$

$V_H = 3.7$ $\qquad$ $M_H = 1$

$V_{HCl} = 25.3$ $\qquad$ $M_{HCl} = 36$

$V_{O_2} = 14.8$ $\qquad$ $M_{O_2} = 32$

$V_{HCl,O_2} = .8(25.3) + .2(14.8) = 23.1$ $\qquad$ $M_{HCl,O_2} = .8(36) + .2(32) = 35.2$

Then

$$Dp = \frac{(1.78 \times 10^{-3})(4.73 \times 10^{2})^{3/2}}{(3.7^{1/3} + 23.1^{1/3})^2} \left(\frac{1}{1} + \frac{1}{35.2}\right)^{1/2} \qquad \text{(A-26)}$$

$$= 1.28\ \text{cm}^2/\text{sec atm}$$

For a flow rate of 10^2 cm^3/min at STP, the linear velocity is given by

$$u = \frac{10^2}{6 \times 10^1} \frac{1}{0.79} \frac{1}{p} \qquad \text{(A-27)}$$

$$= \frac{2.1}{p}\ \text{cm/sec}$$

The reciprocal of the Peclet Number, D/uL, is then equal to

$$\frac{D}{uL} = \frac{1.28}{P} \frac{p}{2.1} \frac{1}{7} \qquad \text{(A-28)}$$

$$= 0.087$$

For flow in an open tube the variance for an initial delta function input is given by

$$\sigma^2 = 2\left(\frac{D}{uL}\right) + 8\left(\frac{D}{uL}\right)^2 \qquad \text{(A-29)}$$

Using the above value of D/uL

$$\sigma^2 = 2(0.087) + 8(0.087)^2 \qquad \text{(A-30)}$$

$$= 0.24$$

$$\sigma = 0.49$$

This value is sufficiently large so that deviations from plug flow should be noticeable.

APPENDIX B

ELECTRON DETACHMENT FROM NEGATIVE IONS

Electron detachment from negative ions can be considered in terms of the following six reactions:

1. $X^- + h \longrightarrow X + e$
2. $X^- + e \longrightarrow X + 2e$
3. $X^- + M \longrightarrow X + M + e$
4. $X^- + X \longrightarrow X_2 + e$
5. $X^- + Z^+ + M \longrightarrow X + Z + M$
6. $X^- + XY^+ \longrightarrow 2X + Y$

Reactions 1-3 essentially represent an ionization of the negative ion. In reaction 4 the electron is released as a result of the liberation of the dissociation energy. A similar process occurs in reactions 5 and 6, here involving the ionization energy. Thompson (69) has studied the detachment of electrons from O^- in pure oxygen. His evaluation of the rates of the various detachment processes shows that the dominant loss mechanism is associative detachment via reaction 4.

Although a study of the detachment of electrons from Cl^- occurring in a hydrogen chloride discharge has not been performed, reaction 4 cannot represent the major loss mechanism in this case. This can be understood in terms of the energy requirements for the process. The detachment energy for Cl^- is 3.7 eV; however, the amount of energy released due to the recombination of chlorine atoms is only 2.48 eV. As a result, the reaction is endothermic by 1.22 eV. The endothermicity of the reaction cannot be supplied by the relative kinetic energies of the ions and atoms since at the temperatures encountered in the discharge these are insufficient. The process can, however, proceed with hydrogen atoms acting as the reaction partner. The rate at which such a detachment mechanism might occur cannot be exceedingly high since this would mean that in the case of the reactive mixture with oxygen Cl^- could remove H atoms faster than O_2, and the over-all chemical reaction would cease to occur.

Of the remaining detachment processes, reactions 5 and 6 are the most likely (70). If it is assumed that one of these reactions is totally responsible for the removal of Cl^-, then an estimate can be made for the rate constant k_d. The ratio of k_1 to k_d is given by

$$\frac{k_1}{k_d} = \frac{(Cl^-)}{(e)} \; \frac{(HCl^+)}{(HCl)} \qquad \text{(B-1)}$$

For $(Cl^-)/(e)$ we can take a value $\gg$ 10 since Thompson (69) shows that $(O^-)/(e)$ is $\sim$ 20 for an oxygen glow discharge. Assuming neutrality of the discharge gives

$$(HCl^+) = (Cl^-) + (e) \tag{B-2}$$

$$\frac{(HCl^+)}{(e)} \gg 11$$

This value of $(HCl^+)/(e)$ can be multiplied times the observed ratio of $(e)/(HCl) \approx 10^{-6}$ to give $(HCl^+)/(HCl) \gg 1.1 \times 10^{-5}$. Thus the ratio of k_1 to k_d is $\gg 1.1 \times 10^{-4}$. Taking $k_1 = 5.6 \times 10^{-11}$ cm^3/molecule sec, we obtain $k_d = 5.1 \times 10^{-7}$ cm^3/molecule sec for $(Cl^-)/(e) = 10$ and $k_d = 2.4 \times 10^{-6}$ cm^3/molecule sec for $(Cl^-)/(e) = 20$. These values are not unreasonable as McDaniel (71) has shown that for reaction 5 occurring in air k_d should be about $10^{-7} - 10^{-6}$ for a pressure of several tens of Torr.

APPENDIX C

REDUCTION OF REACTION KINETICS

The following 14 reactions were considered in the interpretation of the mechanism for the oxidation of hydrogen chloride:

1. $HCl + e \longrightarrow H + Cl^-$
2. $O_2 + e \longrightarrow O + O^-$
3. $H_2O + e \longrightarrow OH + H^-$
4. $Cl_2 + e \longrightarrow Cl + Cl^-$
5. $O + HCl \longrightarrow OH + Cl$
6. $H + O_2 \longrightarrow OH + O$

6a. $H + O_2 + M \longrightarrow HO_2 + M$

6b. $H + HO_2 \longrightarrow 2OH$

7. $OH + HCl \longrightarrow H_2O + Cl$
8. $H + Cl_2 \longrightarrow HCl + Cl$
9. $2\ OH \longrightarrow H_2O + O$
10. $O + OH \longrightarrow O_2 + H$
11. $H + Cl + M \longrightarrow HCl + M$
12. $2\ O + M \longrightarrow O_2 + M$
13. $H + OH + M \longrightarrow H_2O + M$
14. $2\ Cl + M \longrightarrow Cl_2 + M$

The rate of appearance of hydrogen chloride is then given as

$$\frac{d(HCl)}{dt} = - k_1(HCl)(e) - k_5(O)(HCl) - k_7(OH)(HCl) \qquad (C\text{-}1)$$

$$+ \; k_{11}(H)(Cl)(H)$$

For each of the reaction intermediates, the rate of appearance can be set equal to zero under the assumption of a steady state concentration of these species. This gives rise to the set of equations

$$\frac{d(H)}{dt} = 0 = k_1(HCl)(e) + k_3(H_2O)(e) - k_6(H)(O_2) \qquad (C\text{-}2)$$

$$- k_8(H)(Cl_2) + k_{10}(O)(OH)$$

$$+ k_{11}(H)(Cl)(M) + k_{13}(H)(OH)(M)$$

$$\frac{d(O)}{dt} = 0 = 2k_2(O_2)(e) - k_5(O)(HCl) + k_6(H)(O_2) \qquad (C\text{-}3)$$

$$+ k_9(OH)^2 - k_{10}(O)(OH) + 2k_{12}(O)^2(M)$$

$$\frac{d(OH)}{dt} = 0 = k_3(H_2O)(e) + k_5(O)(HCl) + k_6(H)(O_2) \qquad (C\text{-}4)$$

$$k_7(OH)(HCl) - 2k_9(OH)^2 - k_{10}(O)(OH)$$

$$- k_{13}(H)(OH)(M)$$

$$\frac{d(Cl)}{dt} = 0 = k_1(HCl)(e) + 2k_4(Cl_2)(e) + k_5(O)(HCl) \qquad (C\text{-}5)$$

$$k_7(OH)(HCl) + k_8(H)(Cl_2) - k_{11}(H)(Cl)(M)$$

$$- 2k_{14}(Cl)^2(M)$$

Solutions for (H), (O), (OH), and (Cl) in terms of the concentrations of the molecular species cannot be obtained in terms of a sum of whole number exponential terms. To reduce the complexity of equations (C-2) - (C-5), the assumption is that for the forward reaction only those steps leading to the final products need to be considered. In the light of this restriction, reactions 3, 4, 8, 10, 11, and 12 are eliminated, and the remaining eight reactions can be grouped in the manner discussed in Chapter VII. Thus, for the set of reactions 1, 2, 5, 6, 7, and 14, equations (C-1) - (C-5) are simplified to:

$$\frac{d(HCl)}{dt} = - k_1(HCl)(e) - k_5(O)(HCl) - k_7(OH)(HCl) \qquad (C-6)$$

$$\frac{d(H)}{dt} = 0 = k_1(HCl)(e) - k_6(H)(O_2) \qquad (C-7)$$

$$\frac{d(O)}{dt} = 0 = 2k_2(O_2)(e) - k_5(O)(HCl) + k_6(H)(O_2) \qquad (C-8)$$

$$\frac{d(OH)}{dt} = 0 = k_5(O)(HCl) + k_6(H)(O_2) - k_7(OH)(HCl) \qquad (C-9)$$

$$\frac{d(Cl)}{dt} = 0 = k_1(HCl)(e) , k_5(O)(HCl) \qquad (C-10)$$

$$+ k_7(OH)(HCl) - 2k_{14}(Cl)^2(M)$$

Equation (C-6) can then be written as

$$\frac{d(HCl)}{dt} = - 4k_1(HCl)(e) - 4k_2(O_2)(e) \qquad (C-11)$$

In a similar manner, reactions 3, 8, 9, 10, and 14 are considered for the description of the reverse reaction. This leads to:

$$\frac{d(HCl)}{dt} = k_8(H)(Cl_2) \qquad (C-12)$$

$$\frac{d(H)}{dt} = 0 = k_3(H_2O)(e) - k_8(H)(Cl_2) + k_{10}(O)(OH) \qquad (C-13)$$

$$\frac{d(O)}{dt} = 0 = k_9(OH)^2 - k_{10}(O)(OH) \qquad (C-14)$$

$$\frac{d(OH)}{dt} = 0 = k_3(H_2O)(e) - 2k_9(OH)^2 - k_{10}(O)(OH) \qquad (C-15)$$

$$\frac{d(Cl)}{dt} = 0 = k_8(H)(Cl_2) - 2k_{14}(Cl)^2(M) \qquad (C-16)$$

Solving for the concentrations of the intermediate species and introducing these into equation (C-12) gives

$$\frac{d(HCl)}{dt} = \frac{4}{3} k_3(H_2O)(e) \qquad (C-17)$$

In the discussion of the reaction mechanism up to this point, no account has been taken of the manner in which electrons become detached from the negative ions, and the negative ions have, in fact, been treated as if they were the corresponding uncharged atoms. If a detachment step is included in the reaction mechanism, it can be shown that the final form of the over-all rate expression, equation (C-11), does not change.

Let us assume that electron detachment from chlorine anions occurs by reaction 5 of Appendix B, and detachment from oxygen anions by reaction 4. For the forward reaction, equations (C-6) - (C-10) can then be written as

$$\frac{d(HCl)}{dt} = - k_1(HCl)(e) - k_5(O)(HCl) - k_7(OH)(HCl) \qquad (C\text{-}18)$$

$$+ k_{d_5}(Cl^-)(HCl^+)$$

$$\frac{d(H)}{dt} = 0 = k_1(HCl)(e) - k_6(H)(O_2) \qquad (C\text{-}19)$$

$$\frac{d(O)}{dt} = 0 = k_2(O_2)(e) - k_5(O)(HCl) + k_6(H)(O_2) \qquad (C\text{-}20)$$

$$- k_{d_4}(O^-)(O)$$

$$\frac{d(OH)}{dt} = 0 = k_5(O)(HCl) + k_6(H)(O_2) - k_7(OH)(HCl) \qquad (C\text{-}21)$$

$$\frac{d(Cl)}{dt} = 0 = k_5(O)(HCl) + k_7(OH)(HCl) \qquad (C\text{-}22)$$

$$- 2k_{14}(Cl)^2(M) + k_{d_5}(Cl^-)(HCl^+)$$

In addition, the balances for the anions are given by:

$$\frac{d(Cl^-)}{dt} = 0 = k_1(HCl)(e) - k_{d_5}(Cl^-)(HCl^+) \qquad (C\text{-}23)$$

$$\frac{d(O^-)}{dt} = 0 = k_2(O_2)(e) - k_{d_4}(O^-)(O) \qquad (C\text{-}24)$$

The rate of hydrogen chloride appearance is then

$$\frac{d(HCl)}{dt} = -3k_1(HCl)(e) \qquad (C\text{-}25)$$

If reaction 5 of Appendix B had been chosen as the dtachment process for oxygen anions, the final rate expression would have been:

$$\frac{d(HCl)}{dt} = -3k_1(HCl)(e) - 3k_2(O_2)(e) \qquad (C\text{-}26)$$

Thus, the over-all rate expression retains the forms

$$\frac{d(HCl)}{dt} = -Ak_1(HCl)(e) - Bk_2(O_2)(e) \qquad (C\text{-}27)$$

APPENDIX D

DISCUSSION OF THE EXPERIMENTAL MEASUREMENT OF E/p' VERSUS T_e

Almost all the data appearing in the literature on the variation of T_e as a function of E/p' has been taken in a drift tube. The simplest form of this apparatus, originally designed by Townsend (72), is shown in Figure D-1. The drawing shows a diffusion chamber containing a filament, cathode, guard rings, and a segmented anode. The chamber contains the gas to be studied, and a uniform electric field is maintained along the axis of the chamber.

Electrons are emitted continuously from the filament and stream towards the cathode. Those electrons which pass the hole in the cathode drift slowly towards the anode, undergoing diffusion during drift. The electron current to each of the anode segments is measured, and their divergence is represented by $R = I_1/(I_1 + I_2)$. If the cathode hole is treated as a point source of electrons, and it is assumed that neither ionization nor attachment occurs in the gas, then the ratio R can be calculated from a solution to the diffusion problem. This results in

$$R = 1 - \frac{h}{d} e^{-\lambda(h-d)} \qquad \text{(D-1)}$$

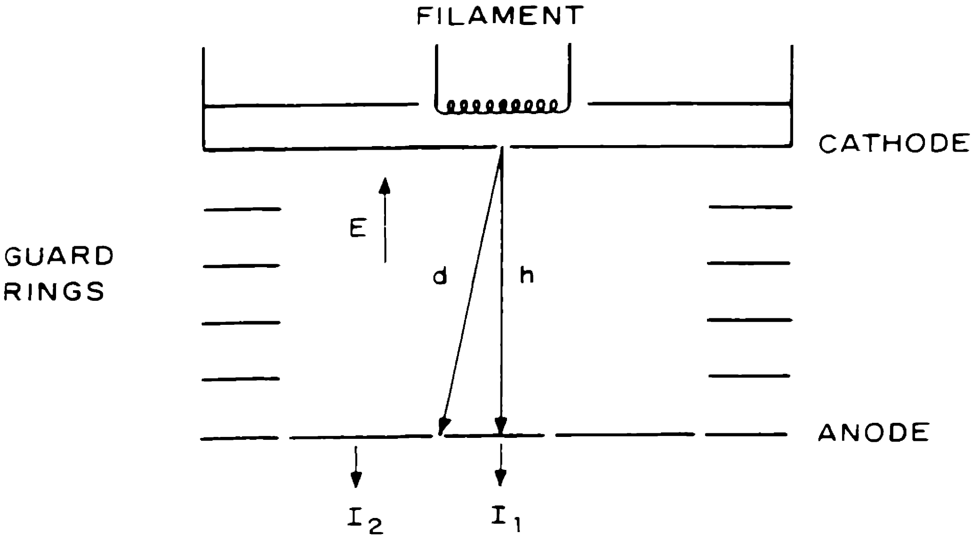
FILAMENT
CATHODE
GUARD RINGS
E
d
h
ANODE
I_2
I_1

FIGURE D-1 SCHEMATIC OF DRIFT TUBE

where h and d are distances shown in Figure D-1 and $\lambda = v_d/2D_e$. Thus, v_d/D_e can be determined from the measured values of R for each value of E/p'. If the possibilities of ionization and attachment are included, Huxley (73) shows that an expression can still be obtained for R in terms of λ.

The problem is now to relate the measured parameter v_d/D_e to T_e. Rose and Clark (74) show that the electron distribution function for a partially ionized gas can be given as

$$f(\bar{r},\bar{v}) = f_o(\bar{r},v) + f_1(\bar{r},\bar{v}) \qquad \text{(D-2)}$$

where $\bar{r}$ and $\bar{v}$ are the position and velocity vectors, v the speed, f_o the symmetric or equilibrium part of the distribution function, and f_1 the second order unsymmetric part of the distribution function. Using this form of the distribution in the calculation of a diffusive flux results in

$$\bar{J}_{diff} = - \bar{\nabla} \int d\bar{v} \; \frac{v^2}{3 \nu_m} f_o \qquad \text{(D-3)}$$

$$= - \bar{\nabla} (D_e n_e)$$

The diffusion coefficient is thus defined as

$$D_e = \overline{v^2/3\,\nu_m} \qquad \text{(D-4)}$$

Similarly, for a flux due to charge mobility in an electric field

$$\bar{j}_{mob} = \bar{E}\int dv\, f_o\, \frac{d}{dv}\left(\frac{4\pi e\; v^3}{3m\;\nu_m}\right) \qquad \text{(D-5)}$$

$$= E(\mu_e\; n_e)$$

If ν_m = constant, equation (D-5) can be integrated to give

$$\mu_e = e/m\,\nu_m \qquad \text{(D-6)}$$

The ratio of the diffusion coefficient to the mobility is given by

$$D_e/\mu_e = \frac{2\bar{\epsilon}}{3e} \qquad \text{(D-7)}$$

where $\bar{\epsilon}$ is the average energy. In addition, if f_o is Maxwellian, then

$$D_e/\mu_e = \frac{kT_e}{e} \qquad \text{(D-8)}$$

Hence, under the limitation that ν_m = constant and that f_o is Maxwellian,

$$\frac{D_e}{v_d} = \frac{kT_e}{eE} \qquad \text{(D-9)}$$

Equation (D-9) provides the necessary relation for converting the drift tube measurements to a value of T_e.

The question which still must be answered is whether the average energies measure in a drift tube correspond to those found in a steady state discharge. This question has been treated by Reder and Brown (75). These authors have solved the transport equation for a fully developed high frequency discharge in helium. On the basis of the calculated distribution function, a plot was constructed of the average electron energy as a function of E_{eff}/p'. These values are illustrated in Figure D-2. Superimposed on this curve are the drift tube data of Townsend and Bailey (72) and values of $\bar{\epsilon}$ calculated for a d.c. discharge by Smit (76). The superposition of the three sets of data shows that not only do the drift tube data give the correct values of $\bar{\epsilon}$ but that these values will not differ between a high frequency and a d.c. discharge provided $E_{dc} = (E_{ac})_{eff}$.

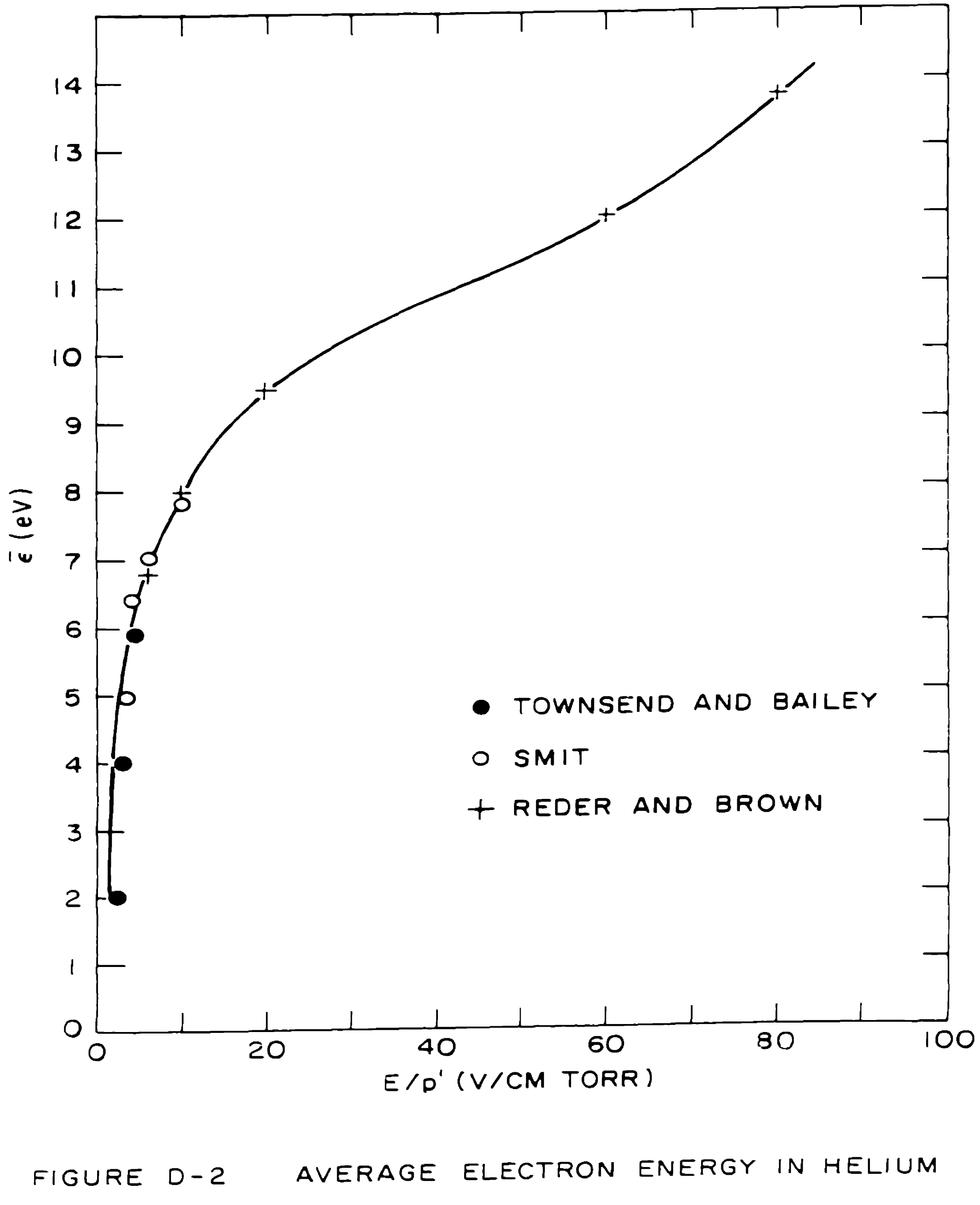

FIGURE D-2 AVERAGE ELECTRON ENERGY IN HELIUM

APPENDIX E

EVALUATION OF THE ASSUMPTION OF A MAXWELLIAN DISTRIBUTION OF ELECTRON ENERGIES

The calculation of the actual distribution of electron energy in an electric discharge requires a solution of the Boltzmann transport equation (77). To perform this solution detailed information must be available on the electron-molecule interaction cross sections for various excitation processes. Since this type of material is most often unavailable and the execution of the solution quite involved, examination is made of two limiting cases.

The first case represents the distribution which results when only elastic collisions are allowed to occur between the electrons and molecules. This form, known as the Druyvesteyn distribution, is given by

$$f_D = 1.04\sqrt{\frac{\epsilon}{\bar{\epsilon}}}\ e^{-0.55(\epsilon/\bar{\epsilon})^2} \qquad \text{(E-1)}$$

where $\bar{\epsilon}$ is the mean energy. The second limiting form represents the condition in which there are strong interactions between the electrons--i.e., by their mutual repulsion--which are responsible for the redistribution of their energies. Under such circumstances a Maxwellian distribution ensues:

$$f_M = \frac{2}{\sqrt{\pi}} \sqrt{\frac{\epsilon}{\bar{\epsilon}}}\, e^{-\epsilon/\bar{\epsilon}} \qquad (E-2)$$

For the Maxwellian distribution an electron temperature, T_e, may be defined as:

$$\bar{\epsilon} = \frac{3}{2} kT_e \qquad (E-3)$$

The concept of an "electron temperature" is often loosely used to describe the mean energy of other energy distributions. For the same mean energy the Maxwellian distribution contains an appreciably larger fraction of electrons at higher energies than the Druyvesteyn

It has been found (78) that the Maxwellian distribution is often a good approximation in molecular gases. This is because these gases have excitation levels (including vibrational levels) widely spread out up to the ionization potential. Hence inelastic losses set in at relatively low energies. The average electron energy is as a consequence low, but the losses are so distributed as to produce an approximately Maxwellian distribution. In rare gases, however, the excitation levels are much closer to the ionization potential, and thus at low mean energies only elastic losses are important. The average energy is much higher than in molecular gases at the same value of E/p', and the Druyvesteyn distribution applies approximately.

APPENDIX F

NOMENCLATURE

A	adjustable constant in equation (21)
A_1	area of chlorine peak on gas chromatogram
A_2	area of hydrogen chloride peak on gas chromatogram
a	discharge tube radius, cm
a	percent of chlorine in the chlorine-hydrogen chloride product mixture
a_j	pre-exponential factor which expresses the characteristics of the excitation function for the j-th level
a_+	pre-exponential factor which expresses the characteristics of the excitation function for ionization
B	adjustable constant in equation (21)
C	adjustable constant in equation (31)
D	adjustable constant in equation (36)
D	molecular diffusion coefficient, cm^2/sec
D_a	ambipolar diffusion coefficient, cm^2/sec
D_e	diffusion coefficient for electrons, cm^2/sec
D_+	diffusion coefficient for positive ions, cm^2/sec
D_-	diffusion coefficient for negative ions, cm^2/sec
E	electric field strength, V/cm
E_{eff}	effective field strength as defined by $$\frac{E}{2}\left(\frac{\nu_m^2}{\nu_m^2+\omega^2}\right)^{1/2}, \text{ V/cm}$$

e	charge on an electron, coulomb
F	molar flow rate, moles/sec
F	force, dynes
g	parameter defined by equation (67)
h	dimensionless electron density
I_{rms}	rms current, amp
J	current density, amp/cm^2
j	particle flux, particles/cm^2 sec
K_n	equilibrium constant
k	Boltzmann constant
k_1	reaction rate constant, cm^3/mole sec
L	discharge length, cm
M	mass of a molecule, gm
m	mass of an electron, gm
N	molecular density, number/cm^3
n_e	electron density, number/cm^3
n_+	positive ion density, number/cm^3
n_-	negative ion density, number/cm^3
P	power, watts
P	power density, watts/cm^3
p	pressure, Torr
p'	reduced pressure as defined by $pT_g/293$, Torr
Q	collision cross section, cm^2
q	detachment cross section, cm^2
R	resistance, ohm

T_e	electron temperature, ^oK
T_g	gas temperature, ^oK
ΔT^*	adjustable constant in equation (25)
u	linear gas velocity, cm/sec
V	volume, cm^3
v	velocity, cm/sec
v_d	drift velocity, cm/sec
v_r	random velocity, cm/sec
x	conversion
y	a parameter defined by equations (24a) and (24b)
z	length, cm
α	the ratio n_-/n_e
α	$(O_2)/(HCl)$
α	number of ionization per cm at one Torr
β	number of attachments per cm at one Torr
γ	the ratio T_e/T_g
Δ	error in measured conversion
Δ_j	fraction of the total discharge energy expended on process j
$\bar{\delta}$	the fraction of its energy which an electron looses on collision
$\bar{\epsilon}$	average energy transferred per collision, eV
$\bar{\epsilon}$	average electron energy, eV
ϵ_j	energy of the j-th excitation level, eV

ϵ_o	permeability of free space
ϵ_u	energy transferred via elastic collisions, eV
ϵ_+	ionization potential, eV
η	number of hydrogen chloride molecules dissociated per unit energy, number/eV
Λ	diffusion length, cm
λ	mean free path, cm
μ_e	electron mobility, cm^2/V sec
μ_+	positive ion mobility, cm^2/V sec
μ_-	negative ion mobility, cm^2/V sec
ν_i	collision frequency for the i-th process, sec^{-1}
ν_m	elastic collision frequency, sec^{-1}
σ	cross section for positive-negative ion recombination
ω	frequency of oscillating electric field, rad/sec

APPENDIX G

LOCATION OF ORIGINAL DATA

The original data on which this thesis is based are contained in three bound notebooks. These are kept by Professor Raymond Baddour in the Department of Chemical Engineering at the Massachusetts Institute of Technology.

APPENDIX H

LITERATURE REFERENCES

1. Blanchet, J. L., "Reactions of Carbon Vapor with Hydrogen and with Methane in a High-Intensity Arc," Sc.D. Thesis in Chemical Engineering, M.I.T., Cambridge, Mass. (1963).

2. Iwasyk, J. M., "The Carbon-Hydrogen System at Temperatures above 2500°C," Sc.D. Thesis in Chemical Engineering, M.I.T., Cambridge, Mass. (1960).

3. Bronfin, B. R., "Fluro-carbon Synthesis in a High-Intensity Carbon Arc," Sc.D. Thesis in Chemical Engineering, M.I.T., Cambridge, Mass. (1963).

4. Glocker, G. and Lind, S.C., Electrochemistry of Gases and Other Dielectrics, John Wiley and Sons, Inc., New York (1939).

5. Jolly, W. L., "The Use of Electric Discharges in Chemical Synthesis" in Techniques of Inorganic Chemistry, Vol. 1, Interscience, New York (1963), p. 179.

6. Kana'an, A. S. and Margrave, J. L., "Chemical Reactions in Electric Discharges" in Advances in Inorganic Chemistry, Vol. 6, Academic Press, New York (1964), p. 143.

7. Shaw, T. M., "Studies of Microwave Gas Discharges: Production of Free Radicals in a Microwave Discharge," General Electric Technical Information Report Number TIS R58ELM 115, General Electric Microwave Laboratory, Power Tube Department, Palo Alto, California.

8. Poole, H. G., "Atomic Hydrogen, I. The of Hydrogen Atoms; II. Surface Effects in the Discharge Tube; III. The Energy Efficiency of Atom Production in a Gas Discharge," Proc. Roy. Soc. A163, 404, 415, 424 (1937).

9. Bak, B. and Rastrup-Anderson, J., "Microwave Discharge Production of Hydrogen Atoms," Acta. Chem. Scand. 16, 111 (1962).

10. Wood, R. W., "Atomic Hydrogen and the Balmer Series Spectrum" Phil. Mag. 44, 538 (1922).

11. Shaw, T. M., "Effect of Water Vapor on the Dissociation of Hydrogen in an Electrical Discharge," J. Chem. Phys. 31, 1142 (1959).

12. Young, R. A., Sharpless, R. L., and Stringham, R. J., "Catalyzed Dissociation of N_2 in Microwave Discharges," J. Chem. Phys. 40, 117 (1964).

13. Elias, L., Ogryzlo, E. A., and Schiff, H. J., "The Study of Electrically Discharged O_2 by Means of an Isothermal Calorimetric Detector," Can. J. Chem. 37, 1680 (1959).

14. Kaufman, F. and Kelso, J. R., "Catalytic Effects in the Dissociation of Oxygen in Microwave Discharges," J. Chem. Phys. 32, 301 (1960).

15. Ogryzlo, E. A., "Halogen Atom Reactions: I. The Electrical Discharge as a Source of Halogen Atoms," Can. J. Chem. 39, 2556 (1961).

16. McCarthy, R. L., "Chemical Synthesis from Free Radicals Produced in Microwave Fields," J. Chem. Phys. 22, 1360 (1954).

17. Coates, A. D., "Microwave Induced Dissociation of n-Hexane," U.S. Dept. Comm. Report AD 409436 (1962).

18. Streitwieser, A. and Ward, H. R., "Organic Compounds in a Microwave Discharge: II. Initial Studies with Toluene and Related Hydrocarbons," J. Am. Chem. Soc. 85, 539 (1963).

19. Dinan, F. J., "The Dissociation of Toluene Vapor in a Radiofrequency Discharge," in preprints of papers presented at the Symposium on Chemical Reactions in Electrical Discharges held at Miami, Florida, by the American Chemical Society (1967).

20. Blaustein, B. D. and Fu, Y. C., "Formation of Hydrocarbons from H_2 and CO in Microwave-Generated Electrodeless Discharges," in preprints of papers presented at the Symposium on Chemical Reactions in Electrical Discharges held at Miami, Florida, by the American Chemical Society (1967).

21. McTaggart, F. K., "Reactions of Carbon Monoxide in a High Frequency Discharge," Aust. J. Chem. 17, 1182 (1964).

22. Hollahan, J. R. and McKeever, R. P., "Radiofrequency Electrodeless Synthesis of Polymers: Reactions of CO, N_2, and H_2," in preprints of papers presented at the Symposium on Chemical Reactions in Electrical Discharges held at Miami, Florida, by the American Chemical Society (1967).

23. Emeleus, H. J. and Tittle, B., "Synthesis of Pentafluorosulphur Chloride and Sulphur Oxide Tetrafluoride in the Microwave Discharge," J. Chem. Soc. (London) 1963, 1644 (1963).

24. Vastola, F. J. and Stacy, W. O., "Plasma Induced Reaction of Hydrogen Sulfide with Hydrocarbons," in preprints of papers presented at the Symposium on Chemical Reactions in Electrical Discharges held at Miami, Florida, by the American Chemical Society (1967).

25. Blackwood, J. D. and McTaggart, F.K., "The Oxidation of Carbon with Atomic Oxygen," Aust. J. Chem. 12, 114 (1959).

26. Vastola, F. J., Walker, P. L., and Wightman, J. P., "The Reaction between Carbon and the Products of Hydrogen, Oxygen, and Water Microwave Discharges," Carbon 1, 11 (1963).

27. Eremin, E. N., Vasil'ev, S. S., and Kobozev, N. I., "Investigation of the Oxidation of Nitrogen in a High Frequency Glow Discharge II," Zh. Fiz. Khim. 9, 48 (1937).

28. Vasil'ev, S. S., "The Molecular and Electron Temperatures and the Number of Effective Collisions during the Chemical Action of Electric Discharges," Vestnik Mos. U., No. 12, 63 (1947).

29. Vasil'ev, S. S., "Generalization of the Formula for the Calculation of Effective Collisions in Electric Discharges," Vestnik. Mos. U., No. 5 (1950).

30. Eremin, E. N., and Mal'tsev, A. N., "Steady State Concentrations of Nitric Oxide in a Discharge. I. Experiments with Air in Wide Vessels," Zh. Fiz. Khim. 30, 1615 (1956).

Mal'tsev, A. N., Eremin, E. N., and Vorob'eva, I. N., "Steady State Concentrations of Nitric Oxide in the Electric Discharge. II. Experiments with Air in a Narrow Tube," Russ. J. Phys. Chem. 33, 79 (1959).

Mal'tsev, A. N., Eremin, E. N., and Meshkova, I. N., "Steady State Concentrations of Nitric Oxide in the Electric Discharge. IV. Influence of the Composition of the Initial Mixture," Russ. J. Phys. Chem. 36, 405 (1962).

Pollo, I., Mal'tsev, A. N., and Eremin, E. N., "Steady State Concentrations of Nitric Oxide in the Glow Discharge. VI. Effect of Composition on the Formation of Nitric Oxide in a Narrow Reactor," Russ. J. Chem. 37, 1130 (1963).

31. Cooper, W. W., "The Oxidation of Hydrogen Chloride in a Microwave Discharge," Sc.D. Thesis in Chemical Engineering, M.I.T., Cambridge, Mass. (1966).

32. Romig, H. F., "Steady State Solutions of the Radiofrequency Discharge with Flow, " Phys. Fl. 3, 129 (1960).

33. Brown, S. C. and MacDonald, A. D., "Limits for the Diffusion Theory of High-Frequency Gas Discharge Breakdown," Phys. Rev. 76, 1629 (1949).

34. Rose, D. J. and Brown, S. C., "High-Frequency Gas Discharge Plasma in Hydrogen," Phys. Rev. 98, 310 (1955).

35. Lathrop, J. W., "Characteristics of Steady State Maintaining Fields in a Microwave Discharge," Ph.D. Thesis in Physics, M.I.T., Cambridge, Mass. (1952).

36. Vasil'ev, S. S., "The Energy Balance and Steady State Distribution of Energy during Physico-Chemical Processes in Electrical Discharges," Zh. Fiz. Khim. 24, 1107 (1950).

37. Lunt, R. W. and Meek, C. A., "The Energy Balance and Energy Efficiencies for the Principal Electron Processes in Hydrogen," Proc. Roy. Soc. A157, 146 (1936).

38. Foner, S. N. and Hudson, R. L., "Mass Spectrometry of the HO_2 Free Radical," J. Chem. Phys. 36, 2681 (1962).

39. Harteck, P. and Kopsch, U.,"Gasreaktionen mit Atomarem Souerstaff," Z. fur Physik, Chem B12, 327 (1931).

40. Greiner, N. R., "Hydroxyl-Radical Kinetics by Kinetic Spectroscopy. I. Reactions with H_2, CO, and CH_4 at 300 °K," J. Chem. Phys. 46, 2795 (1967).

41. Del Greco, F. P. and Kaufman, F., "Lifetime and Reactions of OH Radicals in Discharge Flow Systems," Disc. Faraday Soc. 33, 128 (1962).

42. Kondrat'ev, V. N., Chemical Kinetics of Gas Reactions, Pergamon Press, New York (1964), p. 611.

43. Porter, G., Progress in Reaction Kinetics, Pergamon Press, New York (1965).

44. Campbell, I. M. and Thrush, B. A., "The Association of Oxygen Atoms and their Combination with Nitrogen Atoms," Proc. Roy. Soc. A296, 222 (1967).

45. Bader, L. W. and Ogryzlo, E. A., "Recombination of Chlorine Atoms," Nature 201, 491 (1964).

46. Buchel'nikova, N.S., "Effective Capture Cross Sections for Slow Electrons by Certain Halogen Containing Molecules, O_2, and H_2O," Zh. Eksper. i Teori. Fiz. 35, 1119 (1958).

47. Schulz, G. J., "Cross Sections and Electron Affinity for O^- Ions from O_2, CO, and CO_2 by Electron Impact," Phys. Rev. 128, 178 (1962).

48. Bailey, V. A. and Duncanson, W. E., "On the Behaviour of Electrons Amongst the Molecules NH_3, H_2O and HCl," Phil. Mag. 10, 145 (1930).

49. Fishburne, E. S., "Gaseous Reaction Rates at High Temperatures. II. The Dissociation of Hydrogen Chloride," J. Chem. Phys. 45 (1966).

50. Vasil'ev, S. S. "Kinetic Analysis of Chemical Processes in Electric Discharges," Vestnik Mos. U., No. 8, 79 (1951).

51. Manes, M., "Chemical Equilibrium in Electrically Excited Gases," submitted to Advances in Chemistry Symposium on Electric Discharges in Gases, American Chemical Society, Washington (1967).

52. Potapov, A. V., "Chemical Equilibrium of Multi-temperature Systems," High Temperatures 4, 48 (1966).

53. Kaufman, F., "The Production of Atoms and Simple Radicals in Glow Discharges," in preprints of papers presented at the Symposium on Chemical Reactions in Electrical Discharges at Miami, Florida, American Chemical Society (1967).

54. McDaniel, E. W., Collision Phenomena in Ionized Gases, John Wiley and Sons, Inc., New York (1964), p. 514.

55. Herzberg, G., Molecular Spectra and Molecular Structure, D. Van Nostrand Co., Inc. Princeton (1950).

56. Terenin, A. W., and Neuimin, H. G., "Infrared Emission of the Electric Discharge in Molecular Gases and its Significance for Chemical Kinetics," Acta Physiochimica U.R.S.S. 16, 257 (1942).

57. McAdams, W. H., Heat Transmission, McGraw Hill, New York (1954), p. 172.

58. Bauman, R. P., Absorption Spectroscopy, John Wiley and Sons, Inc., New York (1962), p. 51.

59. Albrecht, G., Ecker, G., and Muller, K. G., "Theorie der Kontraktion der positiven Saule," Z. Naturforch. 17A, 854 (1962).

60. Thompson, J. B., "Negative Ions in the Positive Column of the Oxygen Discharge," Pro. Phys. Soc. (London) 73, 818 (1959).

61. Banerji, D. and Ganguli, R., "On the Distribution of Space-Potential in High-Frequency Glow Discharge," Phil. Mag. 7, 410 (1934).

62. Perel', V. I. and Pinskii, Ya. M., "Effects of an Inhomogeneous AC Field on a High-Frequency Discharge," Sov. Phys.-Tech.Phys. 8, 197 (1963).

63. Golovanivskii, K. S. and Kuzovnikov, A. A., "Effect of Compression of the Positive Column of a Gas Discharge by an Inhomogeneous High-Frequency Field," Sov. Phys.-Tech. Phys. 6, 645 (1962).

64. Dzherpetov, Kh. A., Bulkin, P. S., and Akhmedov, A. R., "Investigation of the Spatial Distribution of the Parameters of a High Frequency Discharge in Helium and Argon," Vestnik Mos. U., No. 3, 71 (1959).

65. Polman, J., "Electron Temperature Measurements in a Radio Frequency Gas Discharge," Physica 34, 310 (1967).

66. McAdams, W., op. cit., p. 466.

67. Sherwood, T. K. and Pigford, R. L., Adsorption and Extraction, McGraw Hill Book Co., Inc., New York (1952), p. 10.

68. Levenspeil, O., Chemical Reaction Engineering, John Wiley and Sons, Inc., New York (1962), p. 265.

69. Thompson, J. B., "The Ion Balance of the Oxygen D.C. Glow Discharge," Proc. Roy. Soc. A262, 819 (1961).

70. McDaniel, E. W., op. cit., p. 386.

71. McDaniel, E. W., op. cit., p. 583.

72. Townsend, J. S. and Bailey, V. A., "The Motion of Electrons in Gases," Phil. Mag. 42, 873 (1921).

73. Huxley, L. G. H., "The Structure of a Stream of Electrons and Ions Drifting and Diffusing in a Gas when Ionization by Collision and Molecular Attachment are Present," Aust. J. Phys. 12, 171 (1959).

74. Rose, D. J. and Clark, M., Plasmas and Controlled Fusion, M.I.T. Press, Cambridge, Mass (1961), p. 63.

75. Reder, F. H. and Brown, S. C., "Energy Distribution Function of Electrons in Pure Helium" Phys. Rev. 95, 885 (1954).

76. Smit, I. A., "Berechnung der Gerschwindigkeitverteilung der Elektronen bei Gasentladung in Helium," Physica 3, 543 (1936).

77. Allis, W. P., "Motion of Ions and Electrons" in Handbuch der Physik, Vol. XXI, Springer-Verlag, Berlin (1956), pp. 383-444.

78. Francis, G., Ionization Phenomena in Gases, Butterworths Scientific Publications, London (1960).

Appendix I

Biographical Note

The author was born on October 16, 1942, in New York City, New York. He attended public school in New York City through the sixth grade. From the seventh grade to the end of high school his education was continued at the McBurney School, also in New York City.

He entered the Massachusetts Institute of Technology in September, 1960. Financial assistance for these undergraduate studies was obtained from a series of scholarships given by the Institute. During the course of his work the author was elected to the Tau Beta Pi Association, the Society of the Sigma Xi, and Phi Lambda Upsilon. He received his Bachelor of Science Degree in Chemical Engineering in June, 1964.

Graduate education in chemical engineering was begun at M.I.T. in the fall of 1964. Financial assistance for these studies was provided by a National Science Foundation Traineeship for 1964-65, a National Aeronautics and Space Administration Traineeship for 1965-66, and a departmental Research Assistanship for 1966-67. In May of 1966 the author received the Eastman Kodak Science Award given by the Department of Chemical Engineering.